

# Analysis Status of the SBS Neutron Two-Photon Exchange Experiment

Ezekiel Wertz  
March 2, 2026

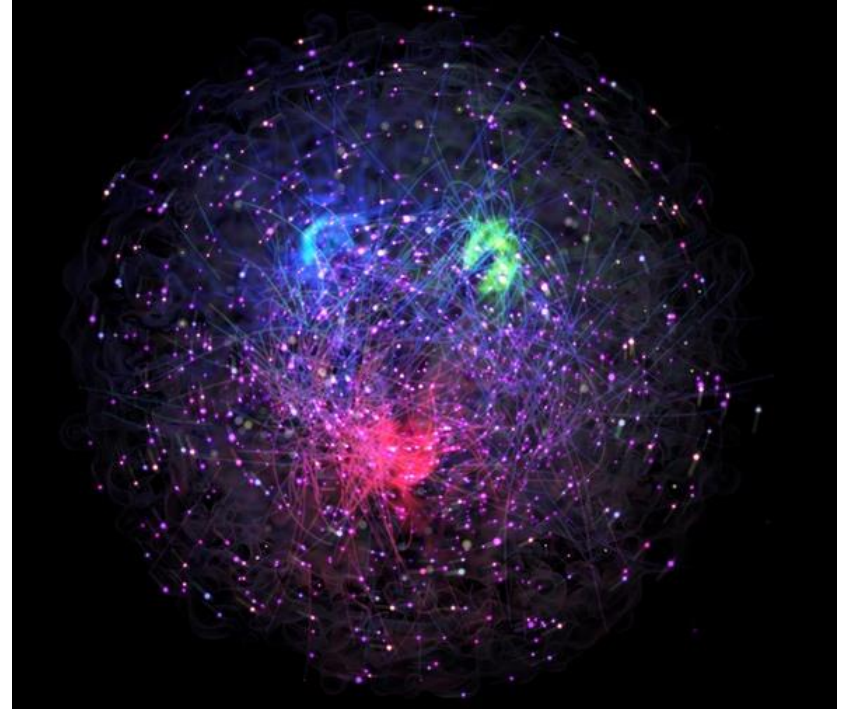
WILLIAM & MARY

School of Computing,  
Data Sciences & Physics



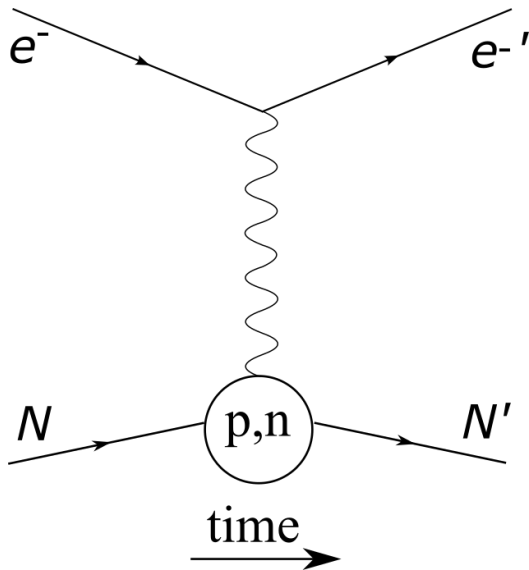
# Outline

- Nucleon Structure & Electromagnetic Form Factors
- SBS nTPE experiment and observable extraction
- Overview of Data Analysis Methods
- Physics Extraction from Data/MC Comparison
- Preliminary neutron Rosenbluth Slope result



# Nucleon Elastic Electromagnetic Form Factors

- Differential Cross-Section represented by a **point-like factor** and a **factor for the internal structure**.
- $G_E(Q^2) = F_1(Q^2) - \tau F_2(Q^2)$  is the **Sachs Electric Form Factor**
- $G_M(Q^2) = F_1(Q^2) + F_2(Q^2)$  is the **Sachs Magnetic Form Factor**
- In a particular reference frame, the Breit frame,  $G_E$  and  $G_M$  are related to the Fourier Transform of the internal charge and magnetization distributions.



$$\begin{aligned} \frac{d\sigma}{d\Omega} &= \frac{\tau \sigma_{\text{Mott}}}{\epsilon(1+\tau)} \left( \frac{\epsilon}{\tau} G_E^2(Q^2) + G_M^2(Q^2) \right) \\ &= \frac{\tau \sigma_{\text{Mott}}}{\epsilon(1+\tau)} (\epsilon \sigma_L + \sigma_T) \end{aligned}$$

$$\epsilon = (1 + 2(1 + \tau) \tan^2(\theta/2))^{-1}$$

## Rosenbluth Separation

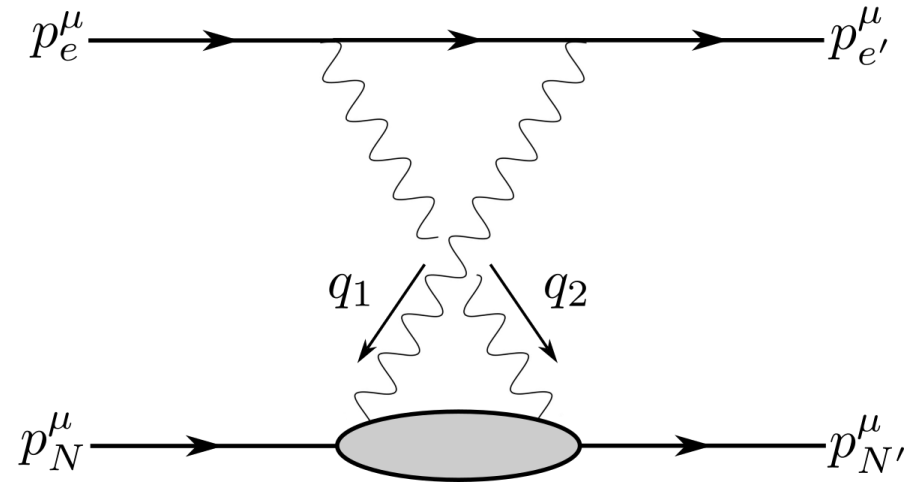
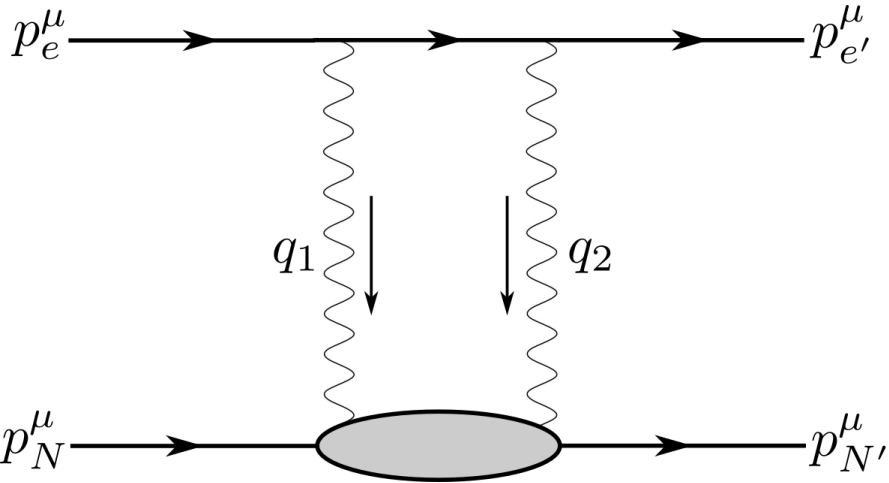
- Fixed  $Q^2$ -value
- Vary electron beam energy and scattering angle, to make measurements at different  $\epsilon$  values

$$\begin{aligned} \sigma_R &= \frac{\epsilon}{\tau} G_E^2(Q^2) + G_M^2(Q^2) \\ &= (\epsilon \sigma_L + \sigma_T) \end{aligned}$$

## Rosenbluth Slope

$$S = \sigma_L / \sigma_T = G_E^2(Q^2) / \tau G_M^2(Q^2)$$

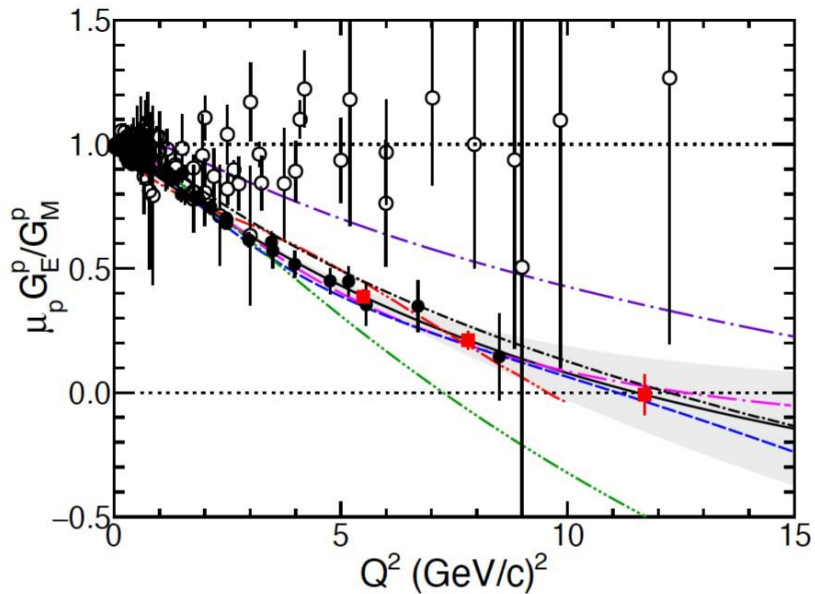
# Two-Photon Exchange



- Higher order diagrams, Two-Photon Exchange (TPE), contribute to the cross-section
- TPE diagrams are difficult to calculate
- Studying TPE effects provides insights into nucleon excitation

# Nucleon Electromagnetic Form Factor World Data

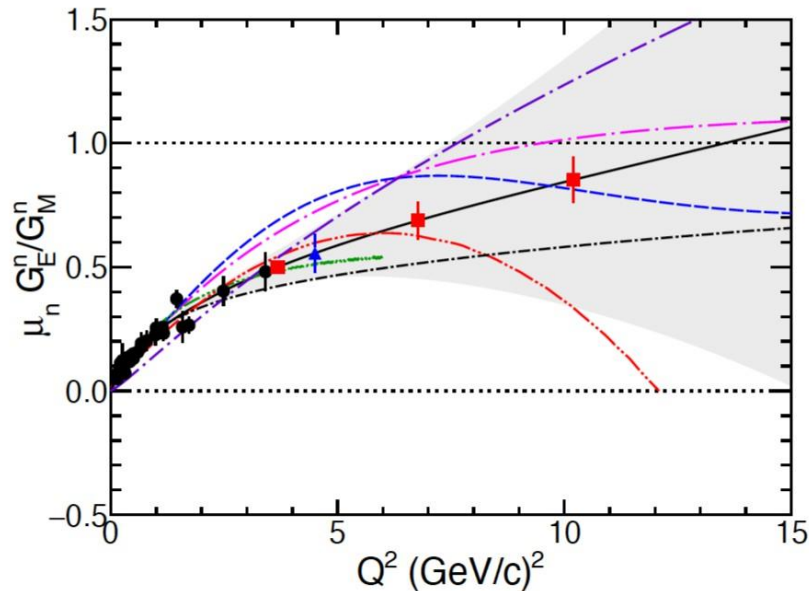
Proton:



- $G_{E,M}^p$  Rosenbluth
- $G_E^{p,n}$  polarization
- SBS projected
- ▲ SBS GEN-RP projected

— Global fit (Ye 2018)

Neutron:

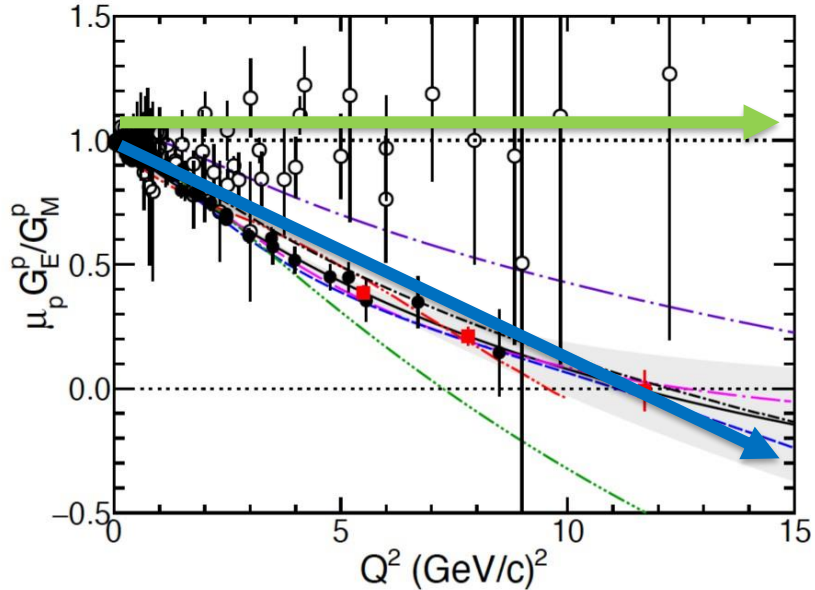


- Xu 2021
- Diehl 2005
- Segovia 2014
- Lomon 2002
- Gross 2008
- Cloet 2012

Plots: Franz Gross *et al.*, *50 Years of Quantum Chromodynamics*

# Proton Form Factor Ratio World Data Discrepancy

Proton:



○  $G_{E,M}^p$  Rosenbluth      ■ SBS projected  
 ●  $G_E^{p,n}$  polarization      ▲ SBS GEN-RP projected

— Global fit (Ye 2018)

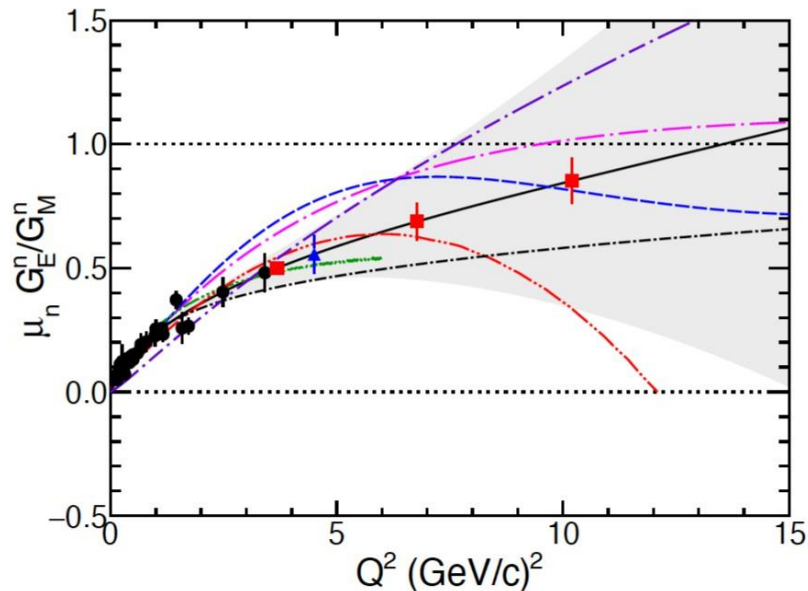
- Primary Methods
  1. Rosenbluth Separation (RS)
  2. Polarization Transfer (PT)
- $G_E^p / G_M^p$  from RS consistent with 1.0
- $G_E^p / G_M^p$  from PT disagrees by 3-4 sigma
- Possible Solution: TPE effects

— Xu 2021      — Lomon 2002  
 — Diehl 2005      — Gross 2008  
 — Segovia 2014      — Cloet 2012

Plots: Franz Gross *et al.*, *50 Years of Quantum Chromodynamics*

# Neutron Form Factor Ratio World Data

Neutron:



○  $G_{E,M}^p$  Rosenbluth      ■ SBS projected  
 ●  $G_E^{p,n}$  polarization      ▲ SBS GEN-RP projected

— Global fit (Ye 2018)

— Xu 2021      — Lomon 2002  
 — Diehl 2005      — Gross 2008  
 — Segovia 2014      — Cloet 2012

- $G_E^n / G_M^n$  only from PT data
- TPE Effects on the neutron not yet experimentally established
- The nTPE experiment is first extraction of  $G_E^n / G_M^n$  from RS

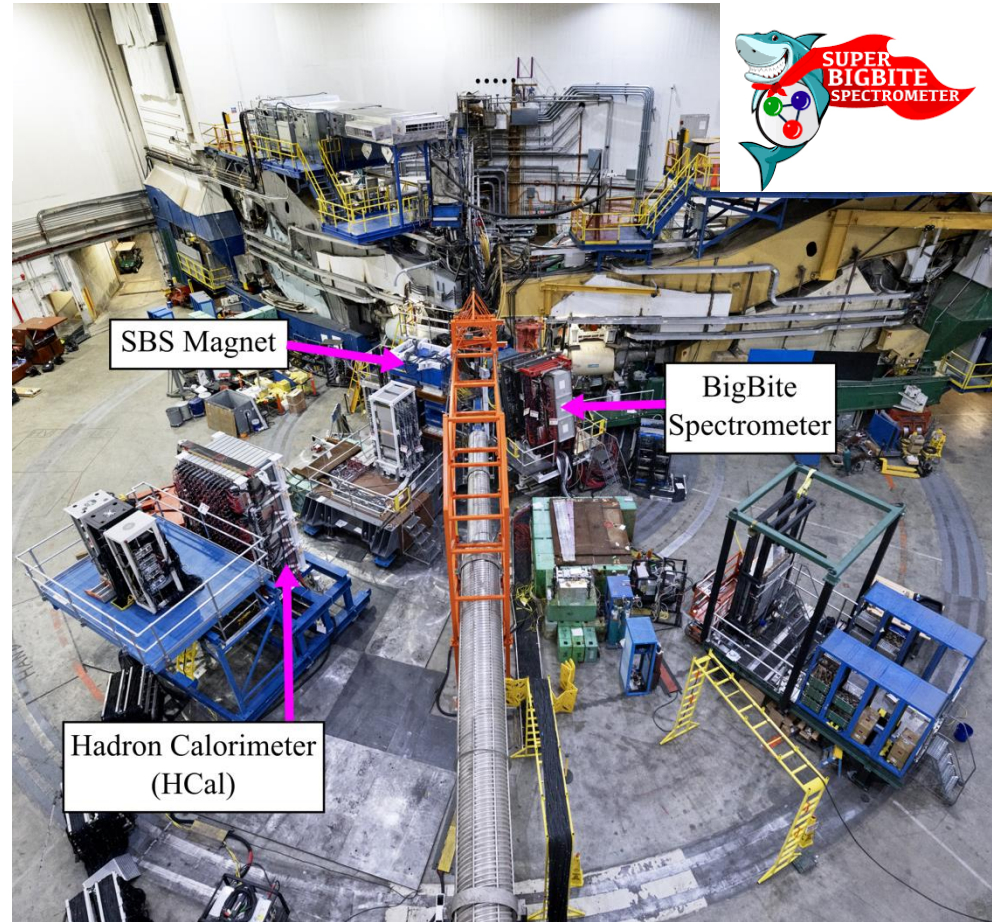
Plots: Franz Gross *et al.*, *50 Years of Quantum Chromodynamics*

# Neutron Rosenbluth Slope Measurement Checklist

1. High intensity electron beam.
2. Source of protons and neutrons.
3. Simultaneous detection of scattered electron and scattered nucleon.
4. Two separate neutron-to-proton cross-section ratio measurements at the same  $Q^2$  with different values of epsilon.

# Super BigBite Spectrometer (SBS) Apparatus in Hall A

- Liquid Deuterium target - source for protons and neutrons
- BigBite Spectrometer – electron arm
- SBS Magnet + HCal – hadron arm



# SBS nTPE and GMn experiments

- neutron Two-Photon Exchange (nTPE) Goal: First measurement of the neutron Rosenbluth slope, extract the neutron electromagnetic form factor ratio. Seeks to quantify TPE effects.
- GMn Goal: Precision measurement of neutron magnetic form factor at high  $Q^2$ .
- GMn and nTPE took data from October 2021 to February 2022.
- SBS-8 and SBS-9 are kinematics for nTPE.

SBS Config.	$Q^2$ (GeV/c) <sup>2</sup>	$\epsilon$	$E_{\text{beam}}$ (GeV)	$\theta_{e'}$ (deg)	$\theta_N$ (deg)	HCal distance (m)	Electron p (GeV)	Nucleon p (GeV)
SBS-4	3.0	0.72	3.728	36.0	31.9	11.0	2.12	2.4
SBS-7	9.8	0.50	7.906	40.0	16.0	14.0	2.66	6.1
SBS-11	13.5	0.41	9.86	42.0	13.3	14.5	2.67	8.1
SBS-14	7.4	0.46	5.965	46.5	17.3	14.0	2.00	4.81
SBS-8	4.5	0.80	5.965	26.5	29.4	11.0	3.58	3.2
SBS-9	4.5	0.51	4.015	49.0	22.0	11.0	1.6	3.2

# The Ratio Method

## Measured Observable:

- Simultaneous measurement of both  $D(e, e'n)$  and  $D(e, e'p)$  reactions for quasi-elastic electron-deuteron scattering.
- Cross-section ratio cancels many systematic effects

$$R = \frac{\left(\frac{d\sigma}{d\Omega}\right)\Big|_{D(e,e'n)}}{\left(\frac{d\sigma}{d\Omega}\right)\Big|_{D(e,e'p)}} = \frac{\left(\frac{d\sigma}{d\Omega}\right)\Big|_{n(e,e')}}{\left(\frac{d\sigma}{d\Omega}\right)\Big|_{p(e,e')}} \cdot f_{nuc} f_{RC} f_{det}$$

## Corrections for Effects:

$$R' = \frac{\left(\frac{d\sigma}{d\Omega}\right)\Big|_{n(e,e')}}{\left(\frac{d\sigma}{d\Omega}\right)\Big|_{p(e,e')}} = R \cdot f_{nuc}^{-1} f_{RC}^{-1} f_{Det}^{-1} = \frac{\frac{\tau\sigma_{Mott}}{\epsilon(1+\tau)} \left(\frac{\epsilon}{\tau} (G_E^n)^2 + (G_M^n)^2\right)}{\left(\frac{d\sigma}{d\Omega}\right)\Big|_{p(e,e')}}}$$

# Neutron Rosenbluth Slope Technique

**Goal:** Extract neutron Rosenbluth Slope,  $S^n = (G_E^n)^2 / \tau_n (G_M^n)^2$

- Consider 2 kinematics with same  $Q^2$ -value and with different values of  $\epsilon$ .
- Consider 2 elastic neutron-to-proton cross-section ratios as described from the Ratio Method.

**Physics Result:**

- Consider ‘super-ratio’ of  $R'$  for two different values of  $\epsilon$ .
- Define  $S^{n(p)} = (G_E^{n(p)})^2 / \tau_{n(p)} (G_M^{n(p)})^2$  and  $\Delta\epsilon = \epsilon_{1,n} - \epsilon_{2,n}$ .

Physics  
Result!

$$S^n = \frac{\left( \frac{R'_{\epsilon_1}}{R'_{\epsilon_2}} - B \right)}{\Delta\epsilon \cdot B} \simeq \frac{(G_E^n)^2}{\tau_n (G_M^n)^2}$$

From Data  
Extraction

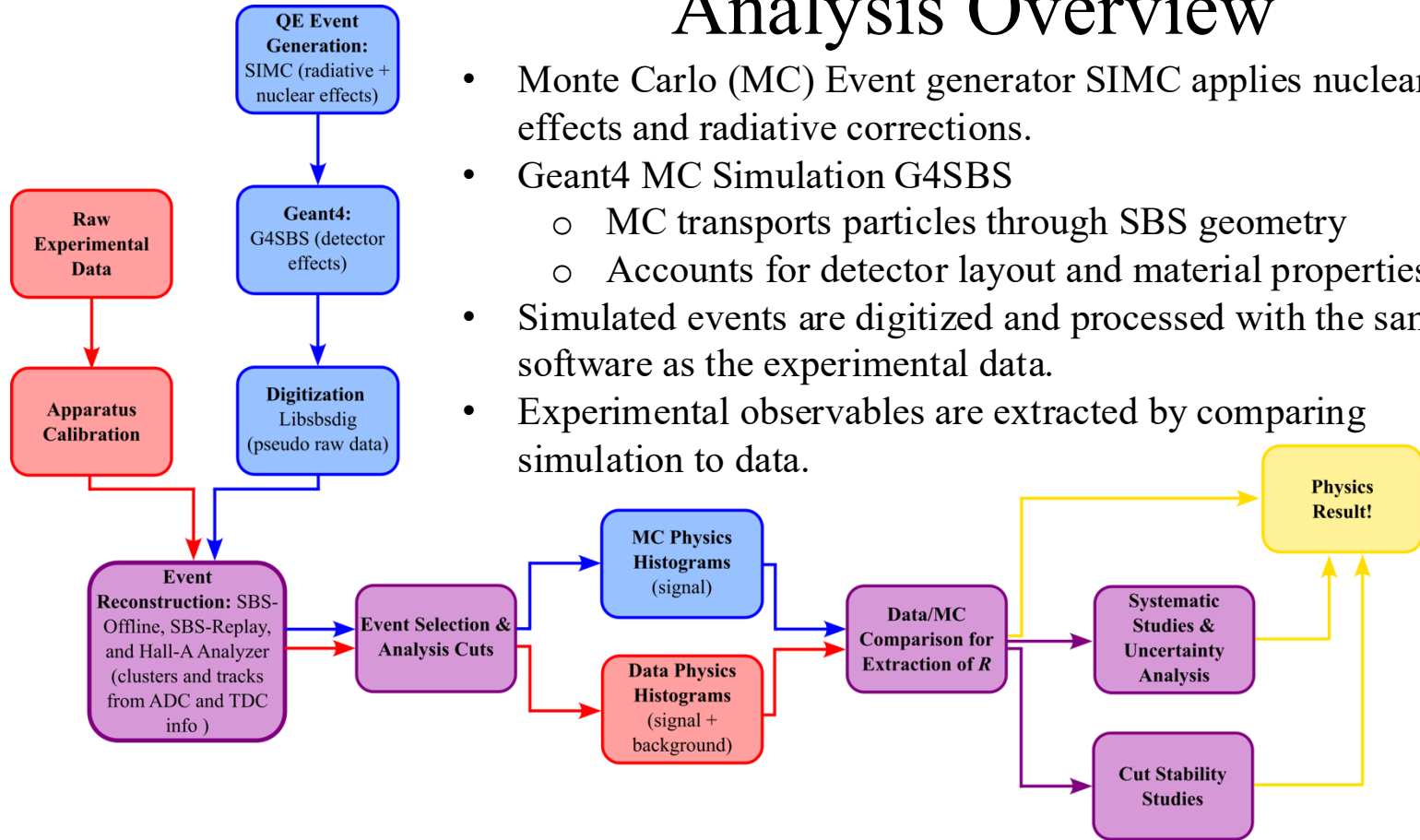
From Kinematic Information

$$B = \frac{\frac{\tau_{\epsilon_{1,n}}}{\epsilon_{1,n}(1 + \tau_{\epsilon_{1,n}})} \frac{\tau_{\epsilon_{2,p}}}{\epsilon_{2,p}(1 + \tau_{\epsilon_{2,p}})}}{\frac{\tau_{\epsilon_{1,p}}}{\epsilon_{1,p}(1 + \tau_{\epsilon_{1,p}})} \frac{\tau_{\epsilon_{2,n}}}{\epsilon_{2,n}(1 + \tau_{\epsilon_{2,n}})}} \frac{(G_M^n)_{\epsilon_1}^2 (G_M^p)_{\epsilon_2}^2}{(G_M^p)_{\epsilon_1}^2 (G_M^n)_{\epsilon_2}^2} \frac{1 + \epsilon_{2,p} S_{\epsilon_2}^p}{1 + \epsilon_{1,p} S_{\epsilon_1}^p}$$

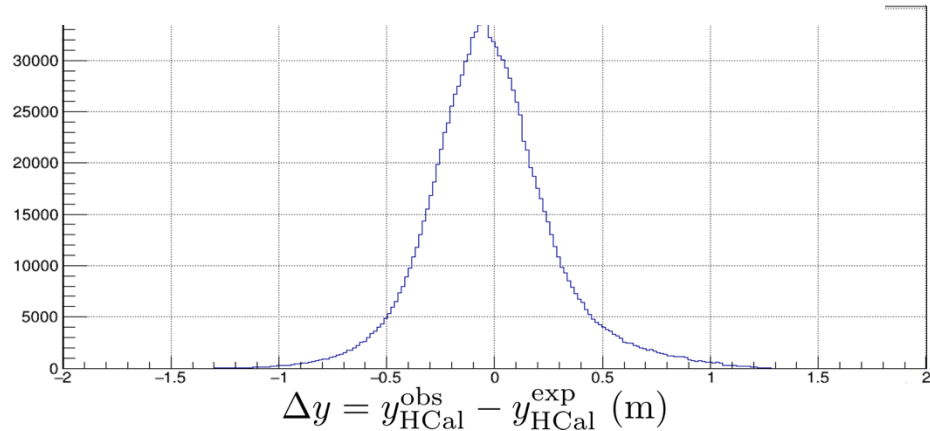
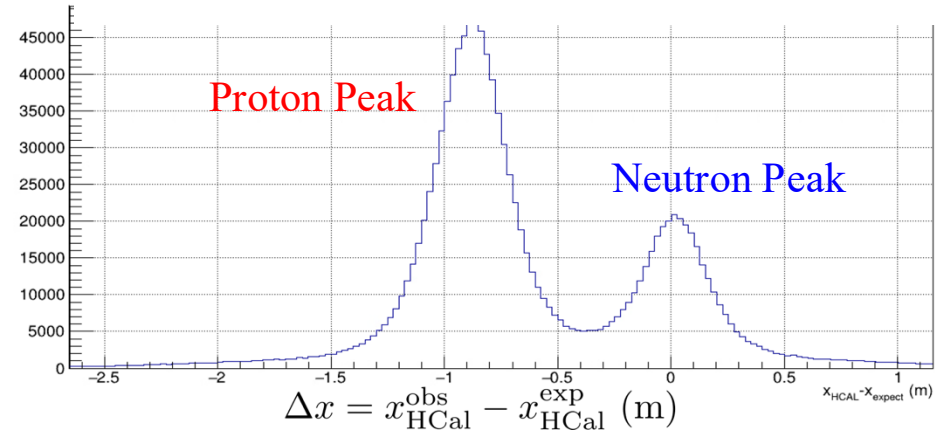
From Global  
Form Factor  
Analysis.

# Analysis Overview

- Monte Carlo (MC) Event generator SIMC applies nuclear effects and radiative corrections.
- Geant4 MC Simulation G4SBS
  - MC transports particles through SBS geometry
  - Accounts for detector layout and material properties
- Simulated events are digitized and processed with the same software as the experimental data.
- Experimental observables are extracted by comparing simulation to data.



# Analysis Methods – Introducing HCal $\Delta x$ and $\Delta y$

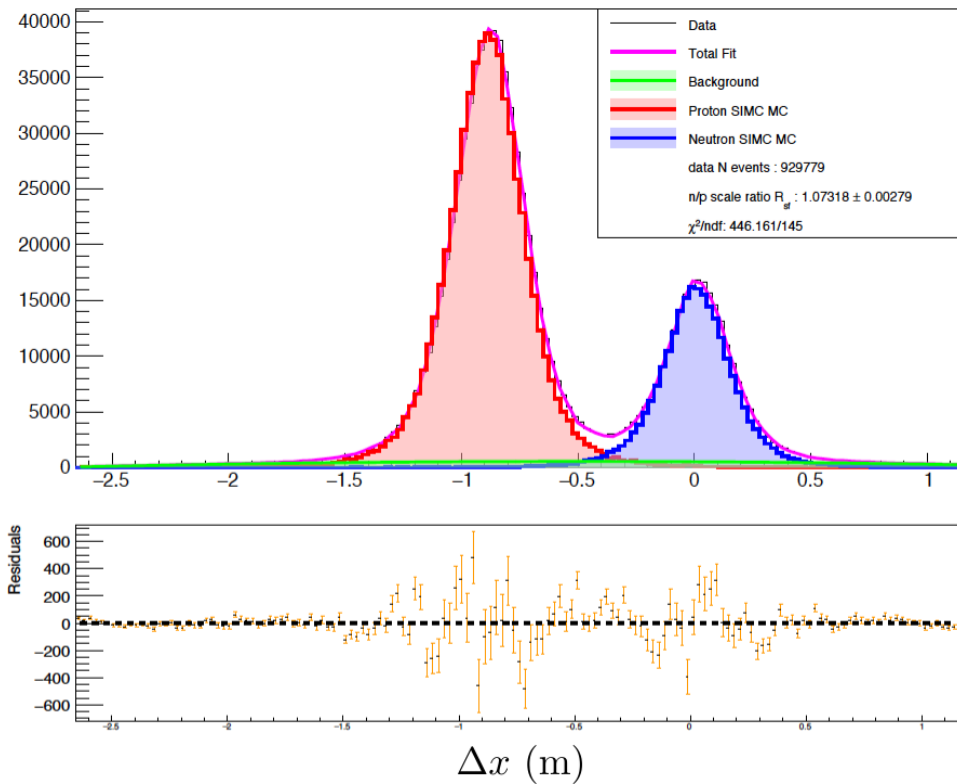


$$Q^2 = 4.5 \text{ (GeV/c)}^2$$

- **Goal:** Separate **protons** and **neutrons** in HCal that came from quasi-elastic scattering events.
- **Reconstruct** the four-vector of  $e'$  using data from the electron arm.

- Calculate the four-vector for a **neutron** that underwent quasi-elastic scattering with  $e'$  and **project** to HCal.
- Plot the **difference** between the **observed** event in HCal and the projected **expected** location.

# $Q^2 = 4.5 \text{ (GeV/c)}^2$ Data-Monte Carlo Comparison



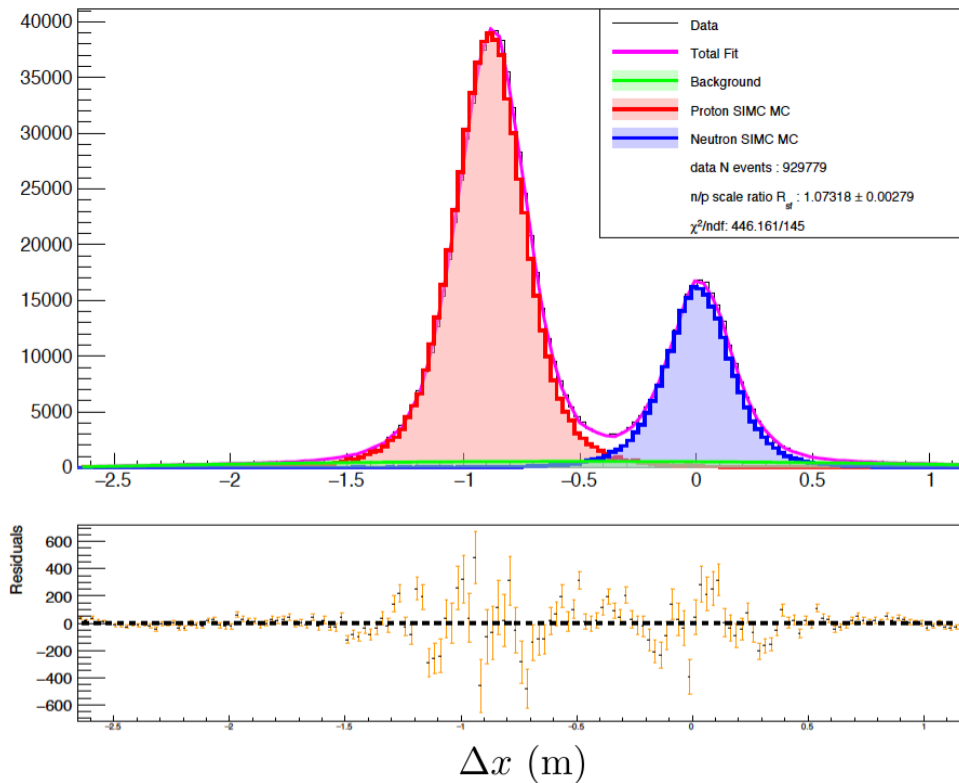
- Fit Equation:

$$f_{total}(x_i) = f_{sf}^p \left( R_{sf}^{n/p} h^n(x_i - \delta_n) + h^p(x_i - \delta_p) \right) + f_{bkgd}(x_i)$$

- Fit Parameters:

- $f_{sf}^p$  - proton scale factor
- $R_{sf}^{n/p}$  - ratio of neutron to proton scale factors
- $\delta_{n(p)}$  - neutron (proton) centroid shift parameters
- $f_{bkgd}$  - parameters associated with the background

# $Q^2 = 4.5 \text{ (GeV/c)}^2$ Data-Monte Carlo Comparison

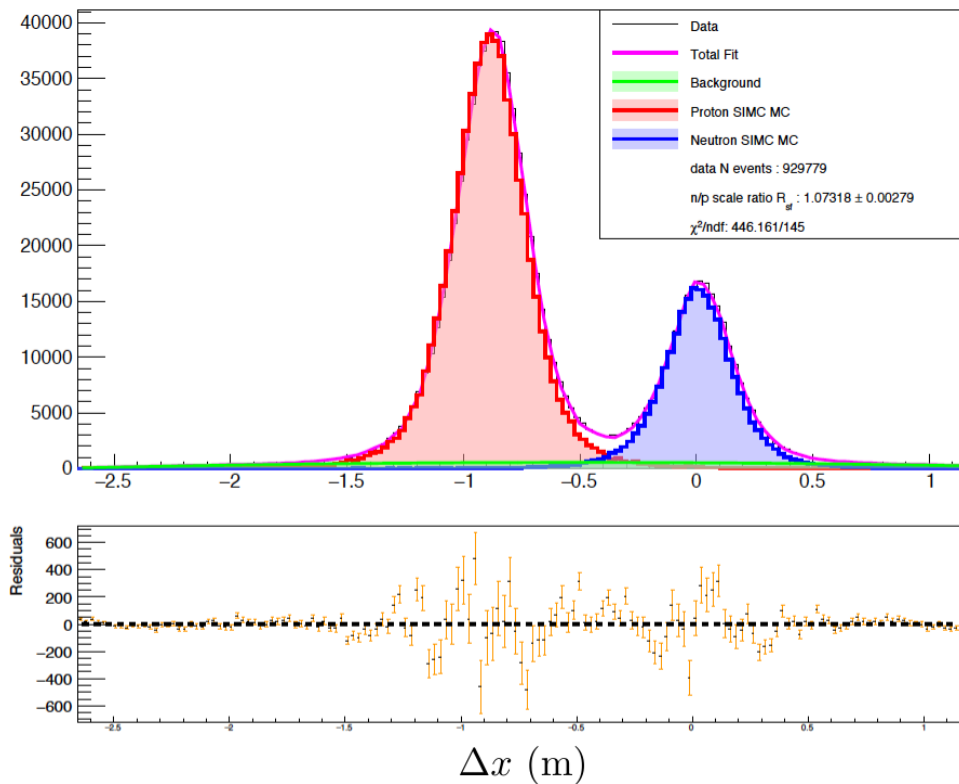


Simulation:

- $D(e, e' n)$  and  $D(e, e' p)$  simulated events realistically account for nuclear, radiative, and detector effects that are present in data.
- Calculate the neutron to proton cross-section ratio identically to the MC

$$\begin{aligned}
 R'_{sim} &= \frac{\left(\frac{d\sigma}{d\Omega}\right)\bigg|_{n(e,e'),sim}}{\left(\frac{d\sigma}{d\Omega}\right)\bigg|_{p(e,e'),sim}} \\
 &= R_{sim} \cdot f_{nuc,sim}^{-1} f_{RC,sim}^{-1} f_{Det,sim}^{-1}
 \end{aligned}$$

# $Q^2 = 4.5 \text{ (GeV/c)}^2$ Data-Monte Carlo Comparison



Extraction:

$$R = R' \cdot f_{nuc} f_{RC} f_{det}$$

$$= R_{sf}^{n/p} \cdot R'_{sim} \cdot f_{nuc,sim} f_{RC,sim} f_{det,sim}$$

Claim:

- Simulation consistently replicates nuclear, radiative, and detector effects that are present in the experimental data.

Implication:

$$\frac{f_{nuc}}{f_{nuc,sim}} \sim 1 \quad \frac{f_{RC}}{f_{RC,sim}} \sim 1 \quad \frac{f_{det}}{f_{det,sim}} \sim 1$$

$$R' = \frac{\left(\frac{d\sigma}{d\Omega}\right)\Big|_{n(e,e')}}{\left(\frac{d\sigma}{d\Omega}\right)\Big|_{p(e,e')}} = R_{sf}^{n/p} \cdot R'_{sim}$$

# Event Selection Criteria

## Good Electron Cuts

### 1. Track Quality

- No. of GEM Layers with Hits
- Track  $\chi^2/ndf$
- Vertex Z position
- BigBite Optics Validity

### 2. PID

- Preshower Energy
- $E_{BBCal}/p$

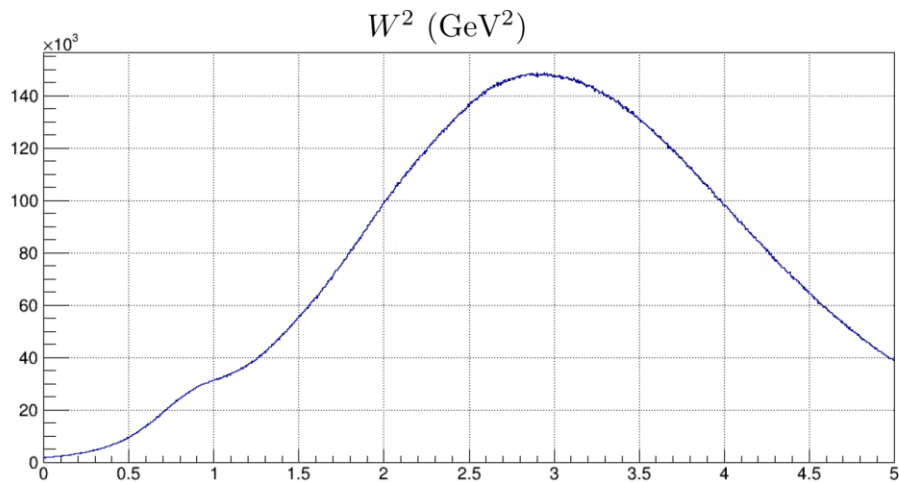
## Quasi-Elastic Event Cuts

- HCal Cluster Energy
- Coincidence Time
- $W^2$
- $\Delta y$
- Fiducial

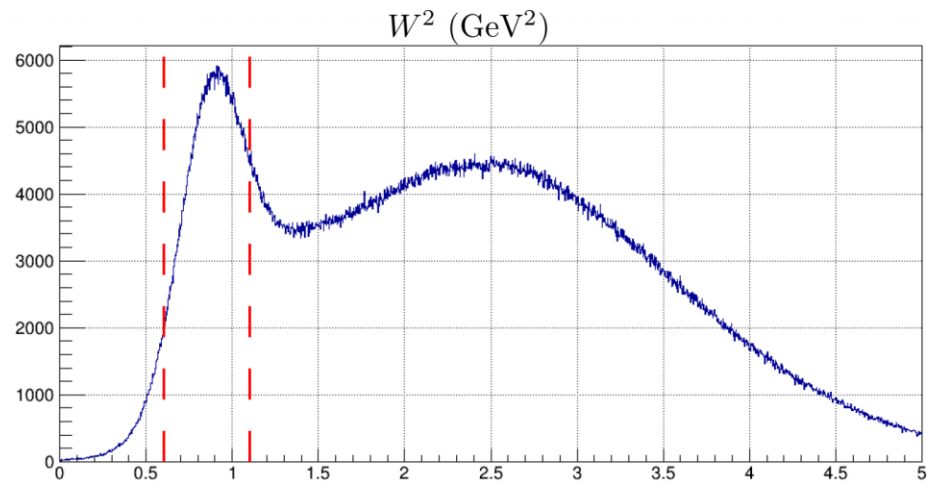
- Cut regions were optimized
- Systematic effects on  $R_{sf}^{n/p}$  due to cut sensitivity were quantified
- Will be reevaluated with pass 3 data and MC files

# $Q^2 = 4.5 \text{ (GeV/c)}^2$ Invariant Mass Squared ( $W^2$ )

No Cuts Applied

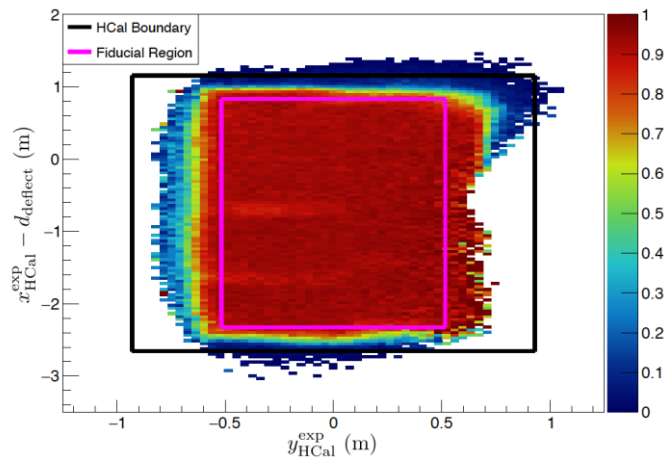
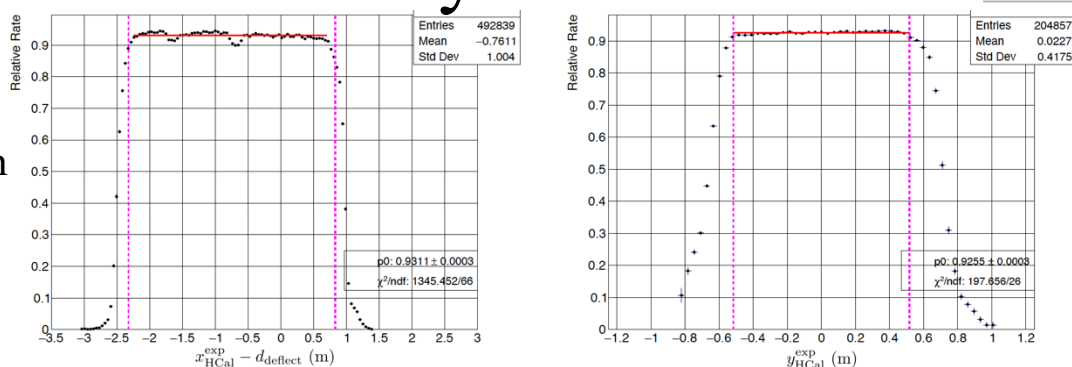


All Other Cuts Applied



# HCal Non-Uniformity in Real Data

- Liquid Hydrogen data
- Clear non-uniformities (dips) in the x-direction
- Highly-likely caused by issues with HCal hardware
- Position-dependent non-uniformities in HCal nucleon detection efficiency could introduce bias to  $R_{sf}^{n/p}$  extractions.
- Will be reevaluated with pass 3 data and MC files

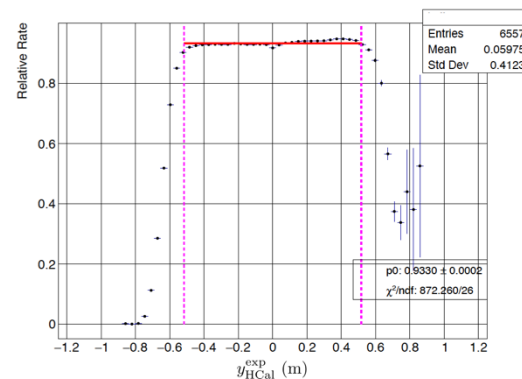
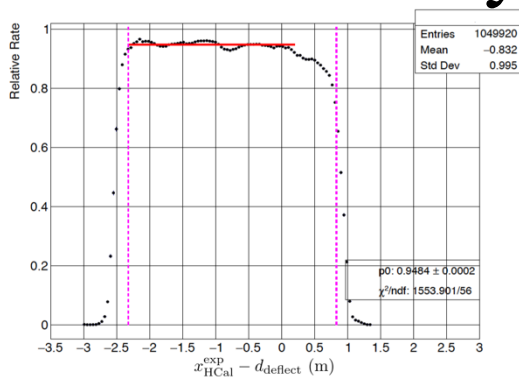


SBS-8,  $Q^2 = 4.5 \text{ (GeV/c)}^2$

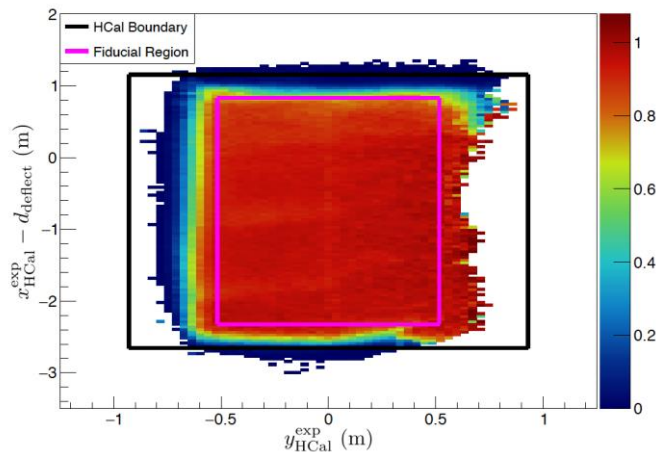
# Position-Dependent Efficiency Correction to MC

- Reweight MC events based on data map
- Treat proton and neutron MC events equally
- Relative efficiency correction factor

$$c(x, y) = \frac{\epsilon_{\text{HCal}}^{\text{data}}(x, y)}{\langle \epsilon_{\text{HCal}}^{\text{data}} \rangle}$$



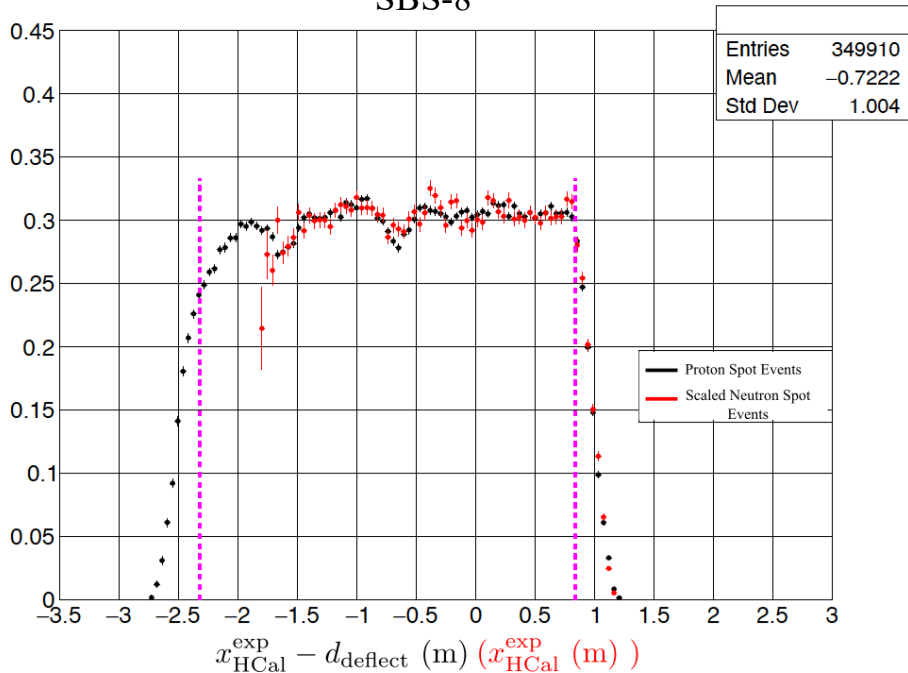
- $\epsilon_{\text{HCal}}^{\text{data}}(x, y)$  is the interpolated position-dependent efficiency value
- $\langle \epsilon_{\text{HCal}}^{\text{data}} \rangle$  is the acceptance-averaged value
- Comparisons of  $\Delta x$  between uncorrected and corrected MC events were used to quantify systematic effects on  $R_{sf}^{n/p}$
- Will be reevaluated with pass 3 data and MC files



SBS-8,  $Q^2 = 4.5 \text{ (GeV/c)}^2$

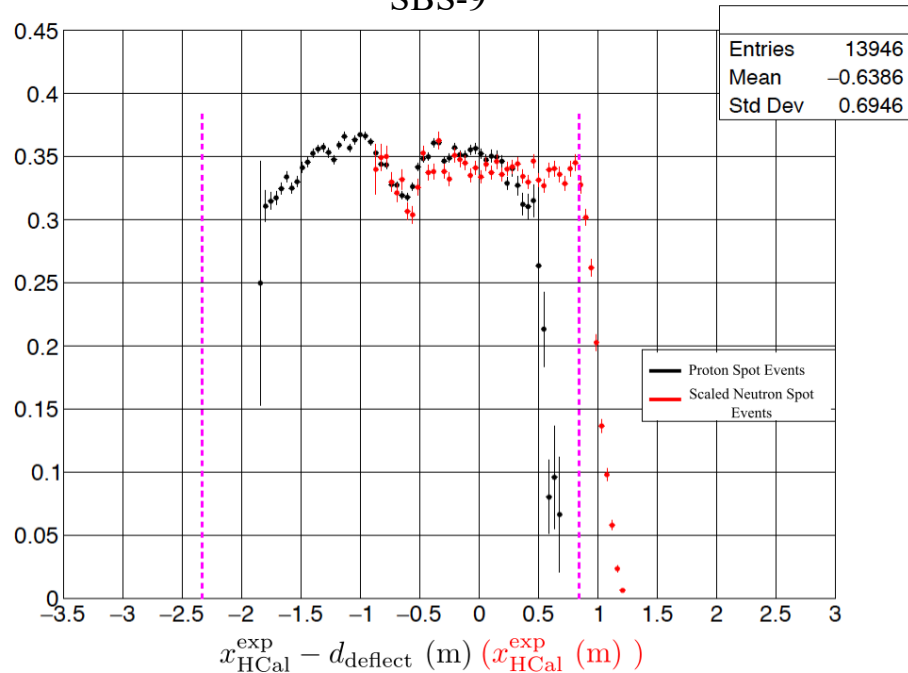
# Proton and Neutron Relative-Rate Comparisons

SBS-8



Proton Spot Events

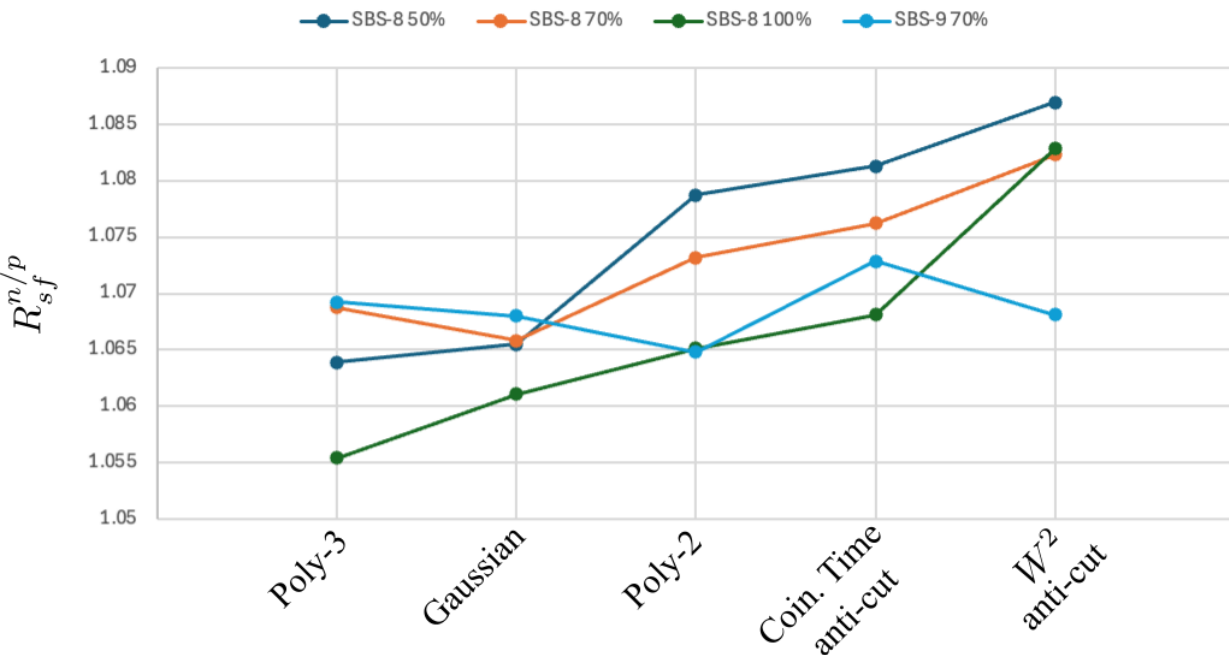
SBS-9



Neutron Spot Events

# Inelastic Background

$R_{sf}^{n/p}$  vs. Functional Form



- Five different functional forms for the background
- The 3 parameterizations provide smooth forms for the background shape
- The 2 anti-cuts are data motivated and attempt to capture events corresponding to background
- Systematic effects on  $R_{sf}^{n/p}$  due to background shape were quantified
- Should incorporate inelastic MC generator with out-of-time events, similar to GMn analysis
- Will be reevaluated with pass 3 data and MC files

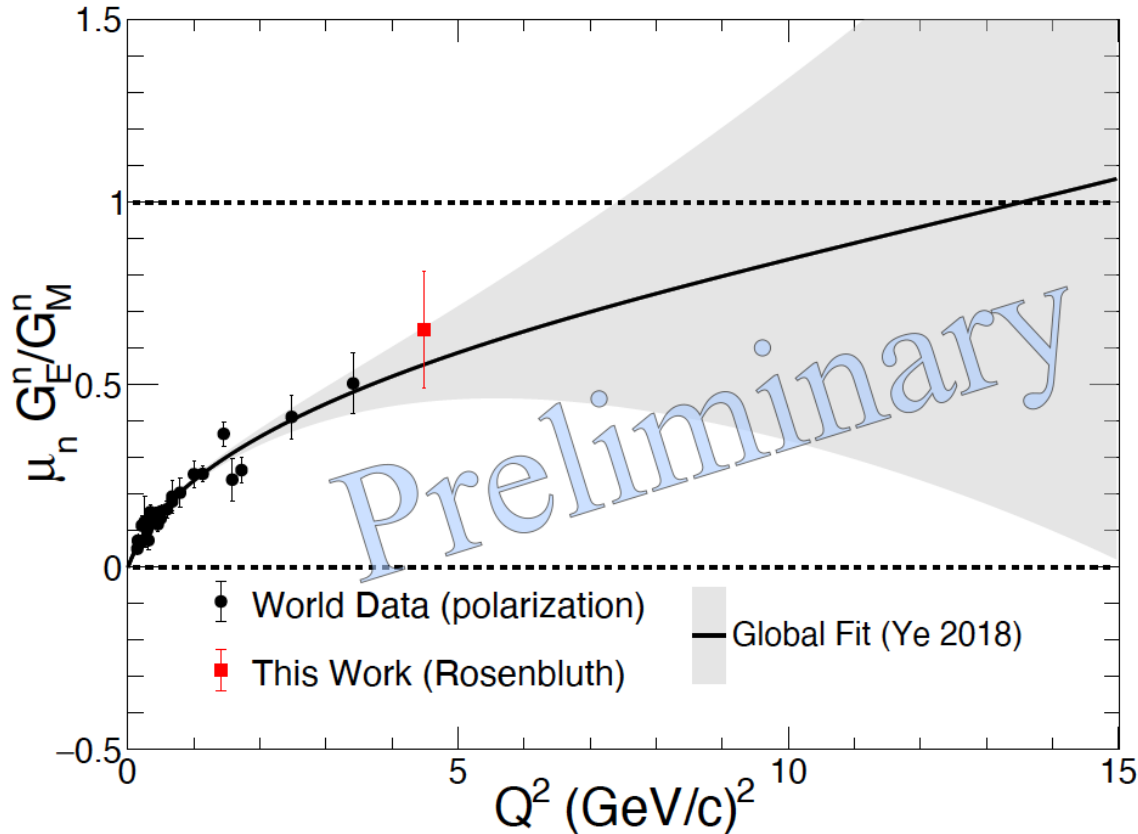
# Neutron Rosenbluth Slope Preliminary Result

$R'_{\epsilon_1}$  is SBS-8 (Weighted Mean),  $R'_{\epsilon_2}$  is SBS-9

For  $Q^2 = 4.48 \text{ (GeV/c)}^2$

Quantity	Value	Uncertainty	Uncertainty (%)
$R'_{\epsilon_1}$	0.3908	0.0038	0.97%
$R'_{\epsilon_2}$	0.3875	0.0032	0.83%
Quantity	Value	Uncertainty	Uncertainty (%)
$\frac{R'_{\epsilon_1}}{R'_{\epsilon_2}}$	1.0085	0.0129	1.28%
$B$	0.98315	0.00281	0.286%
$\Delta\epsilon$	0.281		
$S^n = \frac{\left(\frac{R'_{\epsilon_1}}{R'_{\epsilon_2}} - B\right)}{\Delta\epsilon \cdot B}$	0.0916	0.0476	52%

# Neutron Form Factor Ratio Preliminary Result



For  $Q^2 = 4.48 \text{ (GeV/c)}^2$

$$\begin{aligned}\mu_n \frac{G_E^n}{G_M^n} &\approx \mu_n \sqrt{S^n \tau_n} \\ &= 0.652 \pm 0.160\end{aligned}$$

- Does not account for TPE effects

Conclusions:

- $S^n$  result is consistent with the extrapolation of the global parameterization.
- $S^n$  result suggests an absence of large TPE corrections for the neutron
- $S^n$  result is not precise enough to experimentally expose neutron TPE effects

# Summary

- Nucleon Structure & Electromagnetic Form Factors
- SBS nTPE experiment and observable extraction
- Overview of Data Analysis Methods
- Physics Extraction from Data/MC Comparison
- Preliminary neutron Rosenbluth Slope result

# Outlook

## Remaining Tasks

- Potentially improve Radiative Correction models in MC
- Quantifying systematic effects due to Radiative Corrections for nTPE results: (Implemented for GMn Analysis by P. Datta)
- Updated (Pass-3) data and MC files with improved detector calibrations are available or available soon
- Study effects due to final-state interactions
- Quantify effects due to absolute HCal nucleon detection efficiency
- Reevaluate Inelastic Background systematic uncertainty with improved method (MC Inelastic and Out-Of-Time): (Implemented for GMn Analysis by P. Datta)
- Reevaluate systematic uncertainty associated with Event Selection Cuts

# Thank You!

Special thanks:

PhD advisor: David Armstrong. SBS graduate students John Boyd, Provakar Datta, Anu Rathnayake, Sebastian Seeds, Maria Satnik, Ralph Marinaro, Nathaniel Lashley, Sean Jeffas, Hunter Presley. Hall A/C Staff Arun Tadepalli, Bogdan Wojtkehowski, Jack Segal, Mark Jones, Jessie Butler, Dave Mack. W&M Folks: Todd Averett, Kate Evans, Jack Jackson, Eric Fuchey. GEM Folks: Nilanga Liyanage, Kondo Gnanvo, Holly Szumila-Vance, Evaristo Cisbani, Roberto Perrino. Andrew Puckett. GMn/nTPE Analysis Working Groups. The SBS Collaboration. NSF for supporting this work.

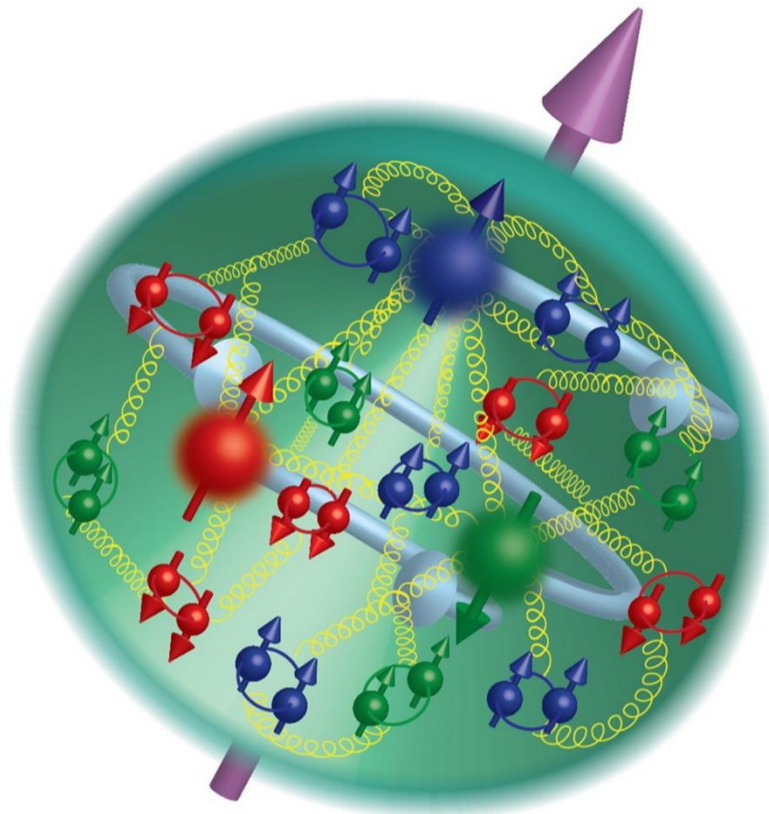


GEM Folks, February 2022. Left to right: Holly Szumila-Vance, Anu Rathnayake, Zeke Wertz, Kondo Gnanvo, Thir Gautam, Sean Jeffas, John Boyd.



DNP Hawaii, November 2023. Left to right: John Boyd, Vimukthi Gamage, Eric Fuchey, Provakar Datta, Zeke Wertz, Sean Jeffas, Hunter Presley, Anu Rathnayake, Sebastian Seeds, Maria Satnik, Andrew Puckett.

# Backup



# Super-Ratio A

	Kine	$\langle Q^2 \rangle$ (GeV/c) <sup>2</sup>	$\langle \epsilon \rangle$	$R'$	$\Delta(R')_{\text{total}}$
$R'_{\epsilon_1}$	SBS-8	4.48	0.799	0.3908	0.0038
$R'_{\epsilon_2}$	SBS-9	4.476	0.518	0.3875	0.0032

$$A \equiv \frac{R'_{\epsilon_1}}{R'_{\epsilon_2}}$$

$$\Delta A = |A| \sqrt{\left(\frac{\Delta(R'_{\epsilon_1})}{R'_{\epsilon_1}}\right)^2 + \left(\frac{\Delta(R'_{\epsilon_2})}{R'_{\epsilon_2}}\right)^2}.$$

$$A = 1.0085 \pm 0.0129.$$

# B term

Quantity	Value	Total Uncertainty
$\frac{\frac{\tau_{n,\epsilon_1}}{\epsilon_{1,n}(1+\tau_{n,\epsilon_1})}}{\frac{\tau_{p,\epsilon_1}}{\epsilon_{1,p}(1+\tau_{p,\epsilon_1})}} \frac{\frac{\tau_{p,\epsilon_2}}{\epsilon_{2,p}(1+\tau_{p,\epsilon_2})}}{\frac{\tau_{n,\epsilon_2}}{\epsilon_{2,n}(1+\tau_{n,\epsilon_2})}}$	1.00044	—
$\frac{\frac{\sigma_{T,\epsilon_1}^n}{\sigma_{T,\epsilon_1}^p}}{\frac{\sigma_{T,\epsilon_2}^p}{\sigma_{T,\epsilon_2}^n}}$	0.99927	0.00017
$\frac{1+\epsilon_{2,p}S_{\epsilon_2}^p}{1+\epsilon_{1,p}S_{\epsilon_1}^p}$	0.98344	0.0028
<i>B</i>	0.98315	0.00281

- Transverse cross-section term is based on Ye et al. 2018 article
  - Proton Rosenbluth Slope term is based on Christ et al. 2022 article
1. [Z. Ye, J. Arrington, R. J. Hill, and G. Lee, Proton and neutron electromagnetic formfactors and uncertainties, Physics Letters B 777, 8 \(2018\).](#)
  2. [M. E. Christy et al., Form Factors and Two-Photon Exchange in High-Energy Elastic Electron-Proton Scattering, Phys. Rev. Lett. 128, 102002 \(2022\).](#)

# Determination Proton Rosenbluth Slope for $B$

$S_{\epsilon_1/\epsilon_2}^p$  is determined from Christy et al. (2022) article and supplemental material, which provides most recent parameterization for RS from only e-p cross-section data.

$$RS = 1 + c_1\tau + c_2\tau^2, \text{ where } c_1 = -0.456299 \pm 0.124409, c_2 = 0.121065 \pm 0.10032, \text{ and } \tau = Q^2/4M_p^2$$

$$\Delta RS = \sqrt{\left(\frac{\partial RS}{\partial c_1} \Delta c_1\right)^2 + \left(\frac{\partial RS}{\partial c_2} \Delta c_2\right)^2 + 2 \frac{\partial RS}{\partial c_1} \frac{\partial RS}{\partial c_2} \text{cov}(c_1, c_2)}$$

$$\frac{\partial RS}{\partial c_1} = \tau, \frac{\partial RS}{\partial c_2} = \tau^2, \text{cov}(c_1, c_2) = -0.778 \Delta c_1 \Delta c_2$$

	Value	Uncertainty	Uncertainty (%)
$RS_{\epsilon_1}$ $= \frac{(\mu_p G_E^p)^2}{(G_M^p)^2}$	0.6151	0.10722	17.4%
$S_{\epsilon_1}^p$ $= \frac{(G_E^p)^2}{\tau_{p,\epsilon_1} (G_M^p)^2}$	0.06186	0.01078	17.4%

	Value	Uncertainty	Uncertainty (%)
$RS_{\epsilon_2}$ $= \frac{(\mu_p G_E^p)^2}{(G_M^p)^2}$	0.6156	0.10674	17.3%
$S_{\epsilon_2}^p$ $= \frac{(G_E^p)^2}{\tau_{p,\epsilon_2} (G_M^p)^2}$	0.06191	0.01074	17.3%

# Neutron Rosenbluth Slope Uncertainty

$$S^n = \frac{(A - B)}{B\Delta\epsilon_n}$$

$$\Delta S^n = \sqrt{\left(\frac{\partial S^n}{\partial A} \Delta A\right)^2 + \left(\frac{\partial S^n}{\partial B} \Delta B\right)^2}$$

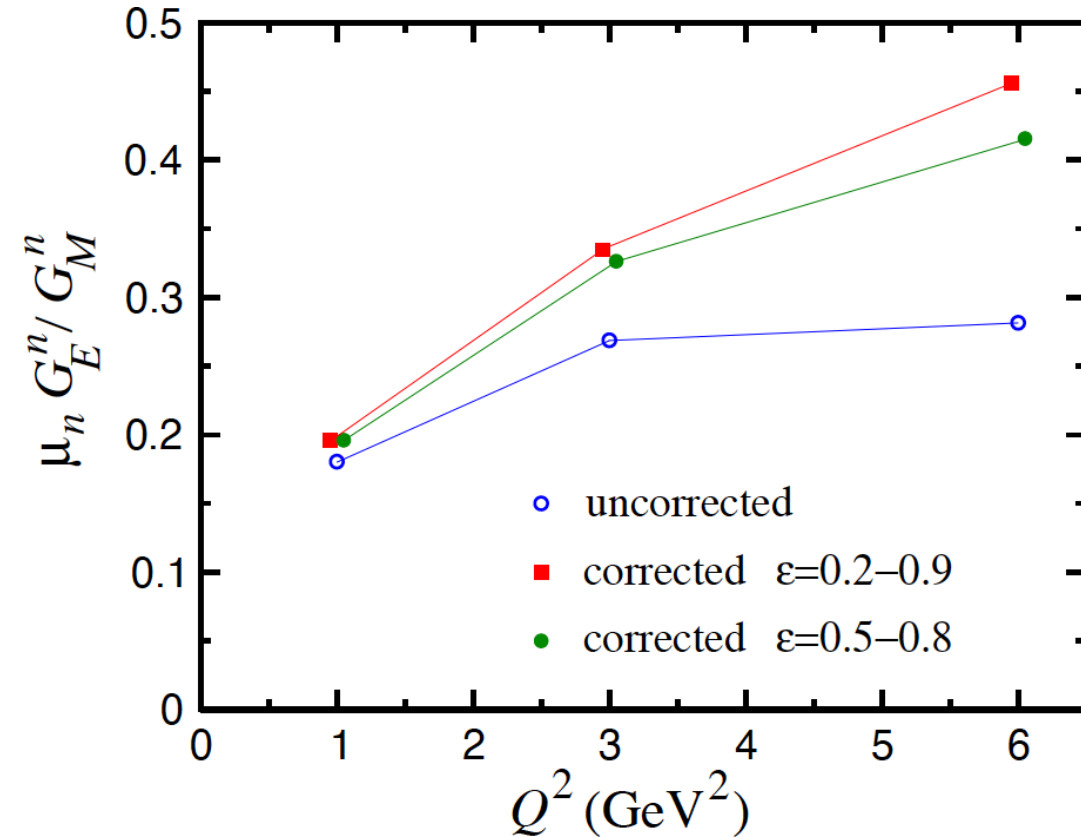
$$\Delta S^n = \sqrt{\left(\frac{1}{B\Delta\epsilon_n} \Delta A\right)^2 + \left(\frac{-A}{B^2\Delta\epsilon_n} \Delta B\right)^2}$$

# Neutron Rosenbluth Slope Preliminary Result

Quantity	Uncertainty Value	Percentage
$\Delta (S^n)_{\text{Exp}}$	0.0465	50.8%
$\Delta (S^n)_{\text{Param}}$	0.0104	11.4%
$\Delta (S^n)_{\text{Total}}$	0.0476	52%

Quantity	Uncertainty Value	Percentage
$\Delta (S^n)_{\text{Stat}}$	0.0144	15.8%
$\Delta (S^n)_{\text{HCDENU}}$	0.0182	19.9%
$\Delta (S^n)_{\text{Cut}}$	0.0227	24.8%
$\Delta (S^n)_{\text{Ine}}$	0.0317	34.7%
$\Delta (S^n)_{\text{Exp}}$	0.0465	50.8%

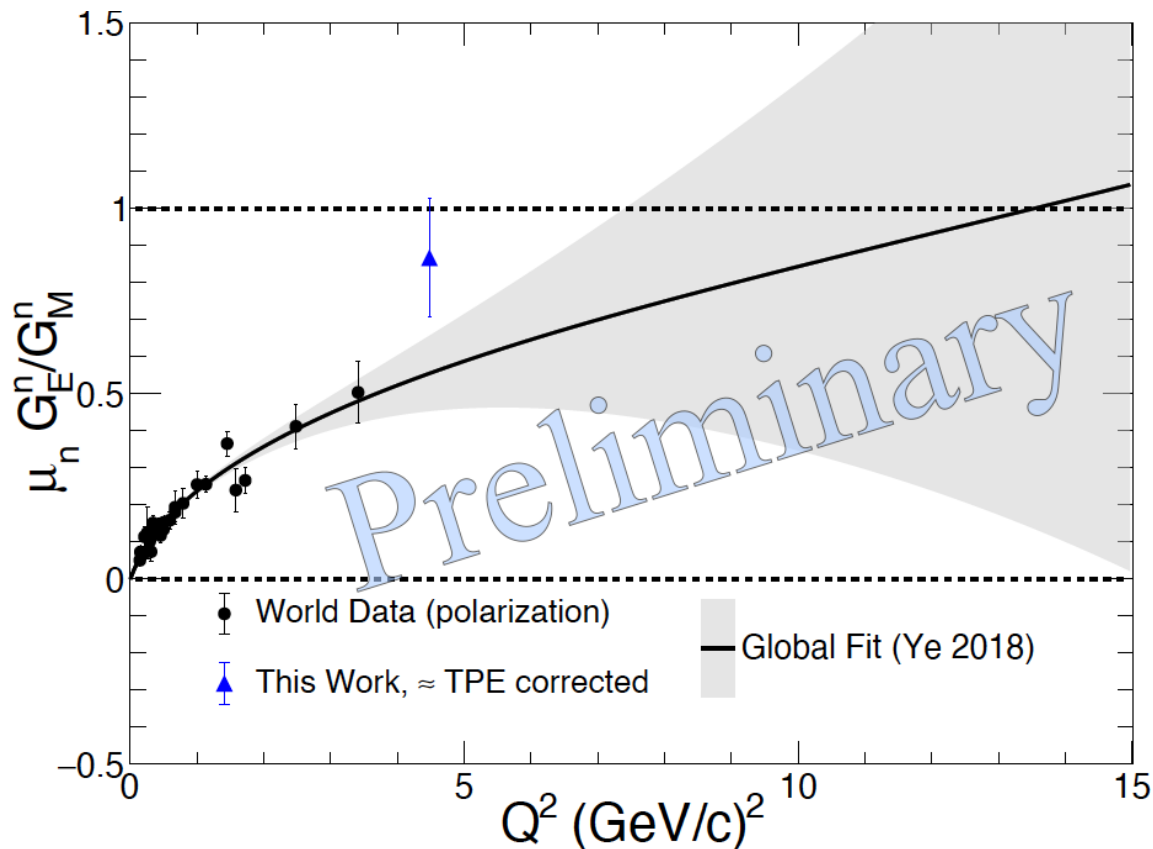
# Neutron TPE from Theory



- Calculates TPE contributions to the unpolarized cross-section by computing scattering amplitude for TPE diagrams.
- For  $Q^2 = 4.5$  (GeV/c)<sup>2</sup>, TPE correcting a Rosenbluth measurement could increase the neutron form factor ratio by 30%

Ref: P. Blunden *et al*, *Two-photon exchange in elastic electron nucleon scattering*

# Neutron Form Factor Ratio Preliminary Result



For  $Q^2 = 4.48 \text{ (GeV/c)}^2$

- Approximately TPE corrected based on Blunden et. al.

$$\mu_n \frac{G_E^n}{G_M^n} + TPE \approx 0.867 \pm 0.160$$

# Neutron TPE from Theory Expanded

$$\delta^{2\gamma} \rightarrow \frac{2\text{Re} \{ \mathcal{M}_0^\dagger \mathcal{M}^{2\gamma} \}}{|\mathcal{M}_0|^2} .$$

TPE modification to the CS. Here  $M_0$  and  $M_{2\gamma}$  are OPE and TPE amplitudes

$$\mathcal{M}^{2\gamma} = e^4 \int \frac{d^4k}{(2\pi)^4} \frac{N_{\text{box}}(k)}{D_{\text{box}}(k)} + e^4 \int \frac{d^4k}{(2\pi)^4} \frac{N_{x\text{-box}}(k)}{D_{x\text{-box}}(k)} .$$

Here  $N_{\text{box}}, N_{x\text{-box}}, D_{\text{box}}, D_{x\text{-box}}$  are matrix elements and propagators, respectively. For TPE diagrams on slide 7

- The TPE amplitude contains finite and IR divergent terms, as well as FFs at the  $\gamma NN$  vertices
- The finite terms can be computed analytically
- There are no IR divergent terms for the neutron

Ref: P. Blunden *et al*, *Two-photon exchange in elastic electron nucleon scattering*

# Neutron TPE from Theory Expanded

$$F_{1,2}(Q^2) = \sum_{i=1}^N \frac{n_i}{d_i + Q^2},$$

FF functional form taken from older world data parameterization available when article published

$$n_N = d_N(F_{1,2}(0) - \sum_{i=1}^{N-1} n_i/d_i).$$

$$F_1^p(0) = 1 \quad F_2^p(0) = \kappa_p$$

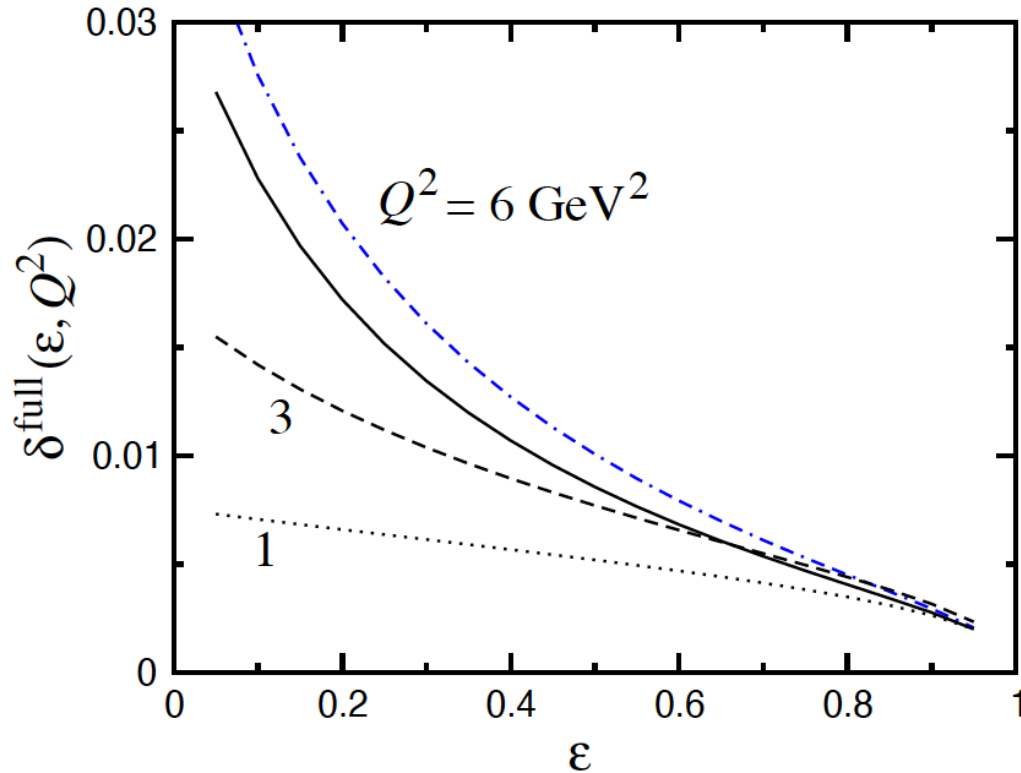
Normalization condition

$$F_1^n(0) = 0 \quad \text{and} \quad F_2^n(0) = \kappa_n$$

	$F_1^p$	$F_2^p$	$F_1^n$	$F_2^n$
$N$	3	3	3	2
$n_1$	0.38676	1.01650	24.8109	5.37640
$n_2$	0.53222	-19.0246	-99.8420	
$d_1$	3.29899	0.40886	1.98524	0.76533
$d_2$	0.45614	2.94311	1.72105	0.59289
$d_3$	3.32682	3.12550	1.64902	—

Ref: P. Blunden *et al*, *Two-photon exchange in elastic electron nucleon scattering*

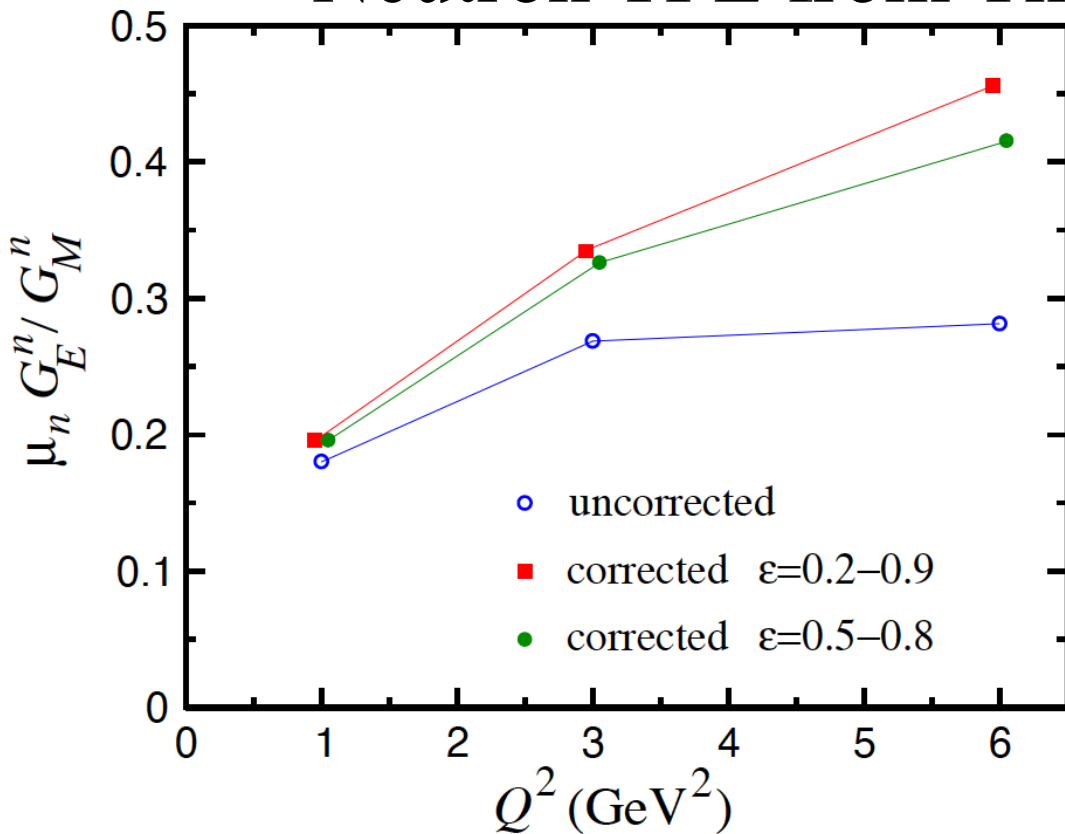
# Neutron TPE from Theory Expanded



- TPE contribution to the unpolarized electron-neutron elastic scattering cross-section
- The dot-dashed curve for  $Q^2 = 6 \text{ GeV}^2$  comes from a particular older world data parameterization
- The other curves come from a different older world data parameterization
- Magnitude of TPE contribution is approx. 3 times smaller than proton
- Sign change is due to negative neutron anomalous magnetic moment

Ref: P. Blunden *et al*, *Two-photon exchange in elastic electron nucleon scattering*

# Neutron TPE from Theory Expanded



- Accounting for the  $\epsilon$  dependence, the correction is applied to the cross-section, reduced cross-section, and then the FF ratio.
- For  $Q^2 = 4.5$  (GeV/c)<sup>2</sup>, TPE correcting a Rosenbluth measurement could increase the neutron form factor ratio by 30%

Ref: P. Blunden *et al*, *Two-photon exchange in elastic electron nucleon scattering*

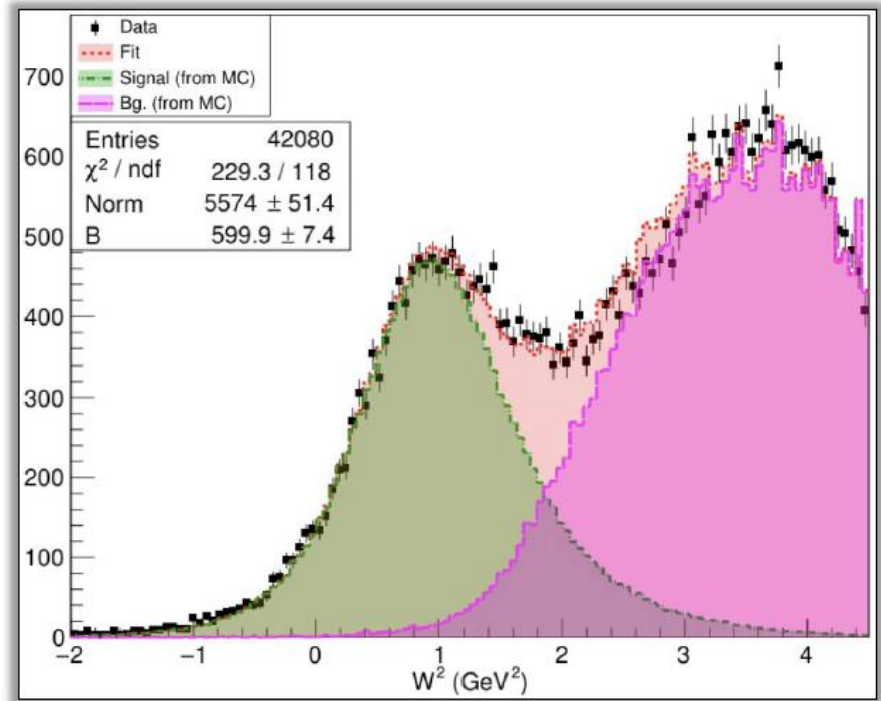
# Improved Inelastic Background Systematic

$Q^2 = 13.6 \text{ (GeV/c)}^2$

## Determination of Inelastic Background

- From MC  $W^2$  distributions of signal and MC inelastic generator events. Select events outside quasi-elastic peak
- Select out-of-time events
- Fit delta x distribution of selected background events
- Use background shape in Systematic uncertainty evaluation

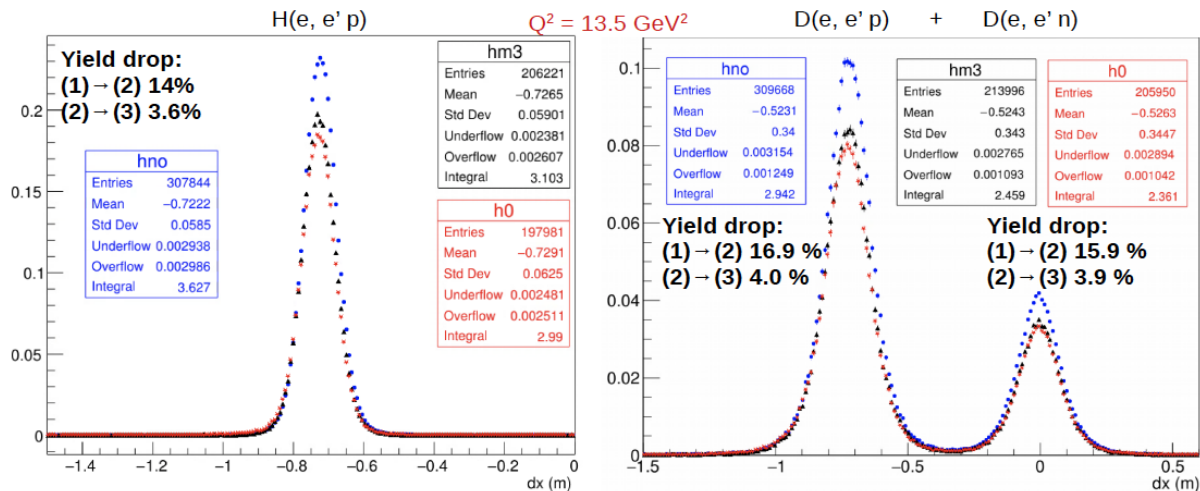
Analysis Credit and Ref: P. Datta APS 2025 Talk



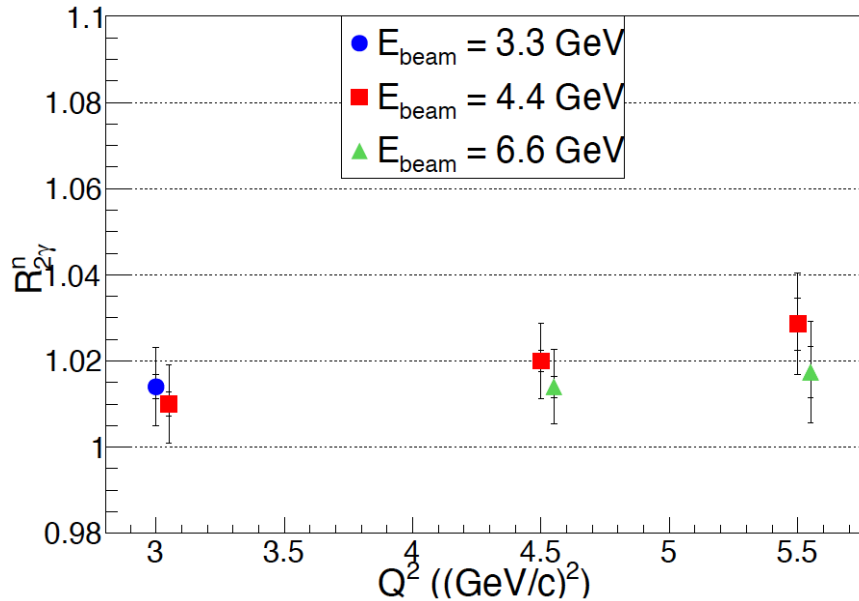
# Systematic: Radiative Corrections

- Radiative corrections (analysis credit: P. Datta, LBNL):
  - SIMC events with the following configurations for radiative effects:
    - ◆ (1) - No radiative corrections i.e. none of the tails are radiated
    - ◆ (2) - One tail = 0 => All (e, e', and p) tails are radiated
    - ◆ (3) - One tail = -3 => All but p tails are radiated
  - SIMC events processed through g4sbs → libsbsdig → SBS-offline;
  - Properly weighted Dx distribution for all types of events with the same selection
  - Extract individual yields and then quantify the correction

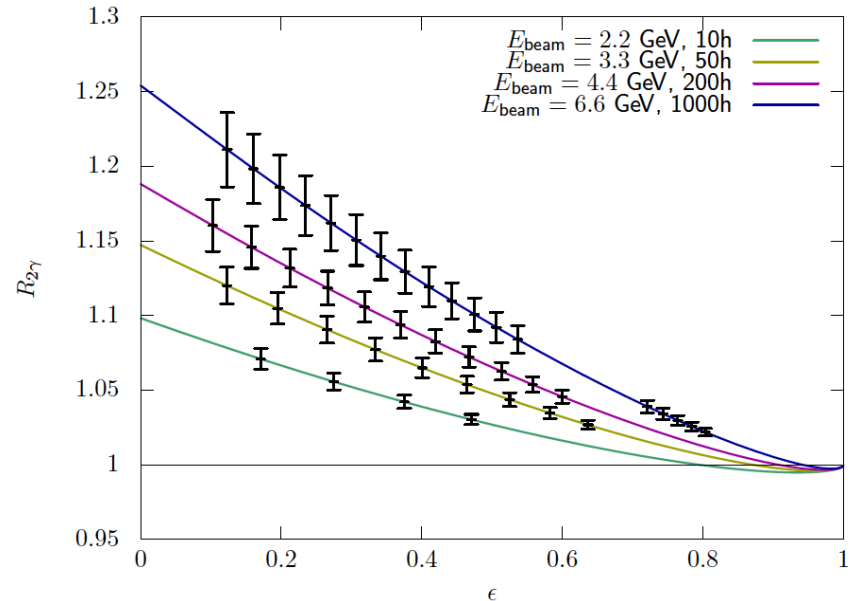
Analysis Credit and Ref:  
P. Datta



# Future TPE Experiments



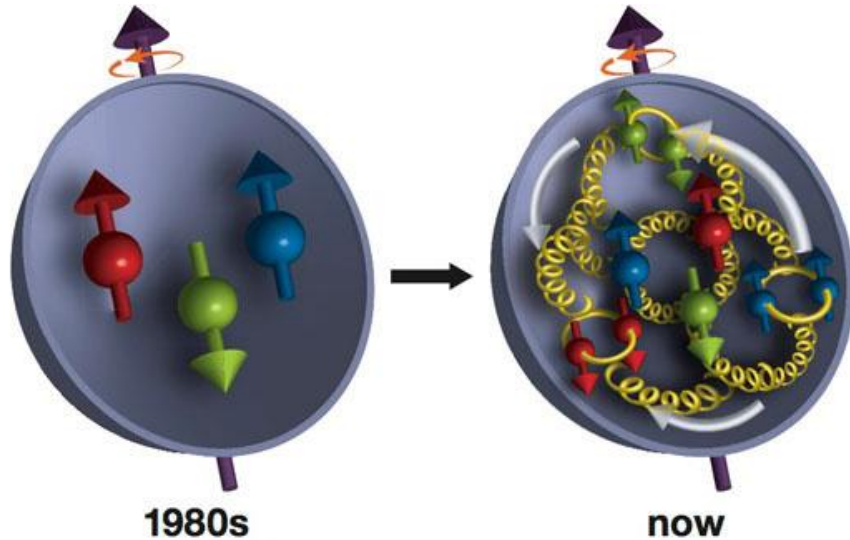
Ref: E. Fuchey *et al*, *Measurement of the Two-Photon Exchange Contribution in the Electron-Neutron and Positron-Neutron Elastic Scattering*



Ref: J. Bernauer *et al*, *Determination of two-photon exchange via  $e^+p/e^-p$  Scattering with CLAS12*

# Nucleon Structure

- Hadrons (including protons and neutrons) have an internal structure!
- Not structureless point-like.
- Complex internal structure of valence quarks, gluons, and quark-antiquark pairs.



## Important Questions:

- How are the charge and magnetization distributed inside a nucleon?
- How do emergent properties of the nucleon arise?
- How does the internal nucleon structure behave at different momentum transfer scales (non-perturbative vs. perturbative regimes)?
- How do the gluon and quark-antiquark pairs contribute?

# BigBite Spectrometer (Electron Arm)

BigBite Dipole Magnet:

- 1.2 T · m
- 53 msr, 1.6 m from target

Tracking:

Gas Electron Multiplier

Cherenkov Detector:

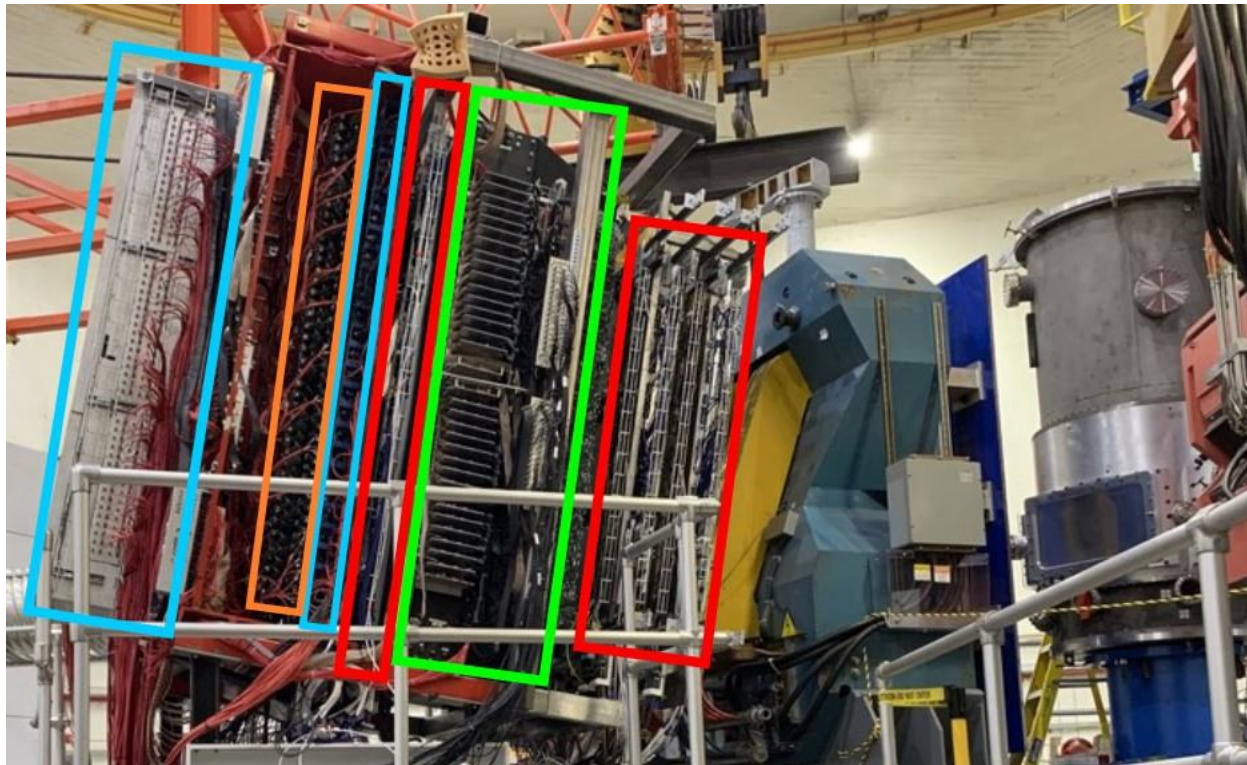
GRINCH

Scintillator Array:

Timing Hodoscope

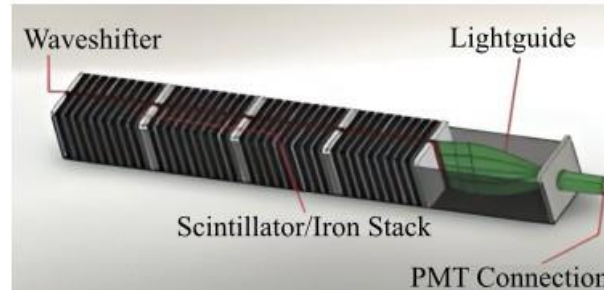
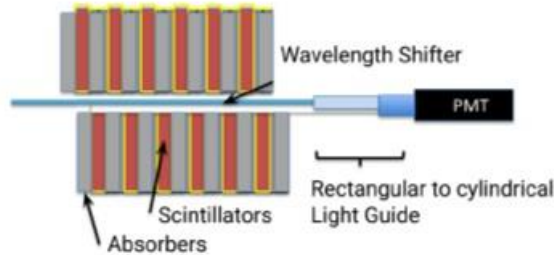
Electron Calorimeter:

BigBite Calorimeter (Preshower  
+ Shower)



# Hadron Calorimeter (HCal)

- SBS magnet is a large dipole magnet
- One module consists of 40 layers of iron absorber and 40 layers scintillator.
- Hadronic showers are created in the iron absorbers and the energy is sampled by scintillators and guided to the PMTs
- 3-4 cm spatial resolution
- 30% energy resolution

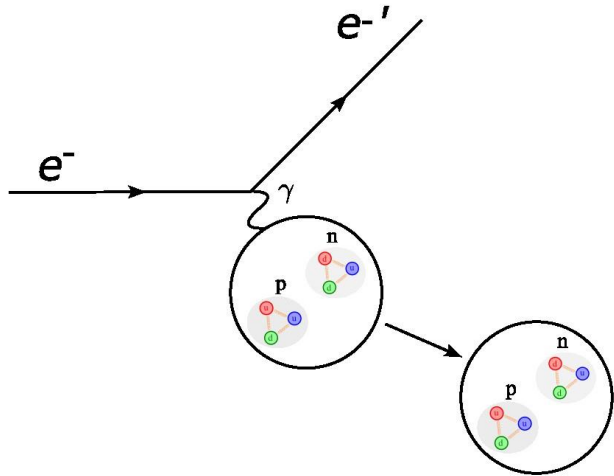


Interior of an HCal module

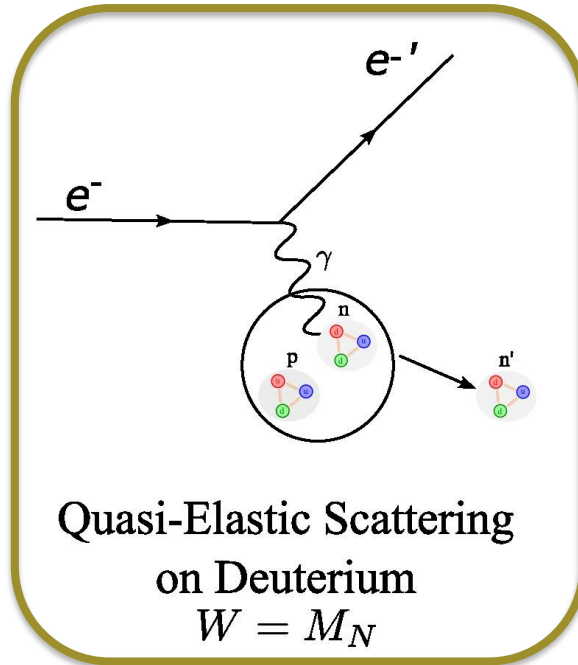


A side view of HCal in Hall A

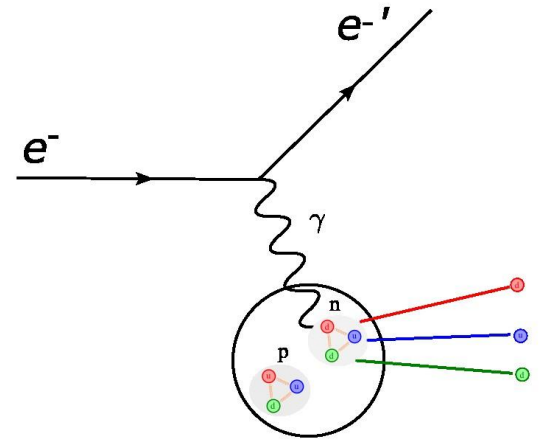
# Quasi-Elastic Scattering



Elastic Scattering on Deuterium  
 $W = M_T$



Quasi-Elastic Scattering  
on Deuterium  
 $W = M_N$



Inelastic Scattering on Deuterium  
 $W > M_N$

- SBS nucleon physics program focuses on quasi-elastic scattering.
- $M_T$  is mass of the target (deuterium)
- $M_N$  is mass of the nucleon

# Quasi-Elastic Scattering

- GMn,  $Q^2 = 3.0 - 13.5 \text{ (GeV/c)}^2$
- nTPE,  $Q^2 = 4.5 \text{ (GeV/c)}^2$
- Need many statistics and strong cuts on the electron arm to resolve the quasi-elastic peak above the inelastic background.

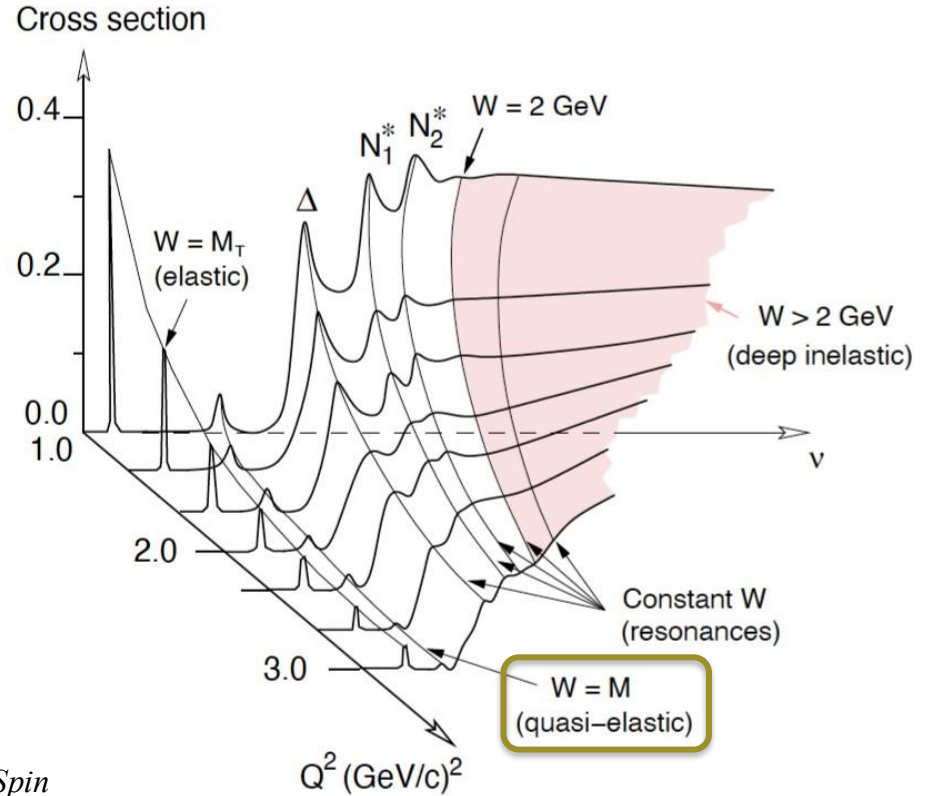
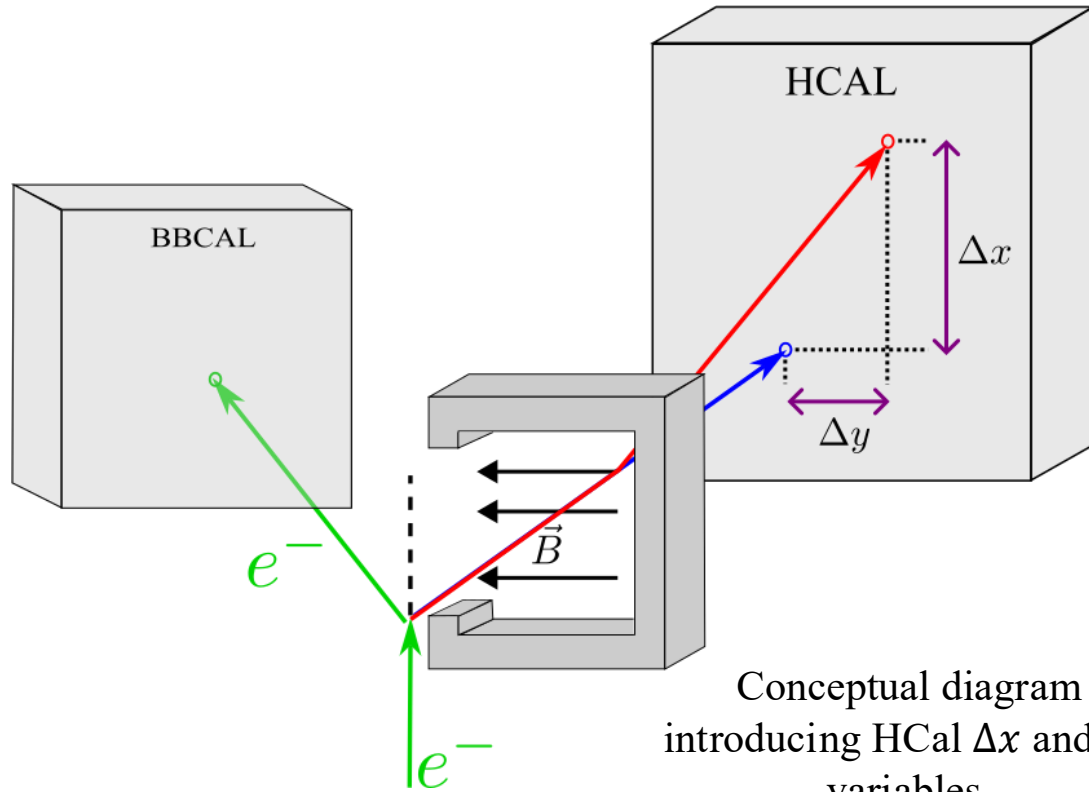


Diagram: Xiaochao Zheng, *Precision Measurement of Neutron Spin Asymmetry  $A_{1n}$  at Large  $x_B$  Using CEBAF at 5.7 GeV*

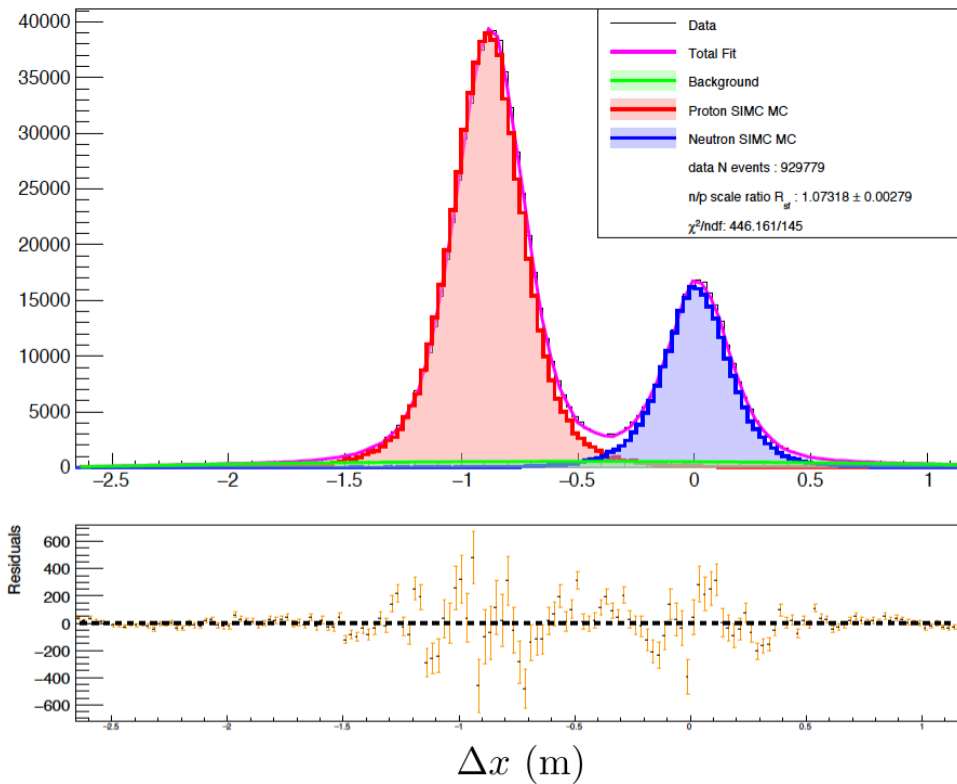
# Analysis Methods – Introducing HCal $\Delta x$ and $\Delta y$



Conceptual diagram  
introducing HCal  $\Delta x$  and  $\Delta y$   
variables.

- Definition of  $\Delta x$  ( $\Delta y$ ): The difference between the observed and the expected nucleon (assuming neutron) position on HCal in the dispersive (non-dispersive) direction.
- Used to separate neutrons and protons

# $Q^2 = 4.5 \text{ (GeV/c)}^2$ Data-Monte Carlo Comparison



- Fit Equation:

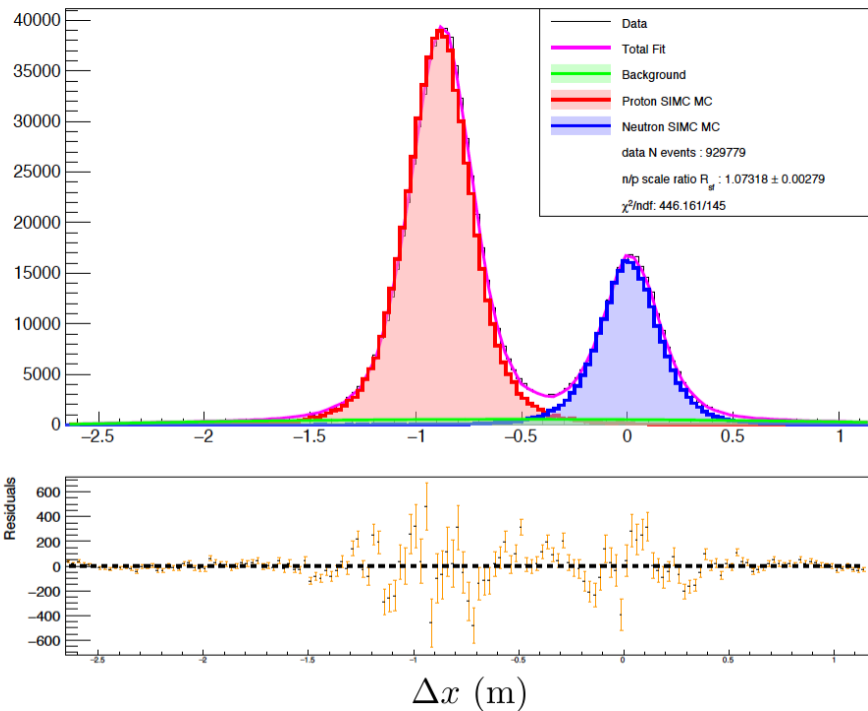
$$\begin{aligned}
 f_{total}(x_i) &= f_{sf}^p \left( R_{sf}^{n/p} h^n(x_i - \delta_n) + h^p(x_i - \delta_p) \right) \\
 &+ f_{bkgd}(x_i)
 \end{aligned}$$

- Fit Parameters:

- $f_{sf}^p$  - proton scale factor
- $R_{sf}^{n/p}$  - ratio of neutron to proton scale factors
- $\delta_{n(p)}$  - neutron (proton) centroid shift parameters
- $f_{bkgd}$  - parameters associated with the background

- Interpretation:  $R_{sf}^{n/p}$  quantifies the relative scaling of the neutron to proton quasi-elastic scattering cross-section as modeled by the simulation and as observed in data.

# $Q^2 = 4.5 \text{ (GeV/c)}^2$ Data-Monte Carlo Comparison



Sources of Systematic Uncertainty:

- Cut Stability
- HCal Nucleon Detection Efficiency
- Inelastic Background

Simulation:

$$R'_{sim} = \frac{\left(\frac{d\sigma}{d\Omega}\right)\bigg|_{n(e,e'),sim}}{\left(\frac{d\sigma}{d\Omega}\right)\bigg|_{p(e,e'),sim}} = R_{sim} \cdot f_{nuc,sim}^{-1} f_{RC,sim}^{-1} f_{Det,sim}^{-1}$$

Extraction:

$$R = R' \cdot f_{nuc} f_{RC} f_{det} = R_{sf}^{n/p} \cdot R'_{sim} \cdot f_{nuc,sim} f_{RC,sim} f_{det,sim}$$

Claim:

- Simulation consistently replicates nuclear, radiative, and detector effects that are present in the experimental data.

Implication:

$$\frac{f_{nuc}}{f_{nuc,sim}} \sim 1 \quad \frac{f_{RC}}{f_{RC,sim}} \sim 1 \quad \frac{f_{det}}{f_{det,sim}} \sim 1$$

$$R' = \frac{\left(\frac{d\sigma}{d\Omega}\right)\bigg|_{n(e,e')}}{\left(\frac{d\sigma}{d\Omega}\right)\bigg|_{p(e,e')}} = R_{sf}^{n/p} \cdot R'_{sim}$$

# Neutron Rosenbluth Slope Technique

- **Goal:** Extract neutron Rosenbluth Slope,  $S^n = (G_E^n)^2 / \tau_n (G_M^n)^2$
- Consider 2 kinematics with same  $Q^2$ -value and with different values of  $\epsilon$ .
- Consider 2 elastic neutron-to-proton cross-section ratios.
- Combine the Ratio Method with a Rosenbluth Technique.

$$R'_{\epsilon_1} = R_{\epsilon_1} \cdot f_{nuc,\epsilon_1}^{-1} f_{RC,\epsilon_1}^{-1} f_{Det,\epsilon_1}^{-1} = \frac{\frac{\tau_{\epsilon_1,n} \sigma_{Mott}}{\epsilon_{1,n} (1 + \tau_{\epsilon_1,n})} (\epsilon_{1,n} \sigma_{L,\epsilon_1}^n + \sigma_{T,\epsilon_1}^n)}{\frac{\tau_{\epsilon_1,p} \sigma_{Mott}}{\epsilon_{1,p} (1 + \tau_{\epsilon_1,p})} (\epsilon_{1,p} \sigma_{L,\epsilon_1}^p + \sigma_{T,\epsilon_1}^p)}$$

$$R'_{\epsilon_2} = R_{\epsilon_2} \cdot f_{nuc,\epsilon_2}^{-1} f_{RC,\epsilon_2}^{-1} f_{Det,\epsilon_2}^{-1} = \frac{\frac{\tau_{\epsilon_2,n} \sigma_{Mott}}{\epsilon_{2,n} (1 + \tau_{\epsilon_2,n})} (\epsilon_{2,n} \sigma_{L,\epsilon_2}^n + \sigma_{T,\epsilon_2}^n)}{\frac{\tau_{\epsilon_2,p} \sigma_{Mott}}{\epsilon_{2,p} (1 + \tau_{\epsilon_2,p})} (\epsilon_{2,p} \sigma_{L,\epsilon_2}^p + \sigma_{T,\epsilon_2}^p)}$$

# Neutron Rosenbluth Slope Technique

## Physics Result:

- Consider ‘super-ratio’ of  $R'$  for two different values of  $\epsilon$ .
- Define  $S^{n(p)} = (G_E^{n(p)})^2 / \tau_{n(p)} (G_M^{n(p)})^2$  and  $\Delta\epsilon = \epsilon_{1,n} - \epsilon_{2,n}$ .

Super-Ratio

$$\frac{R'_{\epsilon_1}}{R'_{\epsilon_2}} = B \cdot \frac{1 + \epsilon_{1,n} S_{\epsilon_1}^n}{1 + \epsilon_{2,n} S_{\epsilon_2}^n}$$

From Kinematic Information

$$B = \frac{\frac{\tau_{\epsilon_{1,n}}}{\epsilon_{1,n}(1 + \tau_{\epsilon_{1,n}})} \frac{\tau_{\epsilon_{2,p}}}{\epsilon_{2,p}(1 + \tau_{\epsilon_{2,p}})}}{\frac{\tau_{\epsilon_{1,p}}}{\epsilon_{1,p}(1 + \tau_{\epsilon_{1,p}})} \frac{\tau_{\epsilon_{2,n}}}{\epsilon_{2,n}(1 + \tau_{\epsilon_{2,n}})}} \frac{(G_M^n)_{\epsilon_1}^2 (G_M^p)_{\epsilon_2}^2}{(G_M^p)_{\epsilon_1}^2 (G_M^n)_{\epsilon_2}^2} \frac{1 + \epsilon_{2,p} S_{\epsilon_2}^p}{1 + \epsilon_{1,p} S_{\epsilon_1}^p}$$

From Global  
Form Factor  
Analysis.

# Neutron Rosenbluth Slope Technique

## Physics Result:

- Consider ‘super-ratio’ of  $R'$  for two different values of  $\epsilon$ .
- Define  $S^{n(p)} = (G_E^{n(p)})^2 / \tau_{n(p)} (G_M^{n(p)})^2$  and  $\Delta\epsilon = \epsilon_{1,n} - \epsilon_{2,n}$ .

Physics  
Result!

$$S^n = \frac{\left( \frac{R'_{\epsilon_1}}{R'_{\epsilon_2}} - B \right)}{\Delta\epsilon \cdot B} \approx \frac{(G_E^n)^2}{\tau_n (G_M^n)^2}$$

From Data  
Extraction

From Kinematic Information

$$B = \frac{\frac{\tau_{\epsilon_{1,n}}}{\epsilon_{1,n}(1 + \tau_{\epsilon_{1,n}})} \frac{\tau_{\epsilon_{2,p}}}{\epsilon_{2,p}(1 + \tau_{\epsilon_{2,p}})}}{\frac{\tau_{\epsilon_{1,p}}}{\epsilon_{1,p}(1 + \tau_{\epsilon_{1,p}})} \frac{\tau_{\epsilon_{2,n}}}{\epsilon_{2,n}(1 + \tau_{\epsilon_{2,n}})}} \frac{(G_M^n)_{\epsilon_1}^2 (G_M^p)_{\epsilon_2}^2}{(G_M^p)_{\epsilon_1}^2 (G_M^n)_{\epsilon_2}^2} \frac{1 + \epsilon_{2,p} S_{\epsilon_2}^p}{1 + \epsilon_{1,p} S_{\epsilon_1}^p}$$

From Global  
Form Factor  
Analysis.

# Event Selection Criteria

## Good Electron Cuts

### 1. Track Quality

- No. of GEM Layers with Hits
- Track  $\chi^2/ndf$
- Vertex Z position
- BigBite Optics Validity

### 2. PID

- **Preshower Energy**
- $E_{BBCal}/p$
- Cut regions were optimized
- Systematic effects on  $R_{sf}^{n/p}$  due to cut sensitivity were quantified

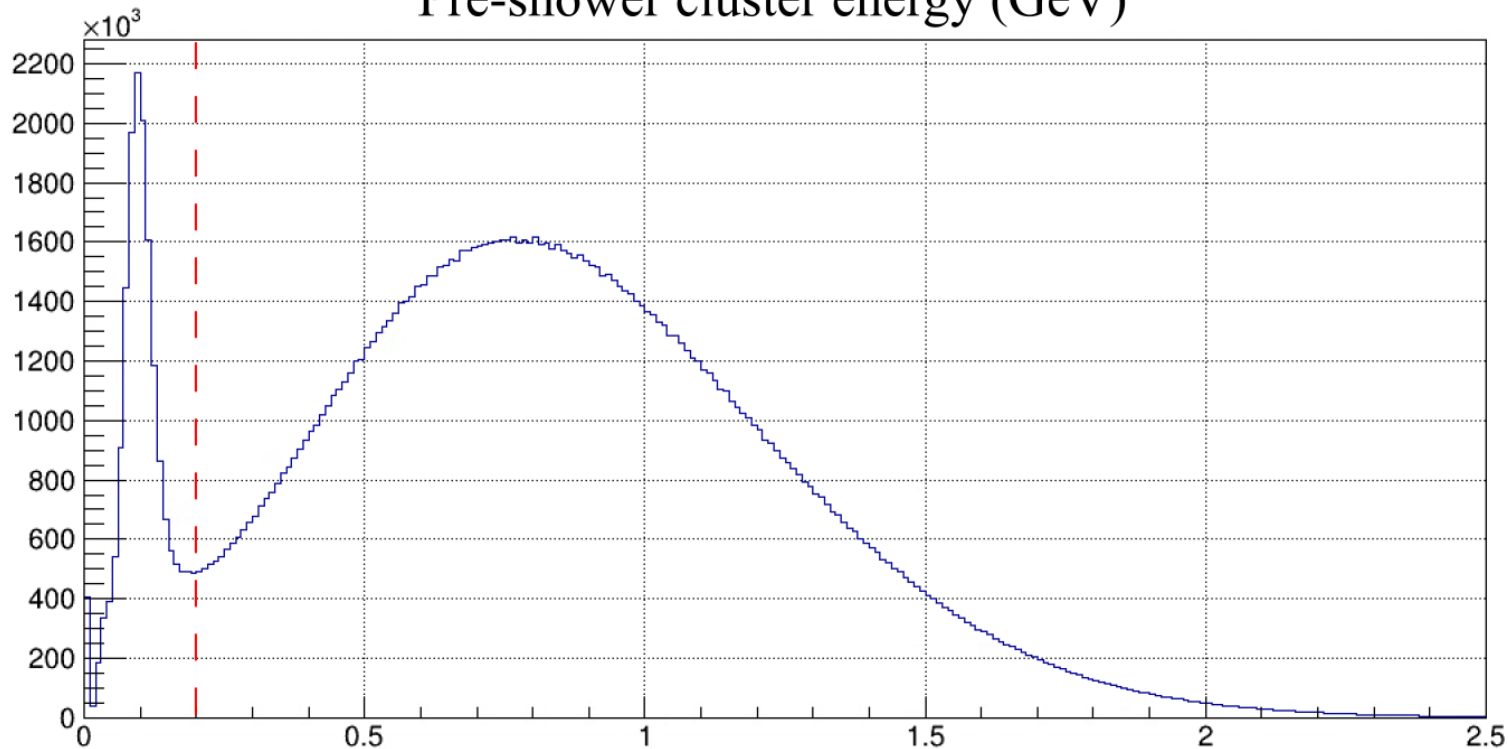
## Quasi-Elastic Event Cuts

- HCal Cluster Energy
- Coincidence Time
- $W^2$
- $\Delta y$
- Fiducial

$$Q^2 = 4.5 \text{ (GeV/c)}^2$$

# Preshower Energy (PID cut)

Pre-shower cluster energy (GeV)



# Extracted $R_{sf}^{n/p}$ Values

Setting	$R_{sf}^{n/p}$	$\Delta \left( R_{sf}^{n/p} \right)_{\text{total}}$	$\Delta \left( R_{sf}^{n/p} \right)_{\text{stat}}$	$\Delta \left( R_{sf}^{n/p} \right)_{\text{sys}}$
SBS-8 50%	1.0787	0.0152	0.0082	0.0128
SBS-8 70%	1.0732	0.0110	0.0028	0.0106
SBS-8 100%	1.0651	0.0133	0.0065	0.0116
SBS-9 70%	1.0648	0.0088	0.0034	0.0081

	Uncertainty Source	Setting			
		SBS-8 50%	SBS-8 70%	SBS-8 100%	SBS-9 70%
$\Delta \left( R_{sf}^{n/p} \right)_{\text{sys}}$	HDENU	0.0003	0.0018	0.0012	0.0053
	Cut S.	0.0078	0.0083	0.0052	0.0054
	Ine. Con.	0.0101	0.0065	0.0103	0.0029
	Total	0.0128	0.0106	0.0116	0.0081

	$\overline{R}_{sf}^{n/p}$	$\Delta \left( \overline{R}_{sf}^{n/p} \right)_{\text{total}}$	$\Delta \left( \overline{R}_{sf}^{n/p} \right)_{\text{uncorr}}$	$\Delta \left( \overline{R}_{sf}^{n/p} \right)_{\text{corr}}$
Value for SBS-8	1.0711	0.0104	0.0054	0.0089

# Extracted $R'$ Values

Setting	$R'$	$\Delta (R')_{\text{total}}$	$\Delta (R')_{\text{stat}}$	$\Delta (R')_{\text{sys}}$
SBS-8 50%	0.3936	0.0055	0.0030	0.0047
SBS-8 70%	0.3916	0.0040	0.0010	0.0039
SBS-8 100%	0.3886	0.0049	0.0024	0.0042
SBS-9 70%	0.3875	0.0032	0.0013	0.0030

	$\bar{R}'$	$\Delta (\bar{R}')_{\text{total}}$	$\Delta (\bar{R}')_{\text{uncorr}}$	$\Delta (\bar{R}')_{\text{corr}}$
Value for SBS-8	0.3908	0.0038	0.0020	0.0032

# Rosenbluth Separation Technique

- Fixed  $Q^2$ -value
- Vary electron beam energy and scattering angle, to make measurements at different  $\epsilon$  values
- Reduced cross-section linear dependence in  $\epsilon$

$$\begin{aligned}\sigma_R &= \frac{\epsilon(1 + \tau)}{\tau} \frac{E}{E'} \frac{d\sigma}{d\Omega} / \sigma_{\text{Mott}} \\ &= \frac{\epsilon}{\tau} G_E^2(Q^2) + G_M^2(Q^2) \\ &= (\epsilon\sigma_L + \sigma_T)\end{aligned}$$

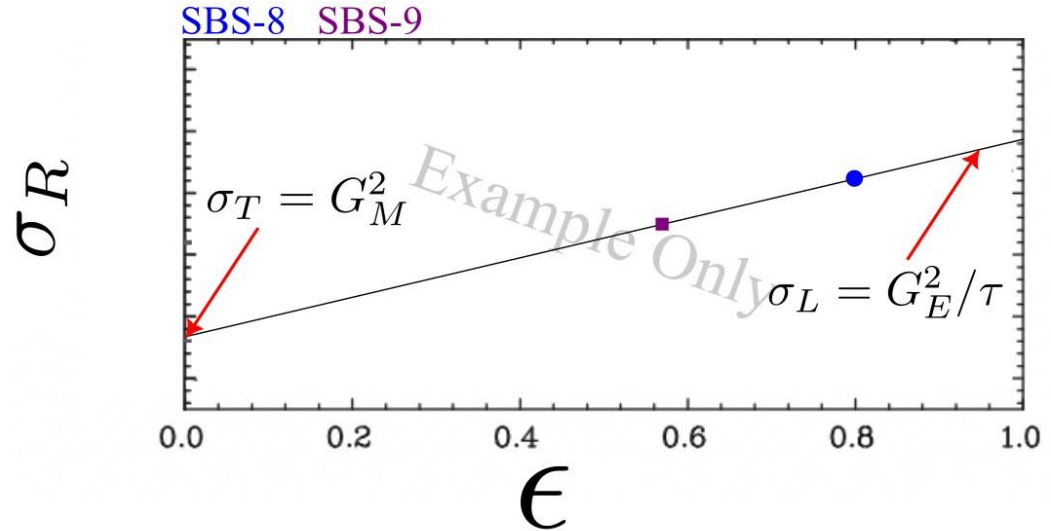
$$\epsilon = (1 + 2(1 + \tau) \tan^2(\theta/2))^{-1}$$

## Rosenbluth Slope

$$S = \sigma_L / \sigma_T = G_E^2(Q^2) / \tau G_M^2(Q^2)$$

# Rosenbluth Separation Technique

$$\begin{aligned}\sigma_R &= \frac{\epsilon(1 + \tau)}{\tau} \frac{E}{E'} \frac{d\sigma}{d\Omega} / \sigma_{\text{Mott}} \\ &= \frac{\epsilon}{\tau} G_E^2(Q^2) + G_M^2(Q^2) \\ &= (\epsilon\sigma_L + \sigma_T)\end{aligned}$$



## Rosenbluth Slope

$$S = \sigma_L/\sigma_T = G_E^2(Q^2)/\tau G_M^2(Q^2)$$

# Targets

## Cryogenic Targets:

- Liquid Hydrogen
  - 19 Kelvin
  - Proton Source
  - Used for apparatus calibrations
- Liquid Deuterium
  - 22 Kelvin
  - Proton and Neutron Source
  - Used for production data

## Solid Targets:

- Used for calibrations, systematics, and optics studies
- Include dummy, carbon hole, and optics foil targets



Target ladder with cryotarget cells.



Target ladder showing solid foil targets.

# Gas Electron Multiplier (GEM)

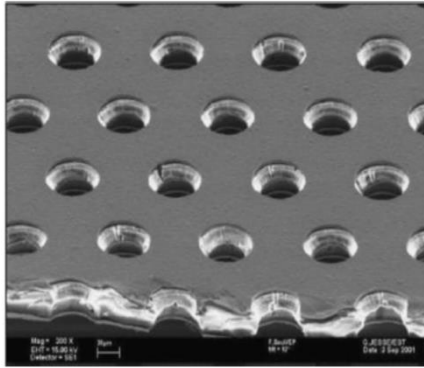


Diagram of a typical GEM electrode

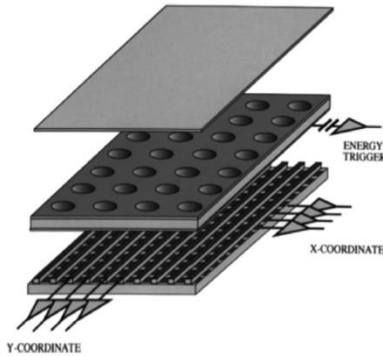
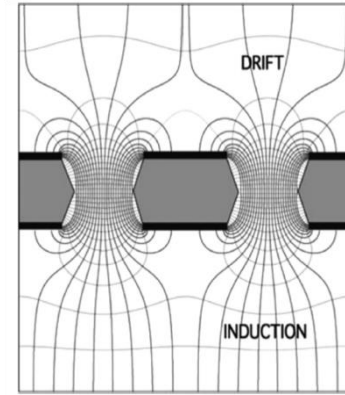


Diagram of a single GEM detector with Cartesian readout

- Type of gaseous ionization detector, reliant on electron avalanche and a subclass of detectors known as Micro-Pattern Gas Detectors (MPGDs).
- Used as tracking detectors, preamplification, drift chambers, time projection chambers, radio imaging.
- Triple GEM detector effective gains typically are  $10^4$  or  $10^5$ .
- $\sim 100 \mu\text{m}$  spatial resolution and  $100\text{-}500 \text{ kHz/cm}^2$  particle rate.



Electric Field in the region of the holes of a GEM electrode

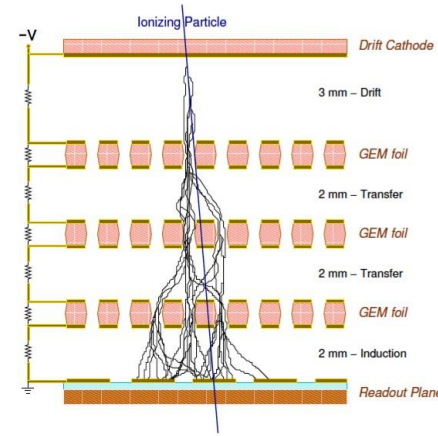
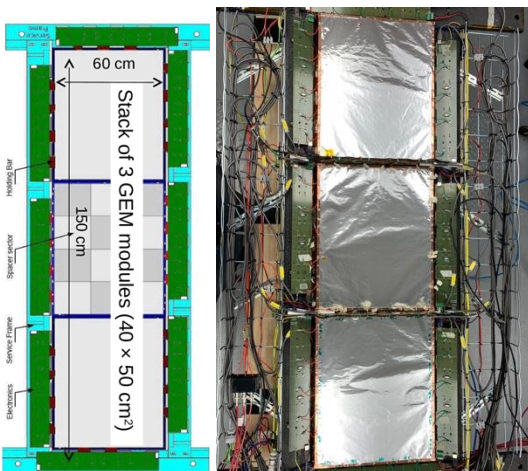
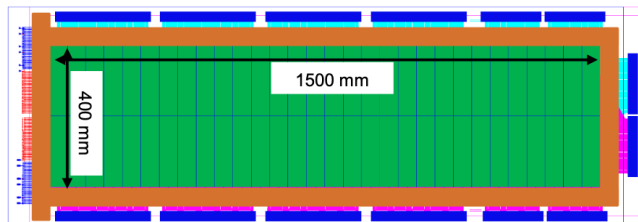


Diagram of a triple GEM detector

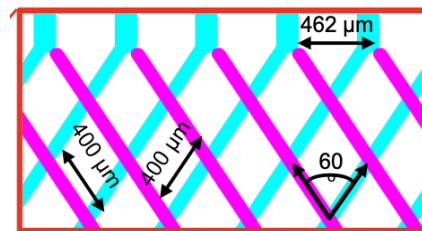
# GEM Detectors for SBS Program



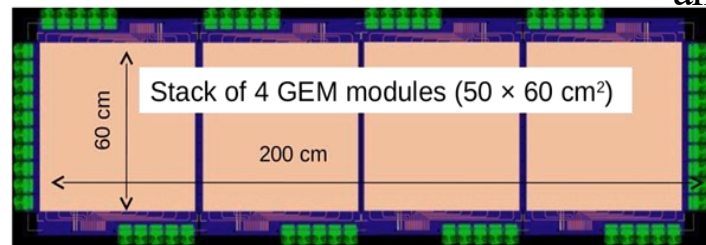
INFN XY-GEM Layer schematic and picture with RF shielding



UVA UV-GEM Layer schematic and picture with RF shielding



- 4 INFN GEM layers prepared for SBS program
- 4 UVA UV-GEM layers prepared for SBS program
- 11 UVA XY-GEM layers prepared for SBS program
- 2 INFN GEM layers operated during  $G_M^n$
- 2 UVA UV-GEM layers operated during  $G_M^n$
- 2 more UVA UV-GEM layers moved to BigBite during  $G_M^n$

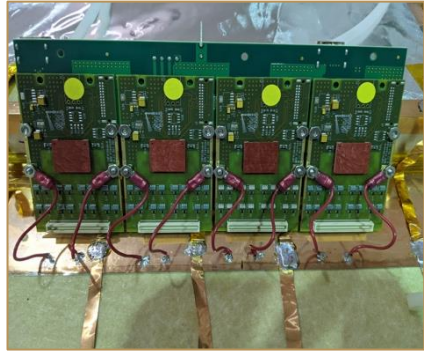


UVA XY-GEM Layer schematic and picture without RF shielding

# GEM DAQ Electronics



INFN Analog Pipeline Voltage (APV25) Card



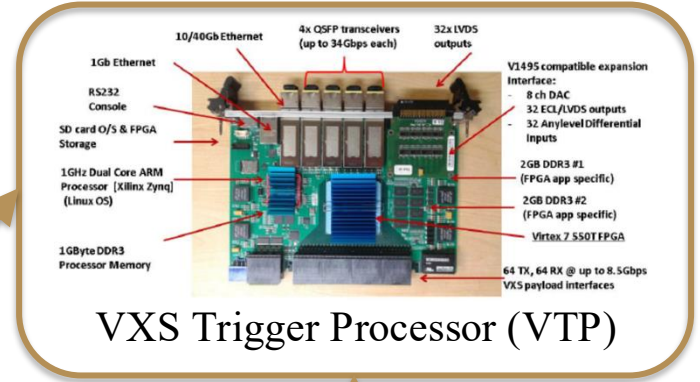
UVA APV25 Card

10 or  
20 m  
HDMI  
Cables



Multi Purpose  
Digitizer (MPD)

Long  
Fiber  
Optic  
Cables

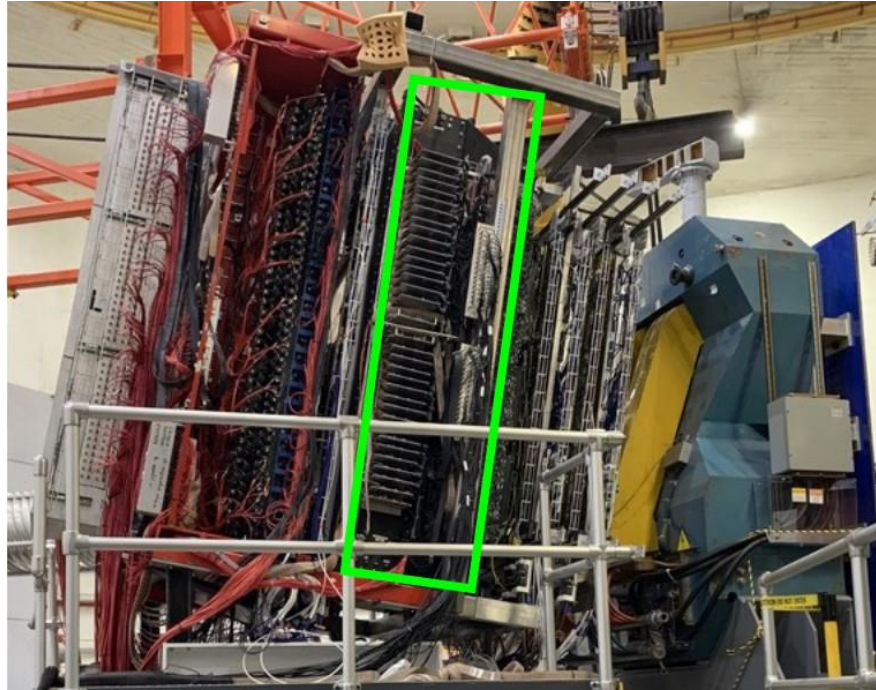


VXS Trigger Processor (VTP)

CODA3 Platform

# Gas RINg CHerenkov (GRINCH)

- PID for electrons and pions
- 510 one-inch PMTs in a honeycomb array
- 4 highly reflective cylindrical mirrors
- Filled with heavy gas:  $C_4F_8$
- Pion Threshold of 2.7 GeV
- NINO front-end cards instrumented for data collection in high-background environment



GRINCH in the BigBite Spectrometer in Hall A



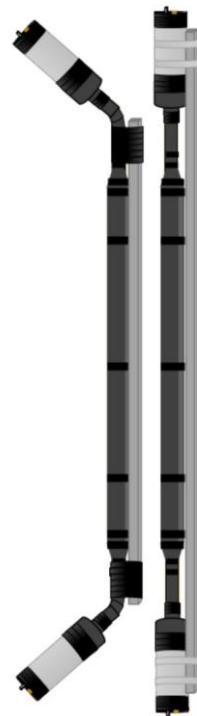
Cylindrical Mirrors  
Inside GRINCH

# Timing Hodoscope

- High precision timing reference
- 90 plastic scintillators with light guides and PMTs on each end
- Alternated straight and curved light guides
- Located between Preshower and Shower
- $\sim 60$  ps timing resolution
- $\sim 5$  cm spatial resolution



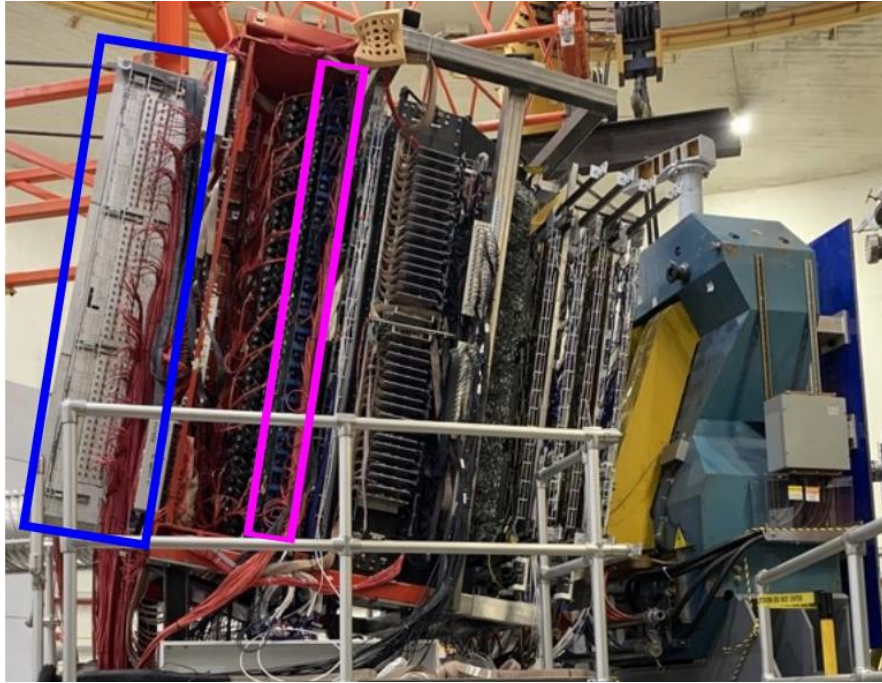
Zoom-in of Timing Hodoscope  
in BigBite Spectrometer



Top-View of  
Scintillator Bar Types

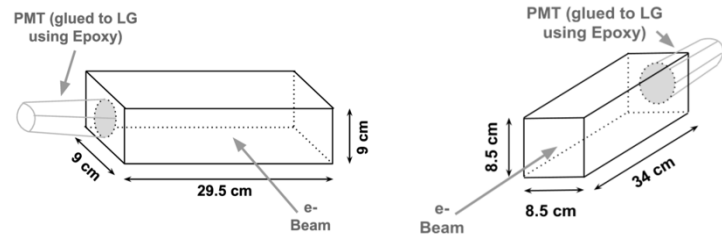
Diagram: Ralph Marinaro, *Performance and Commissioning of the BigBite Timing Hodoscope for Nucleon Form Factor Measurements at Jefferson Lab.*

# BigBite Calorimeter (BBCal)

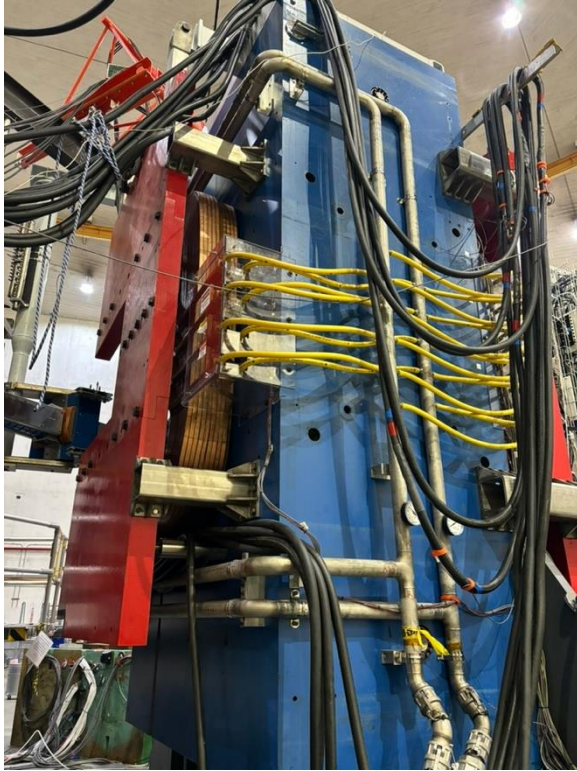


BBCal in BigBite Spectrometer, composed of Preshower and Shower.

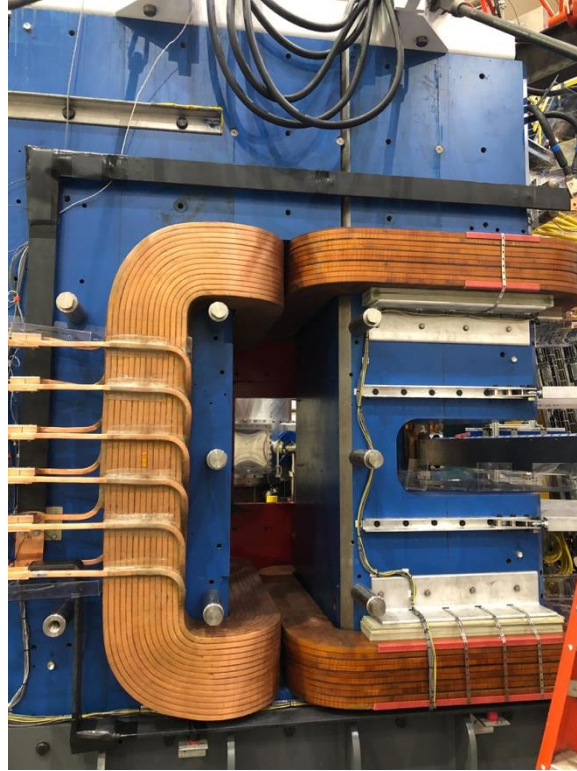
- Preshower and Shower together sample the total energy and position of the scattered electron.
- Electron induces electromagnetic shower in the lead-glass blocks. Light is collected with PMTs.
- Preshower
  - 52 lead-glass blocks perpendicular to  $e'$  track
  - Pions leave a lower energy signal,  $\sim 200 \text{ MeV}/c^2$
- Shower
  - 189 lead-glass blocks parallel to  $e'$  track
  - Electrons deposit remaining energy
- Provides single-arm trigger.
- Allows for energy measurement, constraints on track search region, and pion rejection.



# Super BigBite Magnet



Side View of SBS Magnet



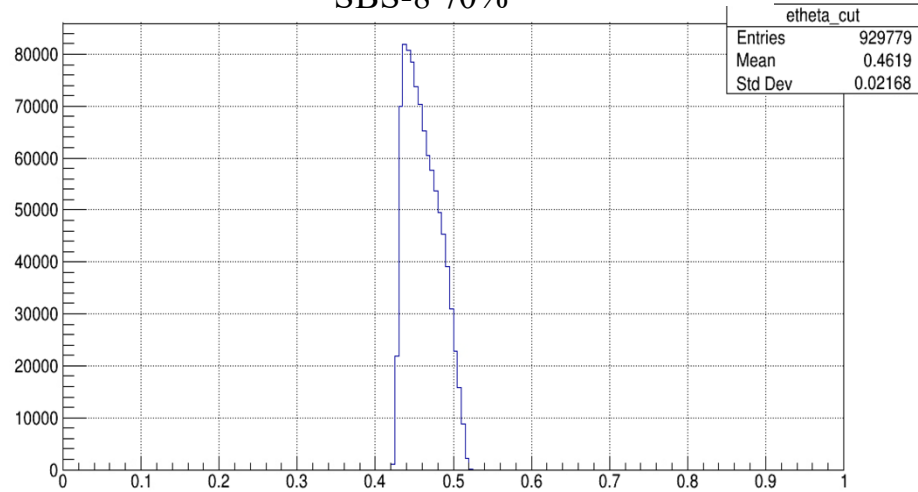
Downstream View of SBS Magnet

- Dipole magnet
- Deflects positively charged particles, differentiating between scattered protons and neutrons.
- 100 tons
- $1.3 \text{ T} \cdot \text{m}$
- 2.1 kA excitation current
- 35 msr, 2.25 m from target

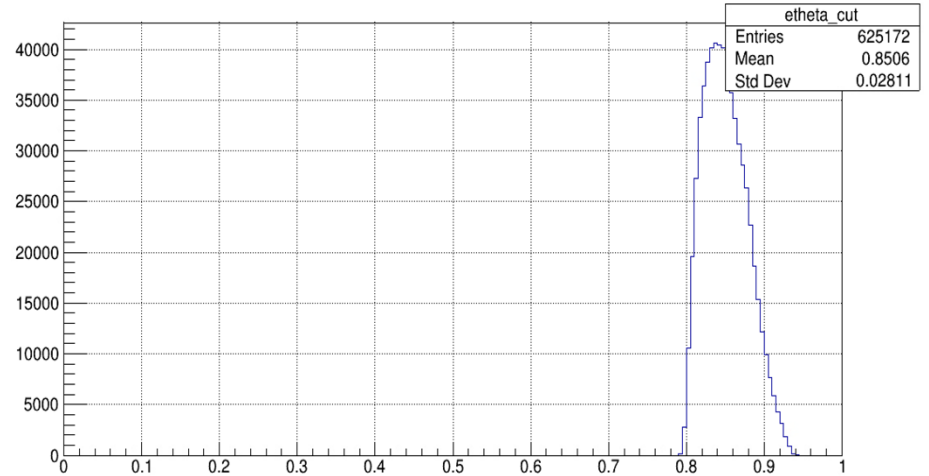
# Theta Scattered Electron Distributions (after all cuts)

For Extraction Theta Scattered Electron values SBS-8: 0.4619 , SBS-9: 0.8506

SBS-8 70%



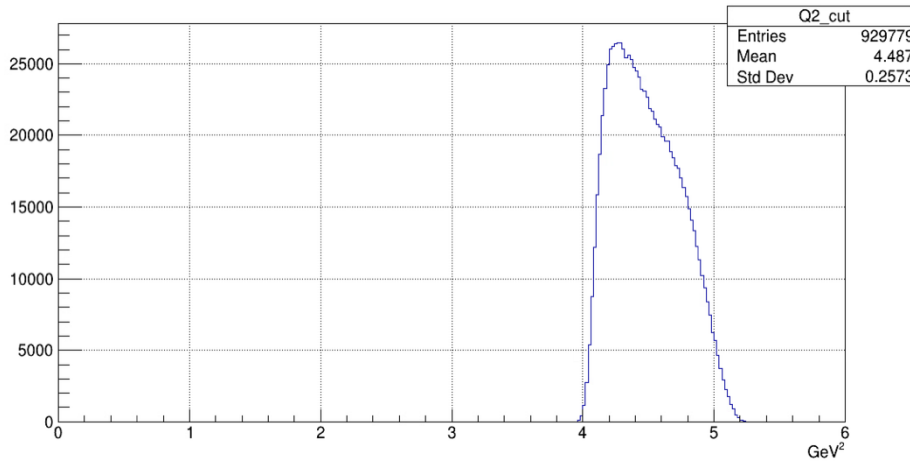
SBS-9 70%  
Theta for Scattered Electron from Reconstruct Track (radians), all cuts



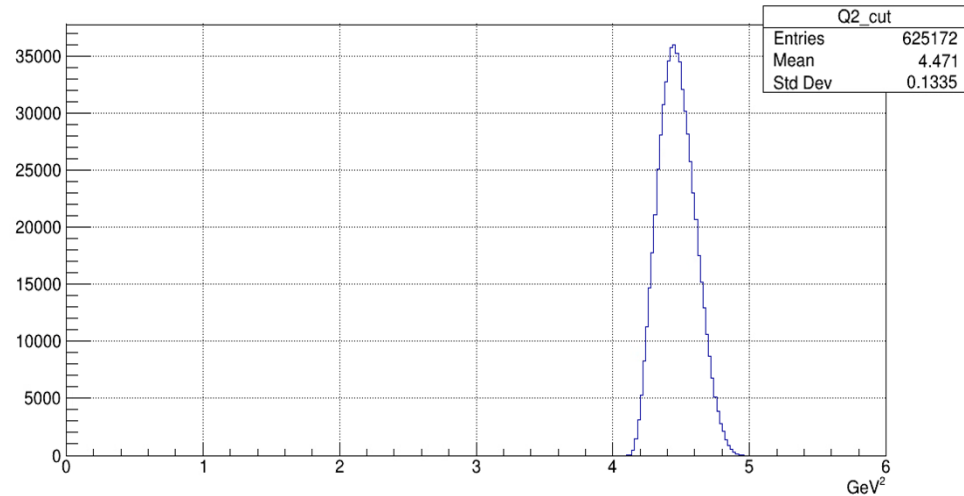
# $Q^2$ Distributions (after all cuts)

For Extraction  $Q^2$  values SBS-8: 4.48, SBS-9: 4.476

SBS-8 70%



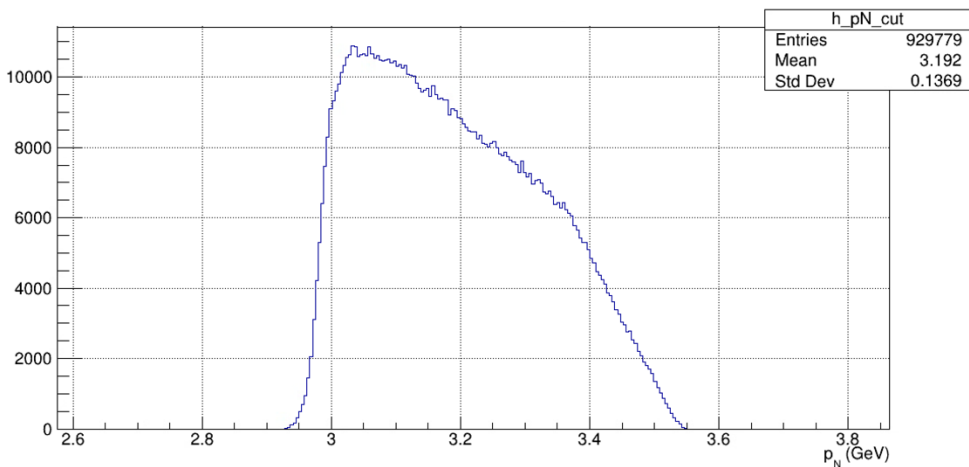
SBS-9 70%



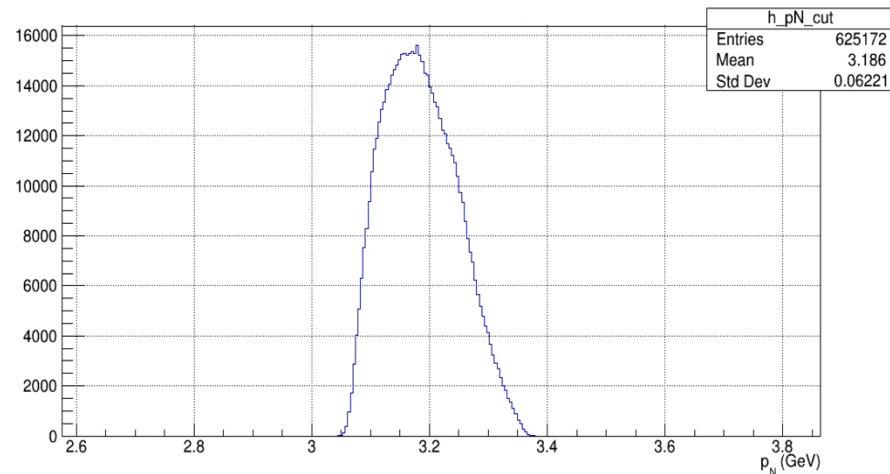
# Scattered Nucleon Momentum Distributions (after all cuts)

For Extraction Scattered Nucleon Momentum values SBS-8: 3.19 , SBS-9: 3.19

SBS-8 70%



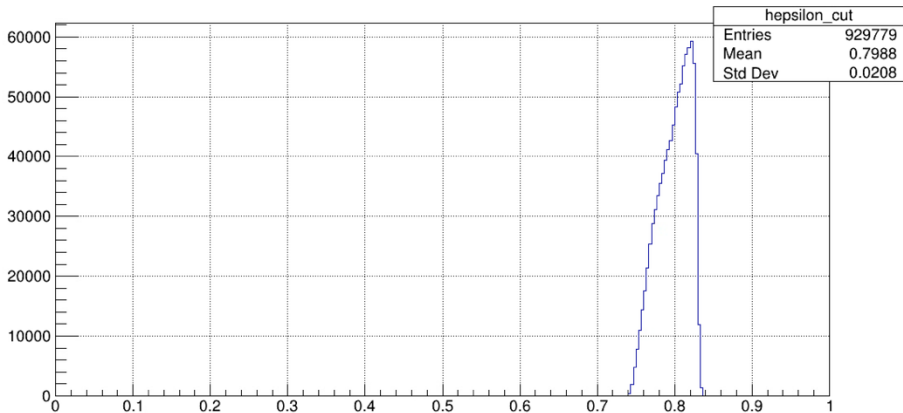
SBS-9 70%



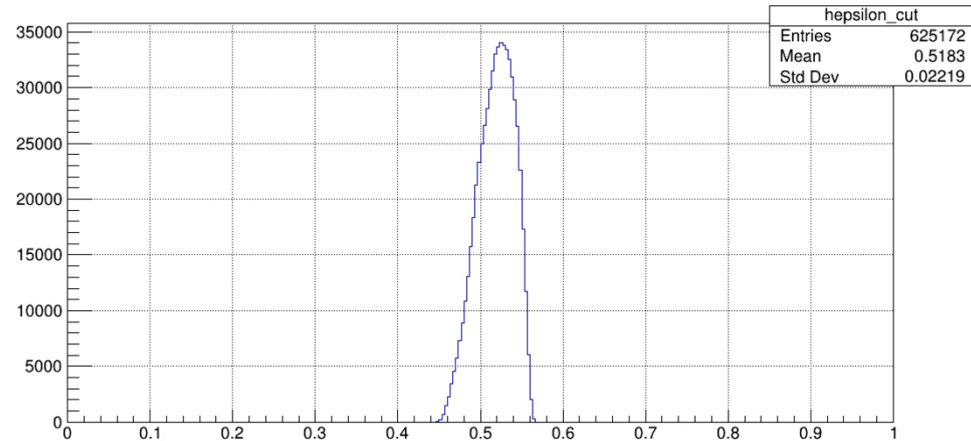
# $\epsilon$ Distributions (after all cuts)

For Extraction  $\epsilon$  values (neutrons) SBS-8: 0.79925 , SBS-9: 0.51802

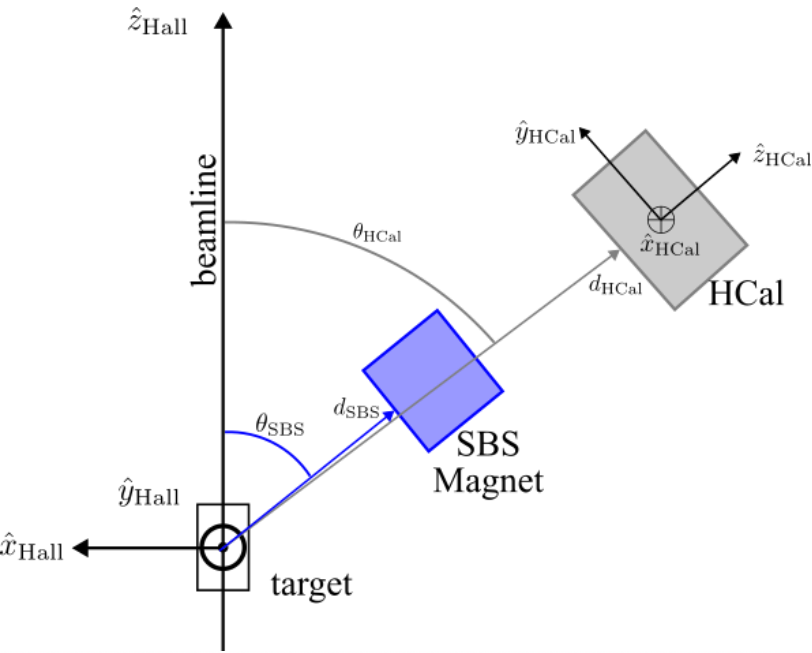
SBS-8 70%



SBS-9 70%



# Analysis Methods – Introducing HCal $\Delta x$ and $\Delta y$



$$\Delta x = x_{\text{HCal}}^{\text{obs}} - x_{\text{HCal}}^{\text{exp}}$$

$$\Delta y = y_{\text{HCal}}^{\text{obs}} - y_{\text{HCal}}^{\text{exp}}$$

$$x_{\text{HCal}}^{\text{exp}} = \left( \vec{h}_{\text{intersect}} - \vec{O}_{\text{HCal}} \right) \cdot \hat{x}_{\text{HCal}},$$

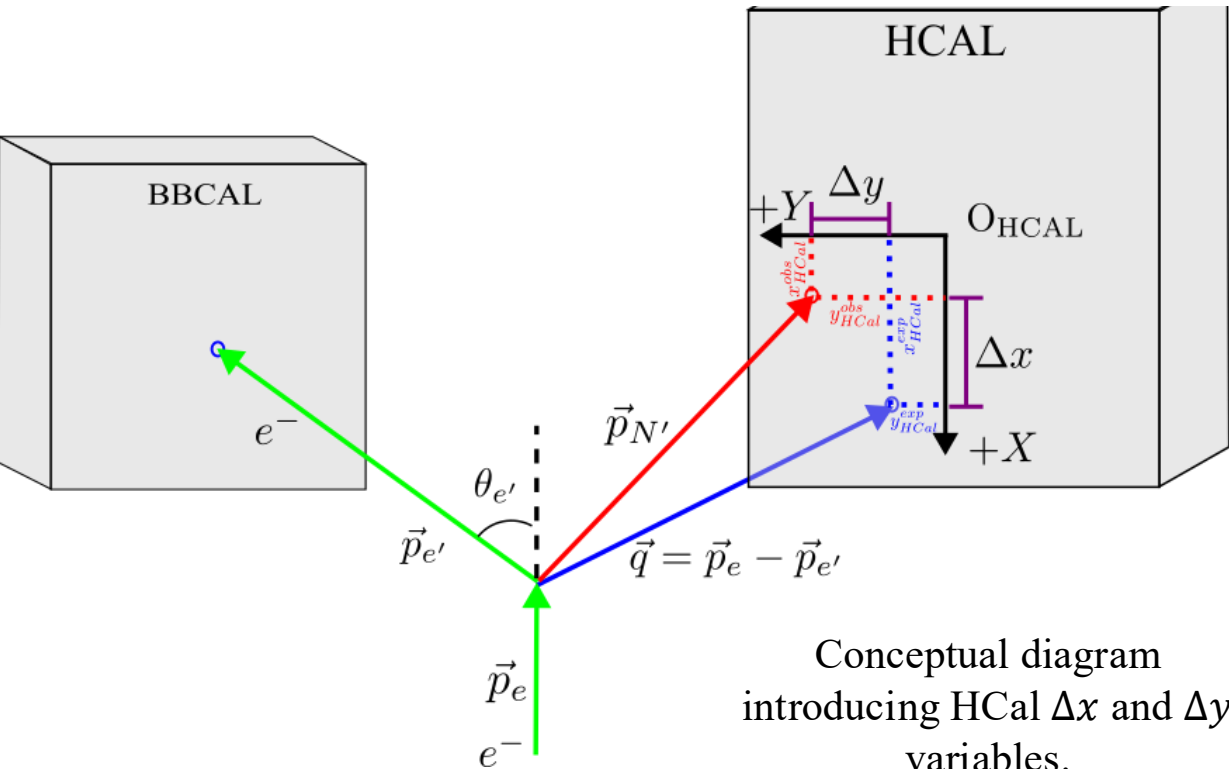
$$y_{\text{HCal}}^{\text{exp}} = \left( \vec{h}_{\text{intersect}} - \vec{O}_{\text{HCal}} \right) \cdot \hat{y}_{\text{HCal}},$$

$$\vec{h}_{\text{intersect}} = \vec{v} + s_{\text{intersect}} \hat{p}_{N'}.$$

$$\left( \vec{O}_{\text{HCal}} - \vec{v} \right) \cdot \hat{z}_{\text{HCal}}$$

$$\hat{p}_{N'} = (\sin \theta_{N'} \cos \phi_{N'}, \sin \theta_{N'} \sin \phi_{N'}, \cos \theta_{N'}) . \quad s_{\text{intersect}} = \frac{\left( \vec{O}_{\text{HCal}} - \vec{v} \right) \cdot \hat{z}_{\text{HCal}}}{\hat{p}_{N'} \cdot \hat{z}_{\text{HCal}}}$$

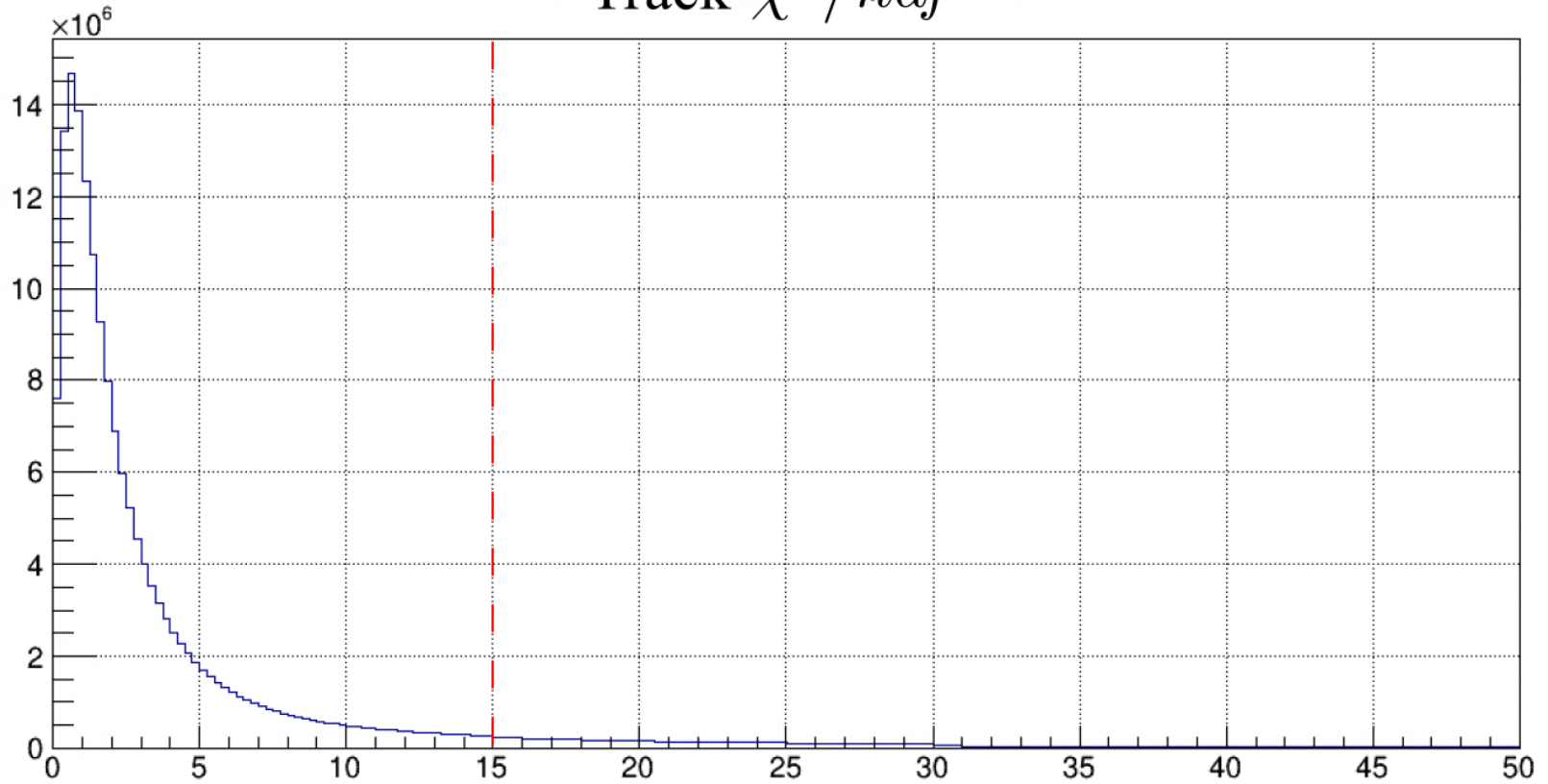
# Analysis Methods – Introducing HCal $\Delta x$ and $\Delta y$



- Definition of  $\Delta x$ : The difference between the observed ( $x_{HCal}^{obs}$ ) and the expected ( $x_{HCal}^{exp}$ ) nucleon position on HCal in the vertical (dispersive) direction.
- Definition of  $\Delta y$ : The difference between the observed ( $y_{HCal}^{obs}$ ) and the expected ( $y_{HCal}^{exp}$ ) nucleon position on HCal in the horizontal (non-dispersive) direction.

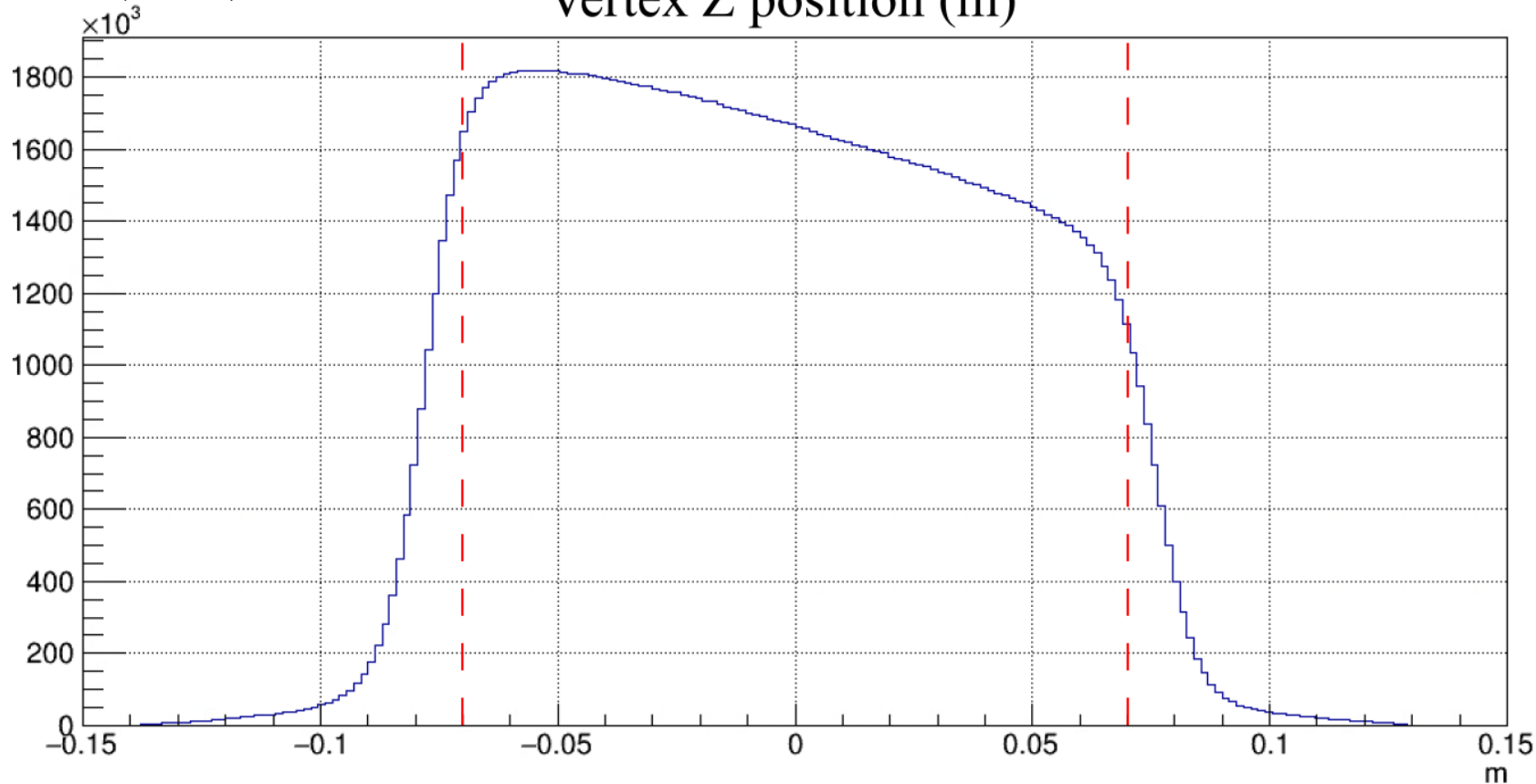
$$Q^2 = 4.5 \text{ (GeV/c)}^2$$

Track  $\chi^2 / ndf$



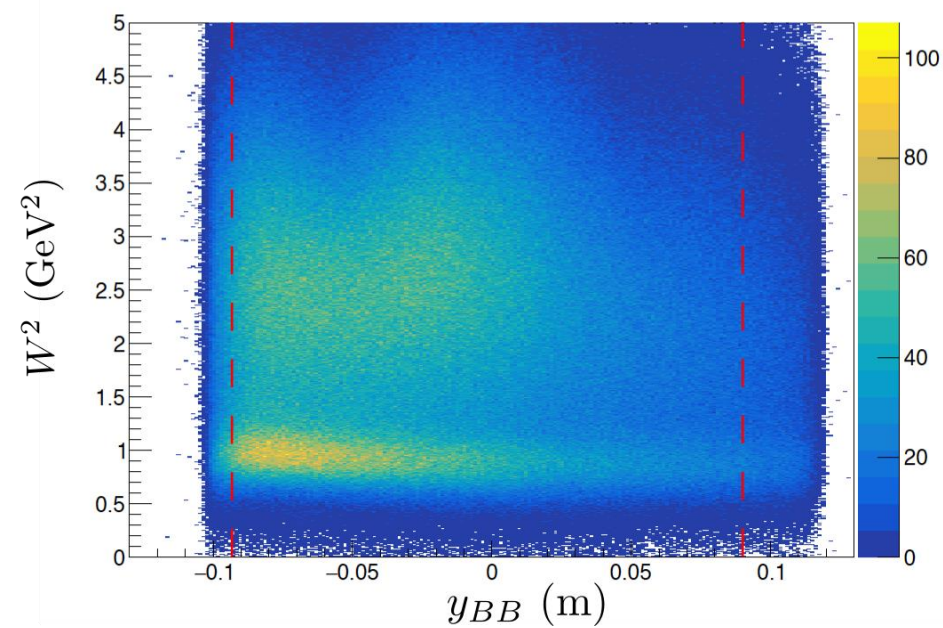
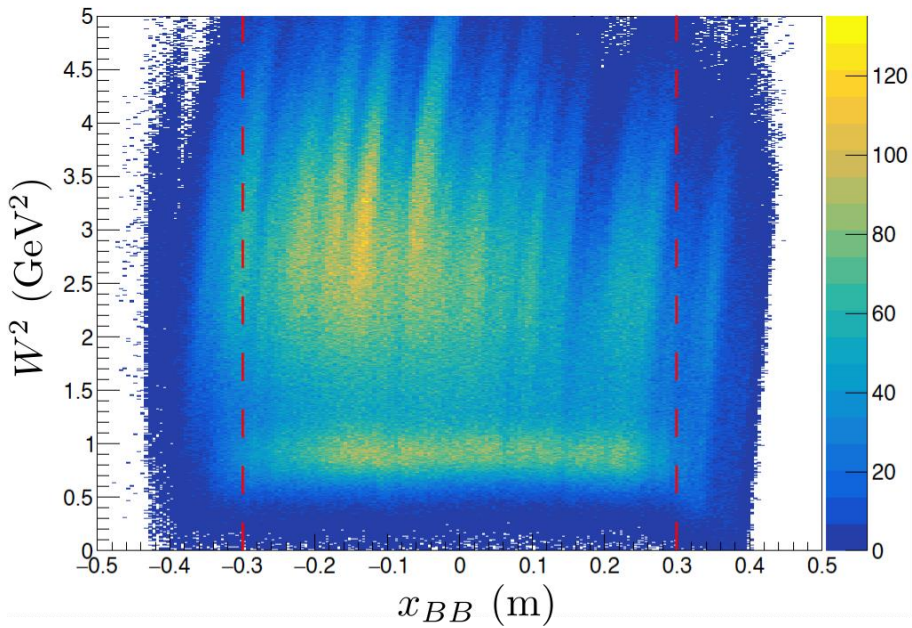
$$Q^2 = 4.5 \text{ (GeV/c)}^2$$

## Vertex Z position (m)



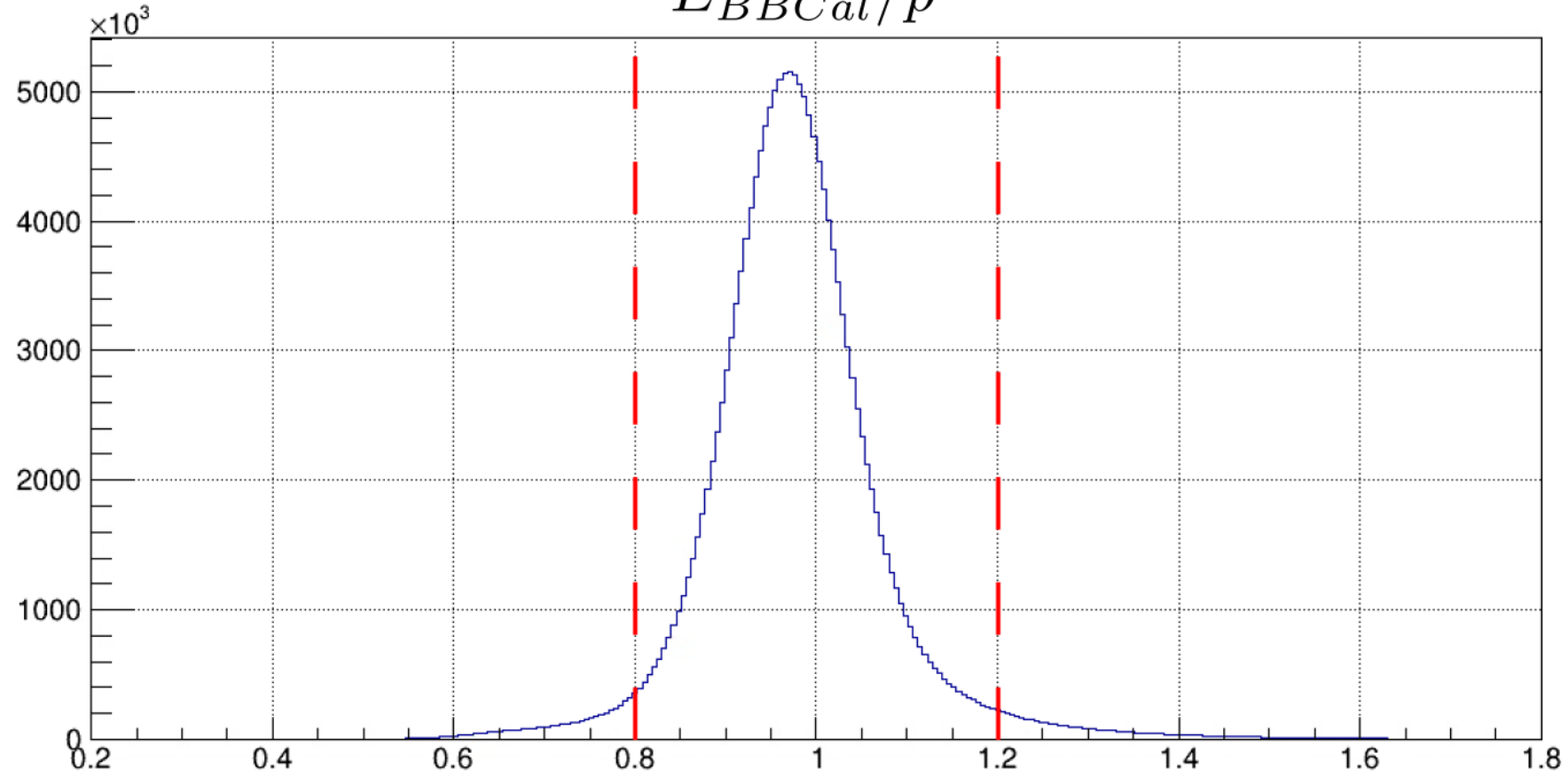
# Optics Validity Cuts

$$Q^2 = 4.5 \text{ (GeV/c)}^2$$



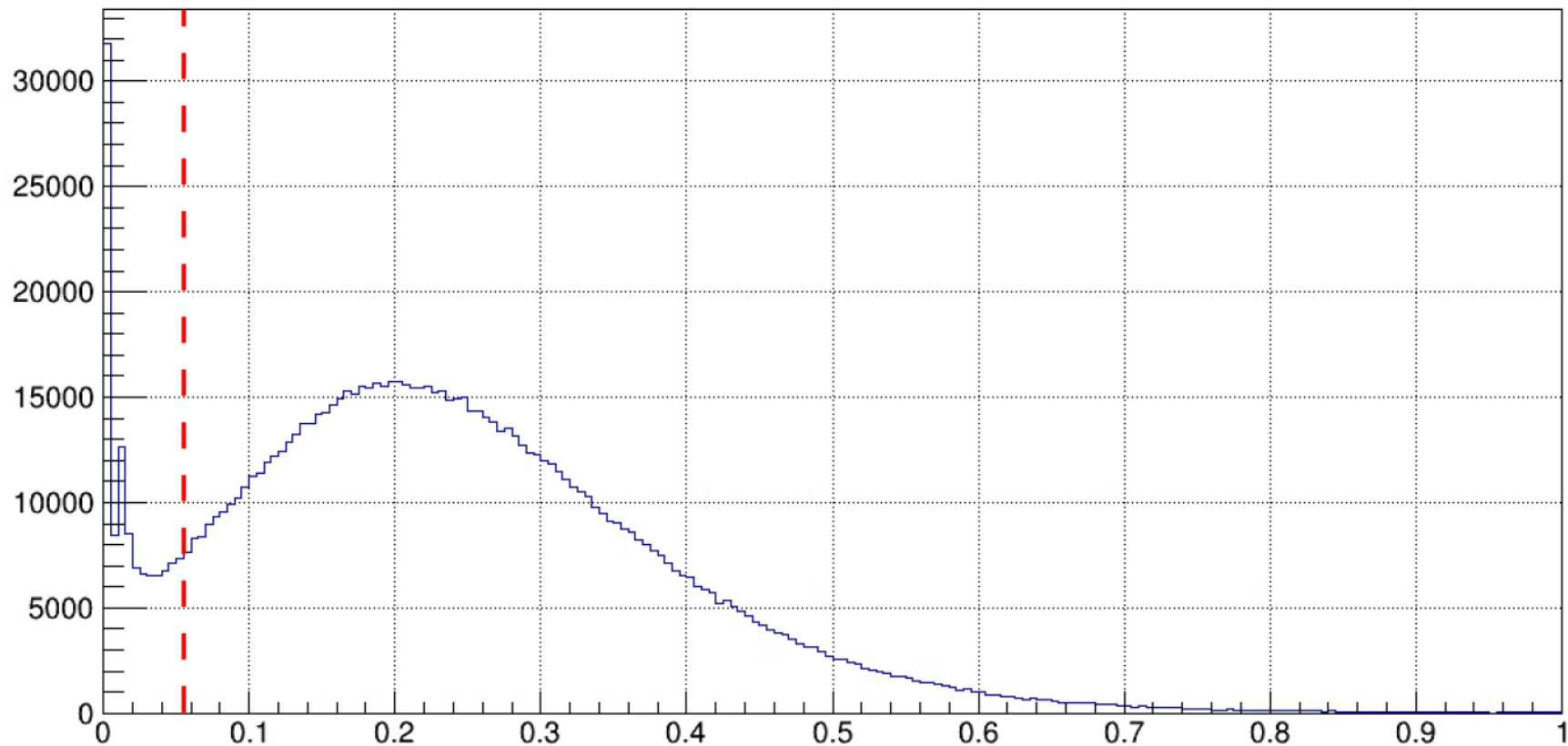
$Q^2 = 4.5 \text{ (GeV/c)}^2$

$E_{BBCal}/p$



$$Q^2 = 4.5 \text{ (GeV/c)}^2$$

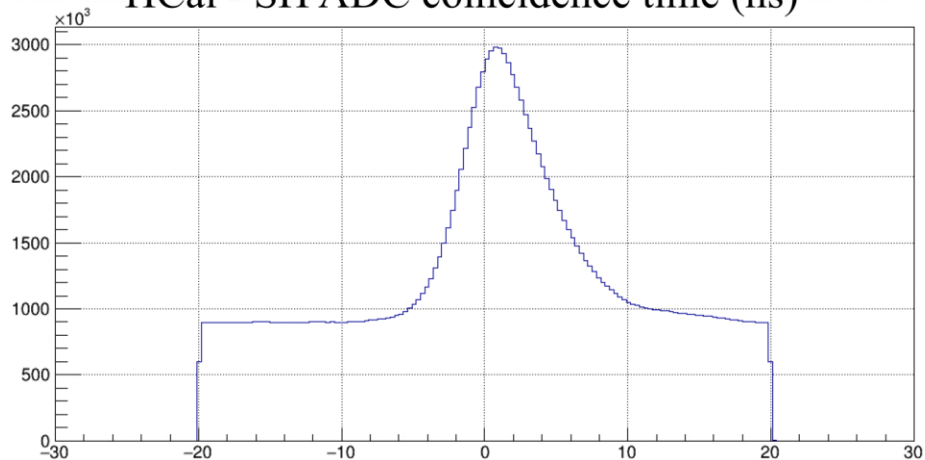
# HCal Cluster Energy (GeV)



$$Q^2 = 4.5 \text{ (GeV/c)}^2$$

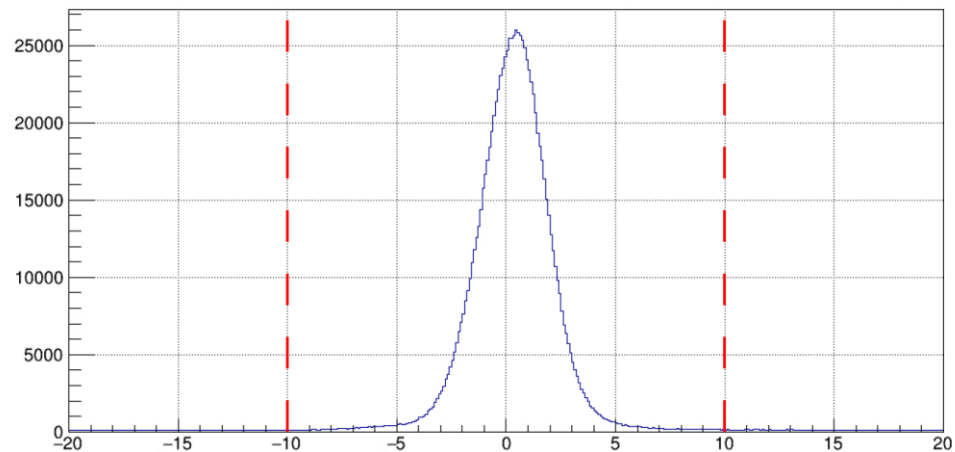
No Cuts Applied

HCal - SH ADC coincidence time (ns)



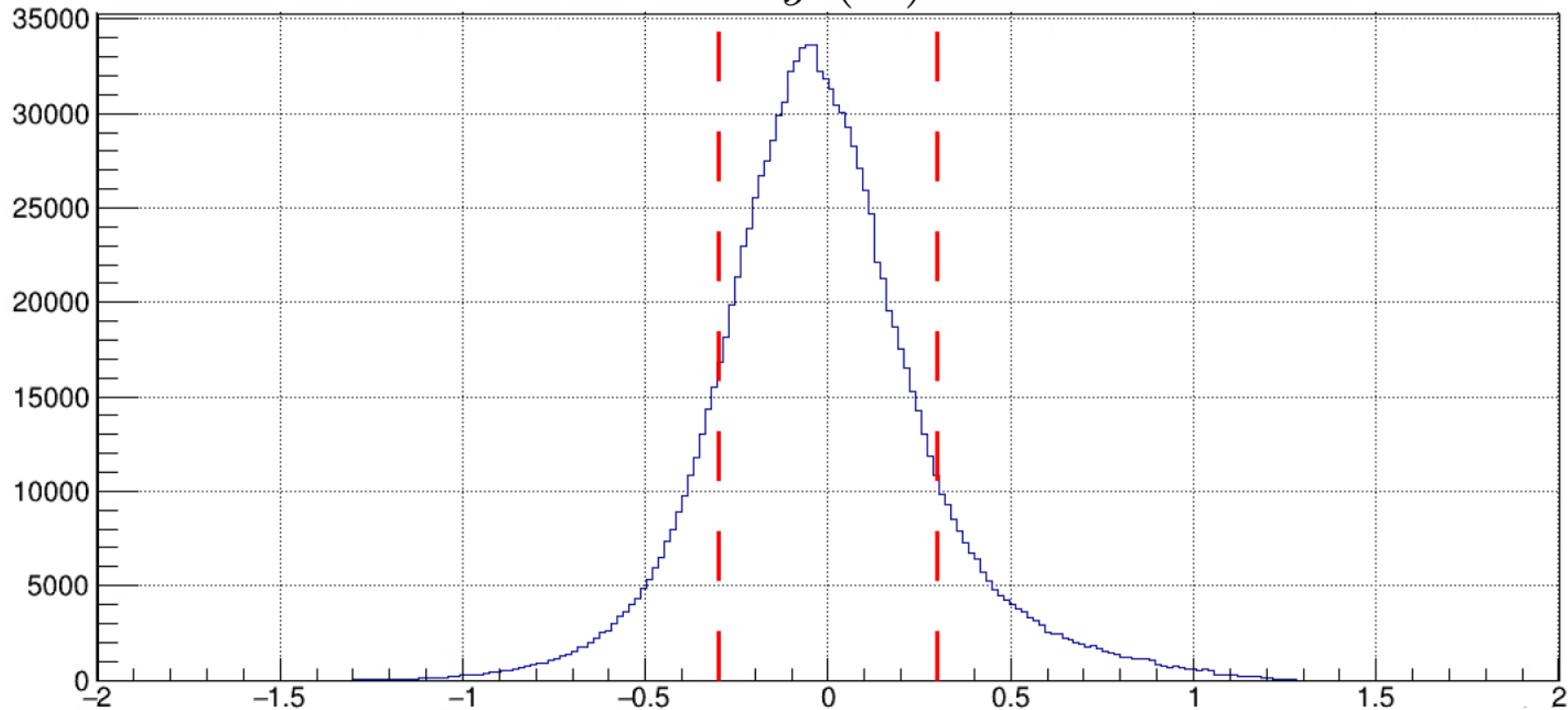
All Other Cuts Applied

HCal - SH ADC coincidence time (ns)

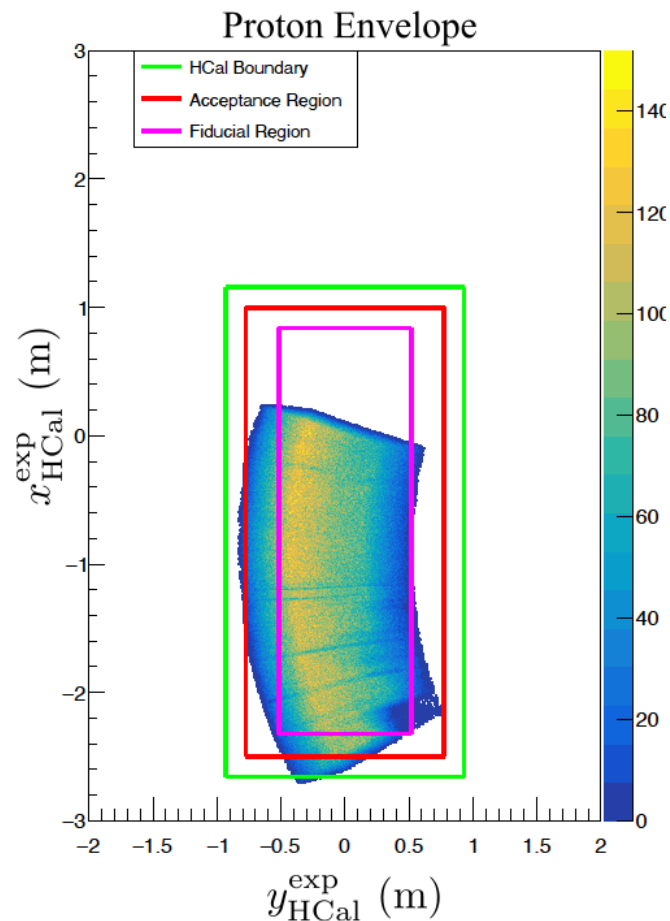
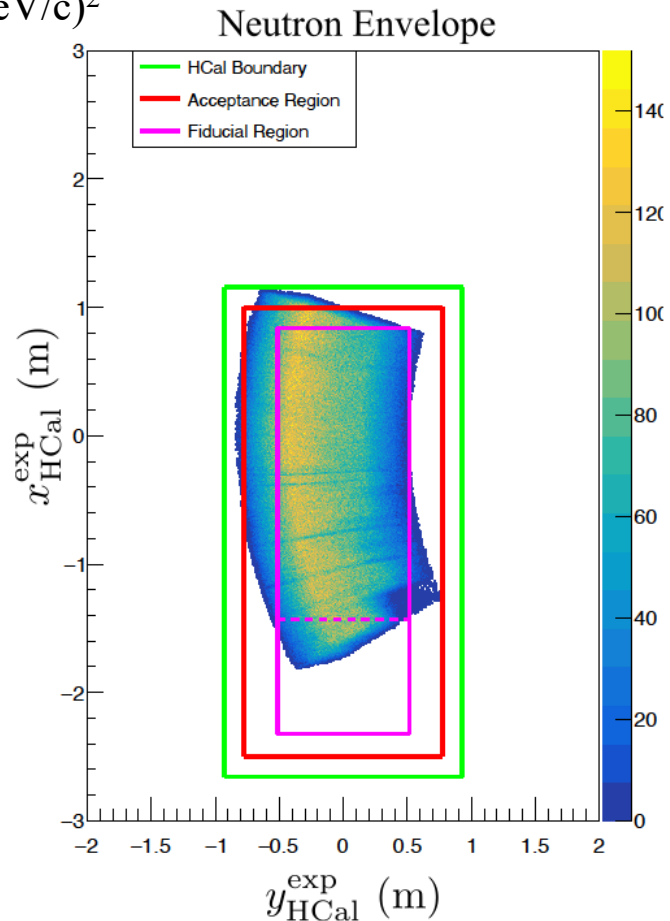


$Q^2 = 4.5 \text{ (GeV/c)}^2$

$\Delta y \text{ (m)}$



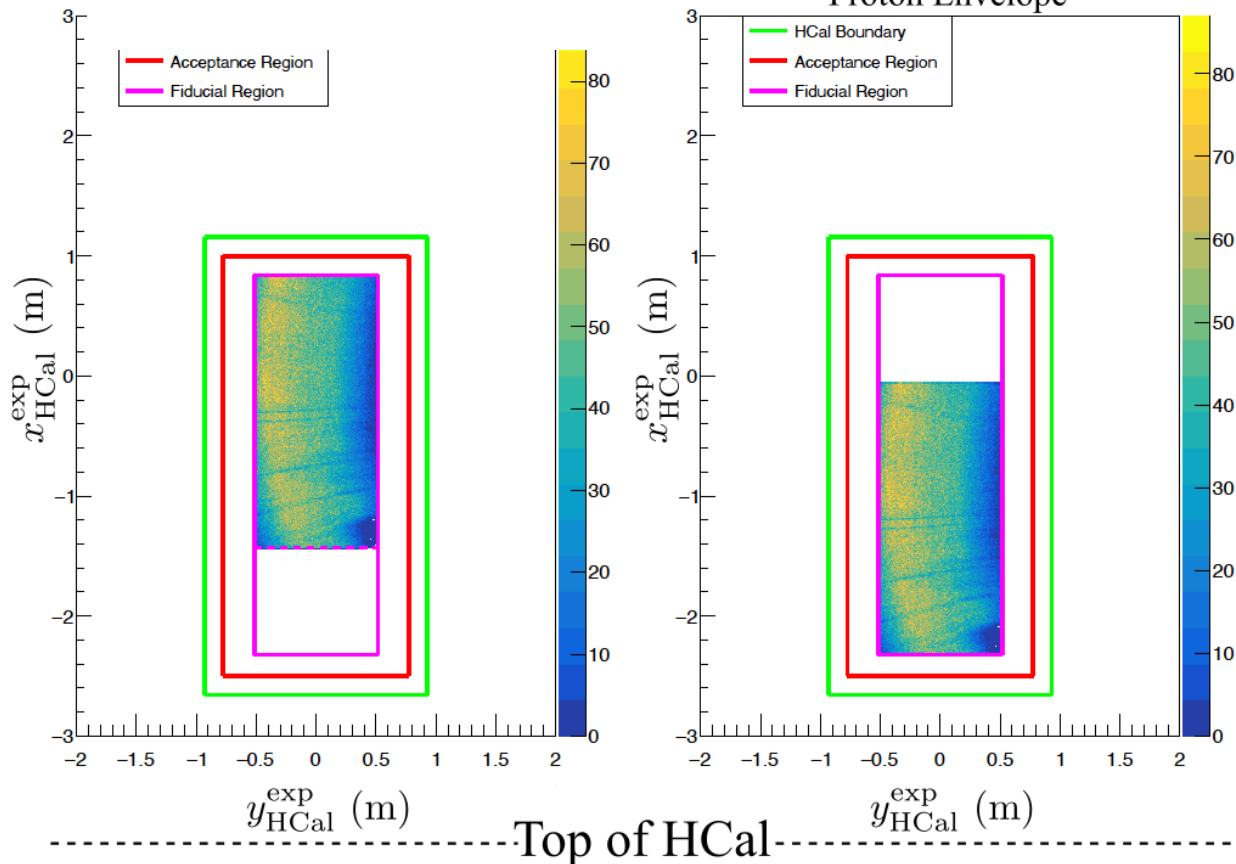
$$Q^2 = 4.5 \text{ (GeV/c)}^2$$



$$Q^2 = 4.5 \text{ (GeV/c)}^2$$

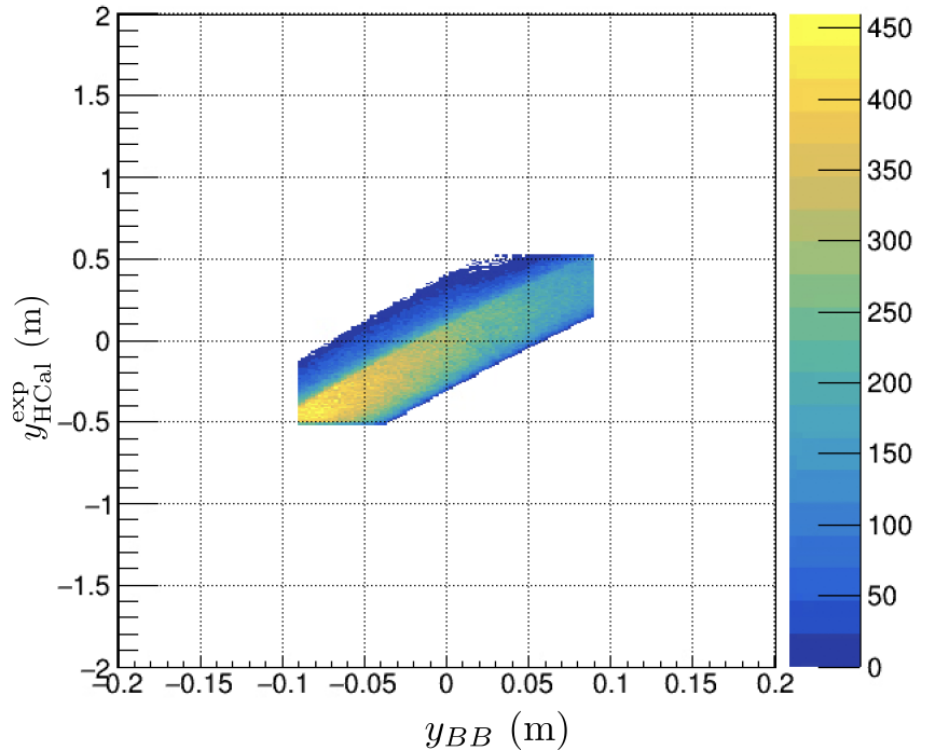
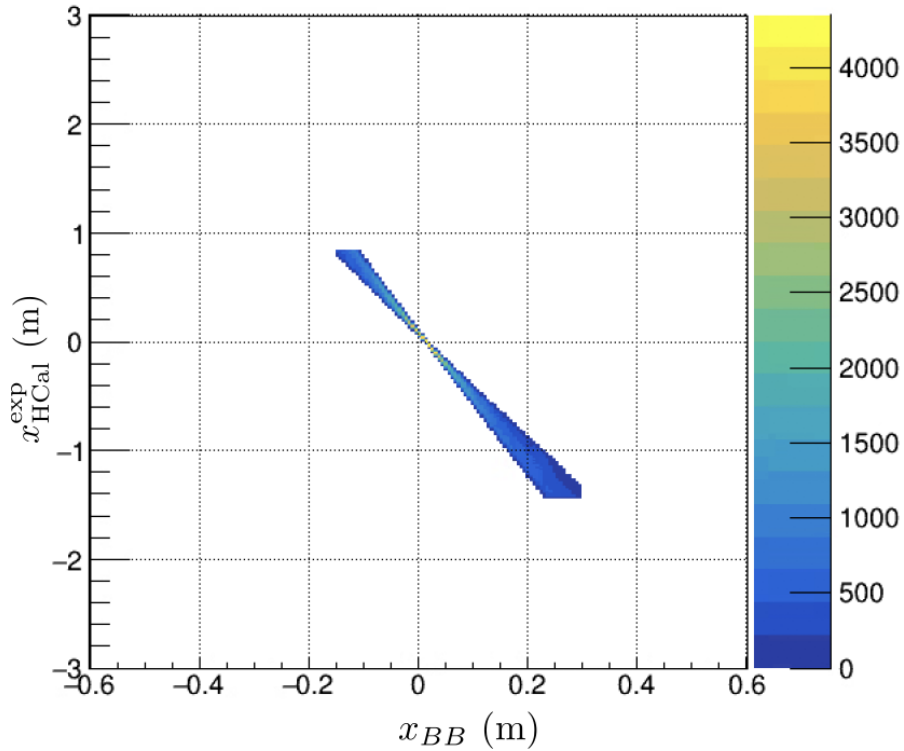
For a given electron event, the Fiducial Cut ensures the event is in the acceptance for both a scattered neutron and proton.

# Fiducial Cut

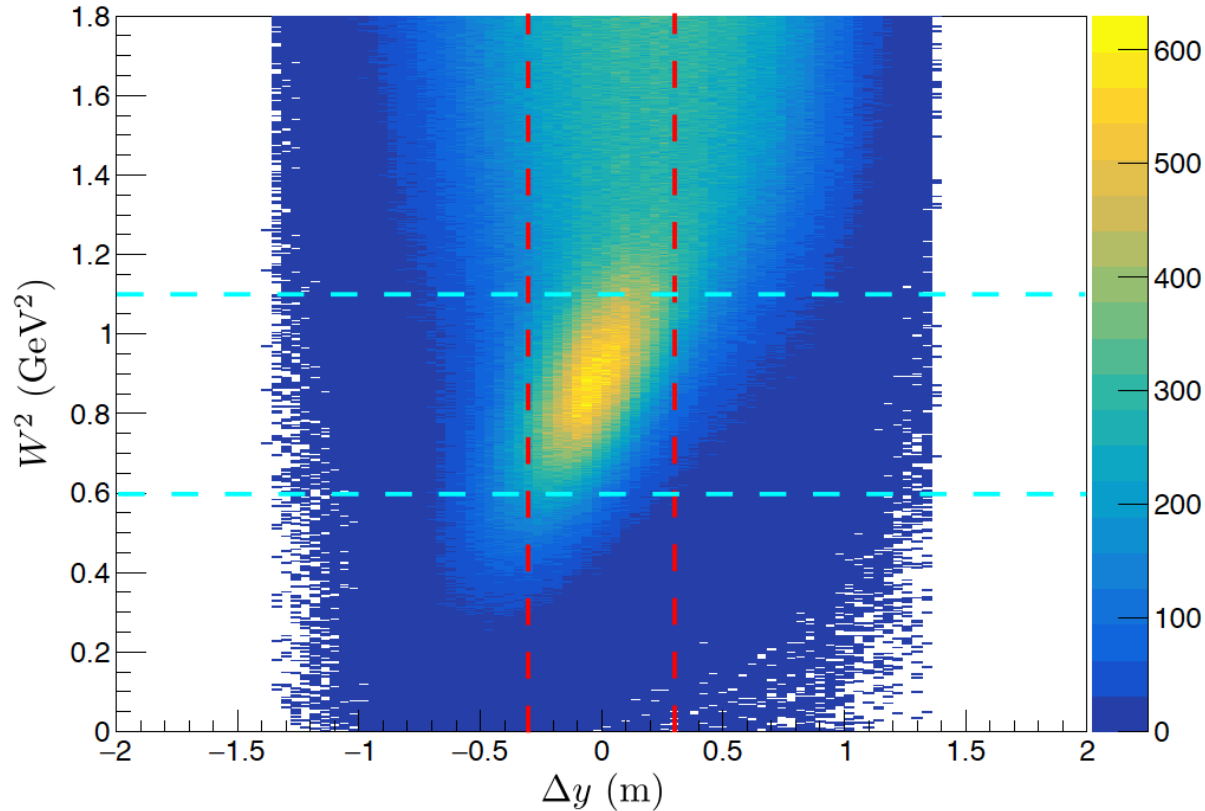


Cut Variable	Optimized Cut Regions			
	SBS-8 50%	SBS-8 70%	SBS-8 100%	SBS-9 70%
$N_{\text{GEMhits}}$	$\geq 3$	$\geq 3$	$\geq 3$	$\geq 3$
Track $\chi^2/ndf$	$\leq 15$	$\leq 15$	$\leq 15$	$\leq 15$
$v_z$ (m)	$[-0.07, 0.07]$	$[-0.07, 0.07]$	$[-0.07, 0.07]$	$[-0.07, 0.07]$
$x_{BB}$ (m)	$(-0.15, 0.30)$	$(-0.15, 0.30)$	$(-0.15, 0.20)$	$(-0.15, 0.30)$
$y_{BB}$ (m)	$(-0.09, 0.09)$	$(-0.09, 0.09)$	$(-0.08, 0.08)$	$(-0.09, 0.09)$
$E_{PS}$ (GeV)	$> 0.2$	$> 0.2$	$> 0.2$	$> 0.2$
$E_{BBCal}/p$	$(0.8, 1.2)$	$(0.8, 1.2)$	$(0.8, 1.2)$	$(0.8, 1.2)$
$E_{HCal}$ (GeV)	$\geq 0.055$	$\geq 0.055$	$\geq 0.055$	$\geq 0.05$
$\Delta t$ (ns)	$[-10, 10]$	$[-10, 10]$	$[-10, 10]$	$[-10, 10]$
$W^2$ (GeV <sup>2</sup> )	$[0.6, 1.1]$	$[0.6, 1.1]$	$[0.6, 1.1]$	$[0.65, 1.1]$
$\Delta y$ (m)	$[-0.3, 0.3]$	$[-0.3, 0.3]$	$[-0.3, 0.3]$	$[-0.3, 0.3]$
$x_{HCal}^{\text{exp}}$	$(-2.32, 0.83)$	$(-2.32, 0.83)$	$(-2.32, 0.83)$	$(-2.32, 0.84)$
$y_{HCal}^{\text{exp}}$	$(-0.51, 0.51)$	$(-0.51, 0.51)$	$(-0.51, 0.51)$	$(-0.5, 0.5)$

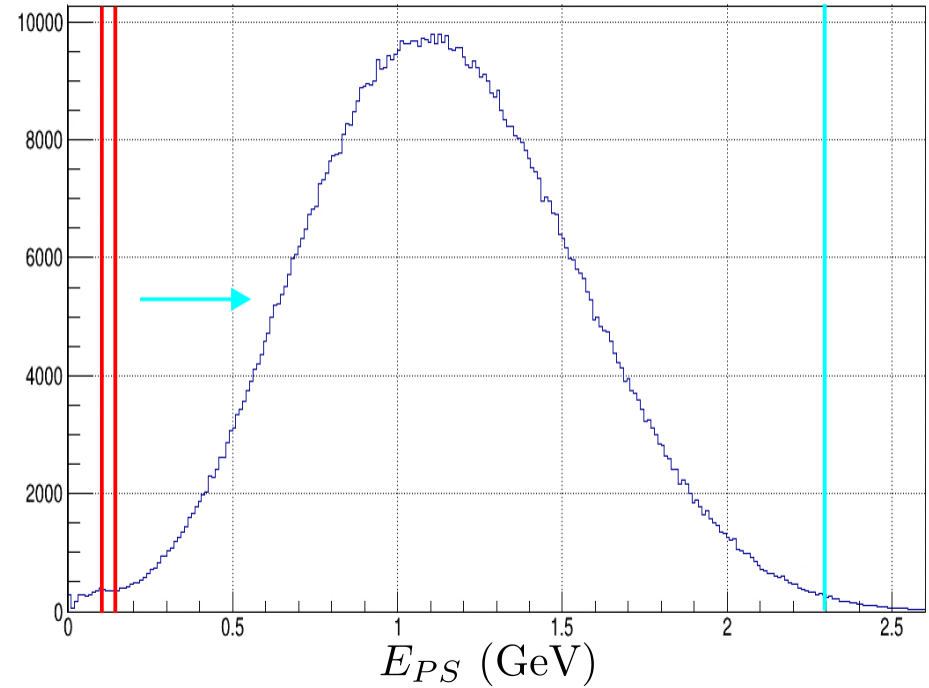
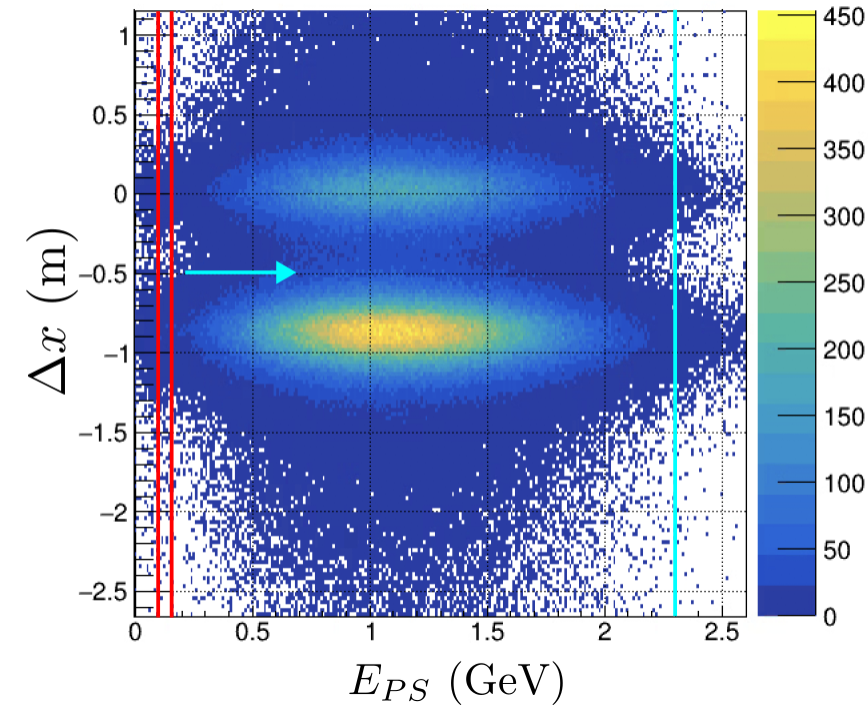
# Correlated Cut Variables Pt 1



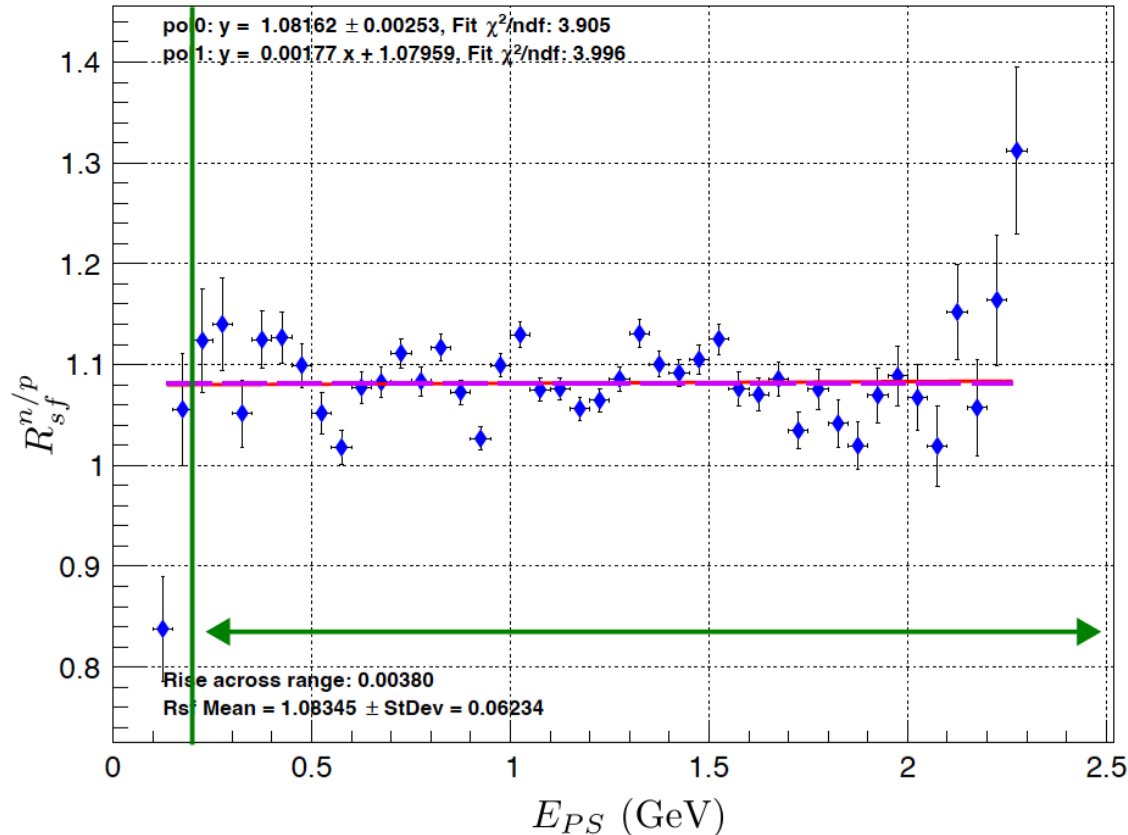
# Correlated Cut Variables Pt 2



# Cut Region Optimization

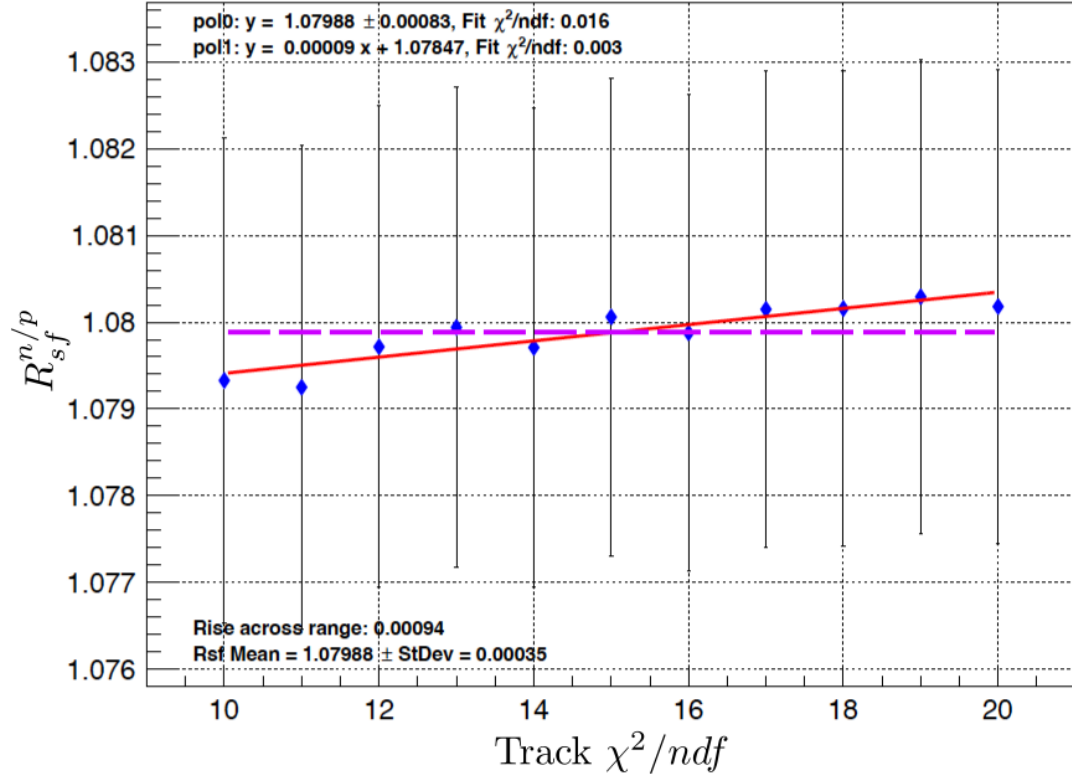
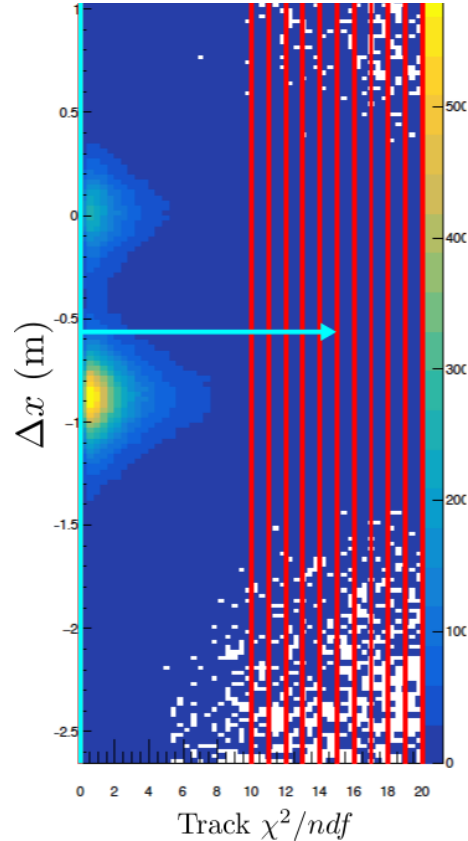


# Cut Region Optimization

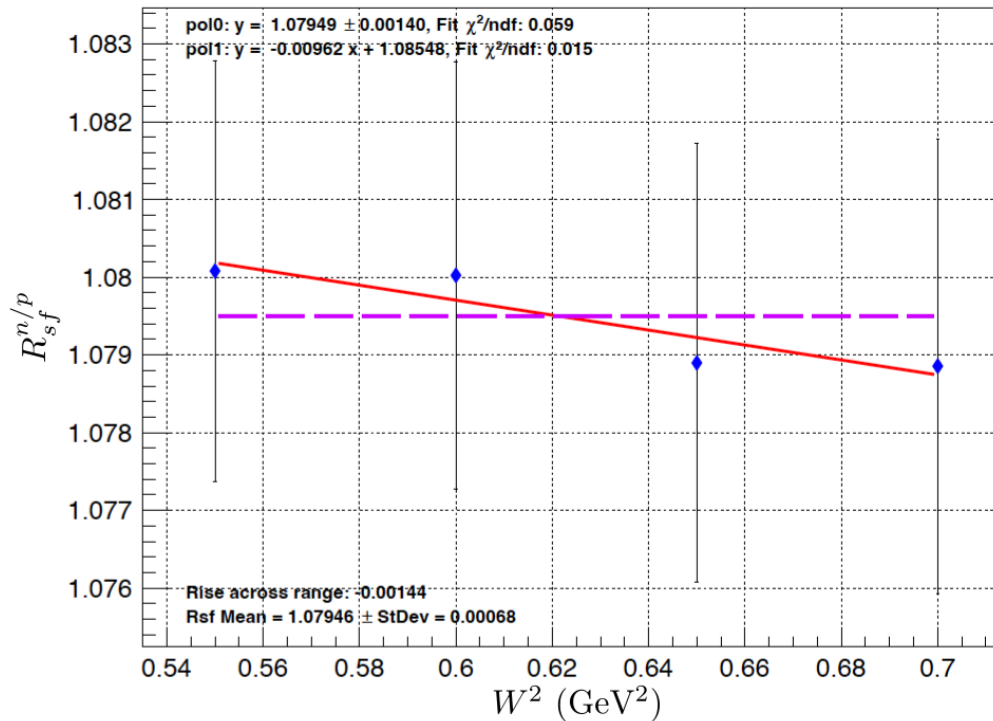
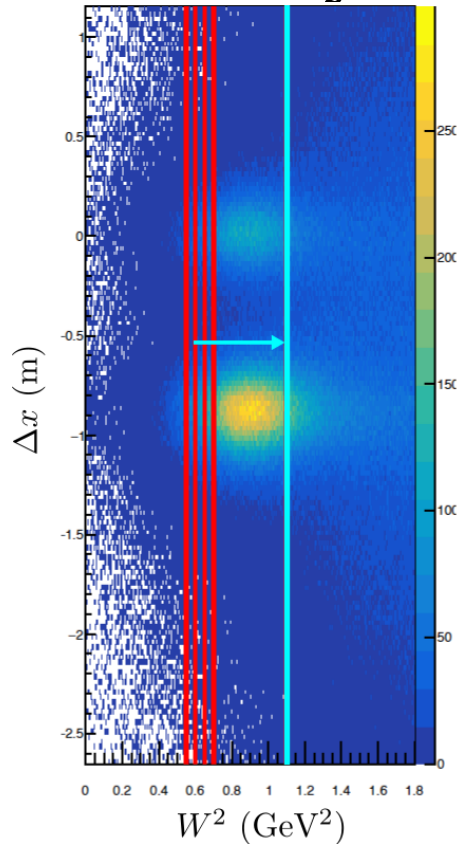


Cut Variable	Systematic Uncertainty Contribution			
	SBS-8 50%	SBS-8 70%	SBS-8 100%	SBS-9 70%
$N_{\text{GEMhits}}$	0.0025	0.0061	0.0029	0.00007
Track $\chi^2/ndf$	0.0005	0.0005	0.0002	0.0014
$v_z$ (m)	0.0017	0.00003	0.0003	0.0009
$x_{BB}$ (m)	0.0012	0.0044	0.0021	0.0019
$y_{BB}$ (m)	0.0014	0.0013	0.0023	0.0007*
$E_{PS}$ (GeV)	0.0002	0.0002	0.0006	0.0005
$E_{\text{BBCal}}/p$	0.0002	0.0007	0.0013	0.0003
$E_{\text{HCal}}$ (GeV)	0.0006	0.0002	0.0003	0.0002
$\Delta t$ (ns)	0.0027	0.0023	0.0022	0.0030
$W^2$ (GeV <sup>2</sup> )	0.0063	0.0007*	0.0012	0.0035
$\Delta y$ (m)	0.0041*	0.0019	0.0012*	0.0010*
$x_{\text{HCal}}^{\text{exp}}$	0.0006*	0.0002*	0.0006*	0.0008*
$y_{\text{HCal}}^{\text{exp}}$	0.0007*	0.0007*	0.0013*	0.0011
$\Delta \left( R_{sf}^{n/p} \right)_{\text{cuts}}$	0.0078	0.0083	0.0052	0.0054

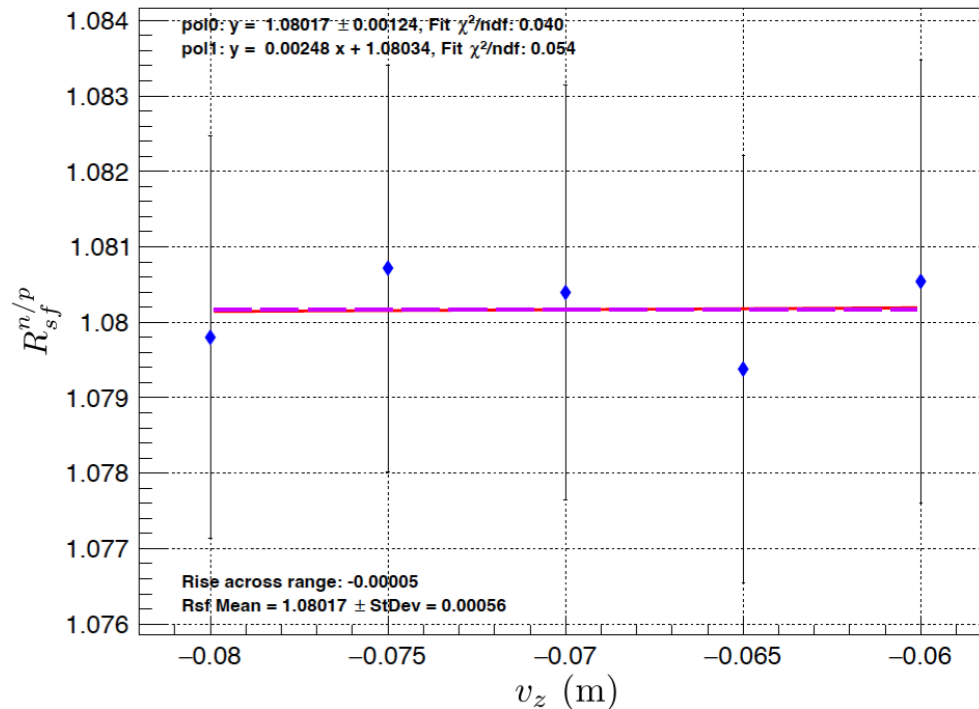
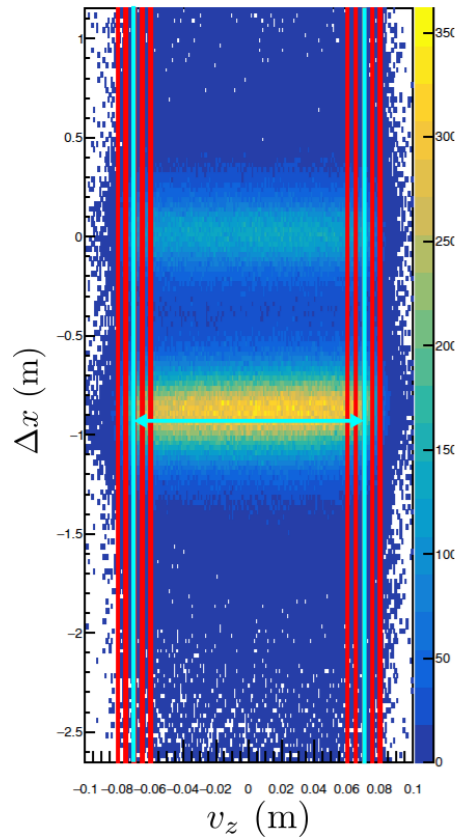
# Cut Systematic One Boundary



# Cut Systematic Two Separate Boundary

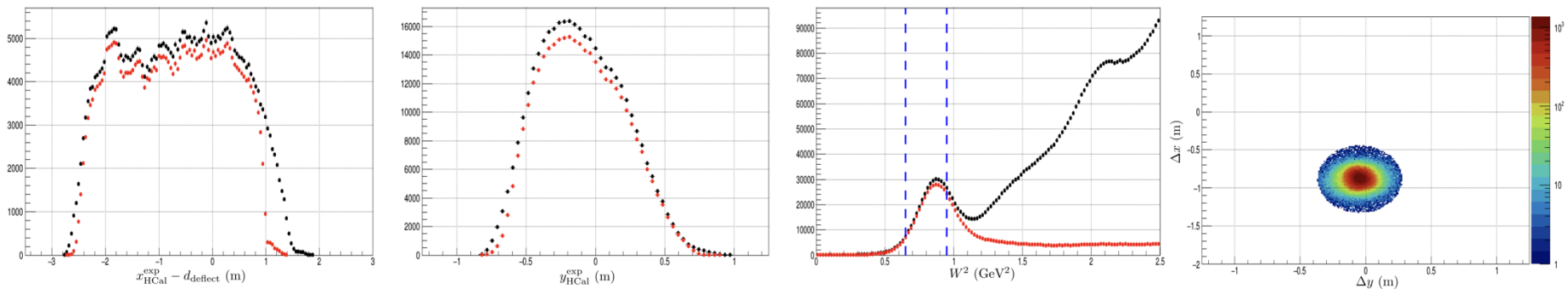


# Cut Systematic Two Boundary Symmetric

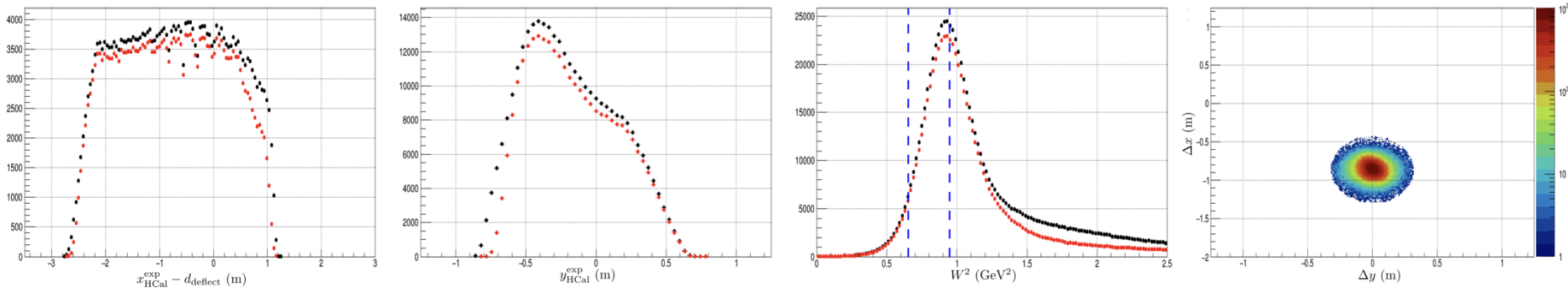


# Proton Relative Rate Information

Data

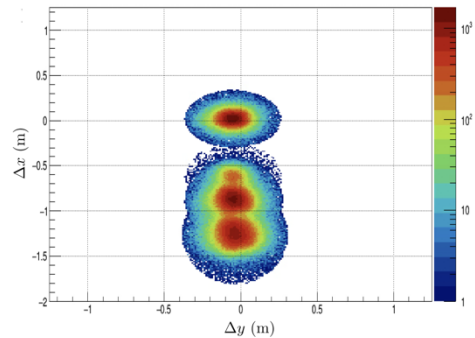
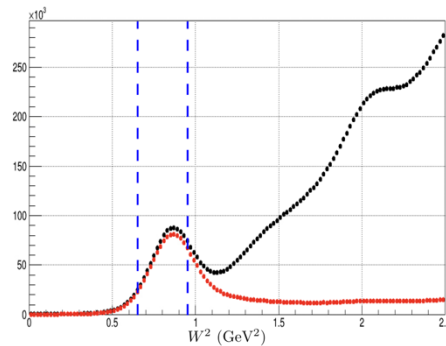
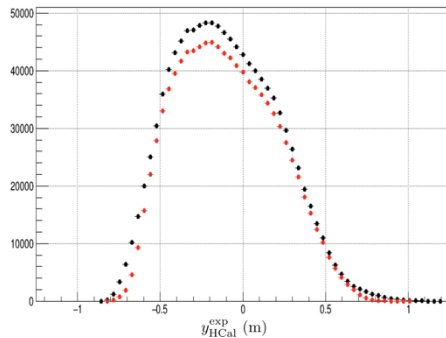
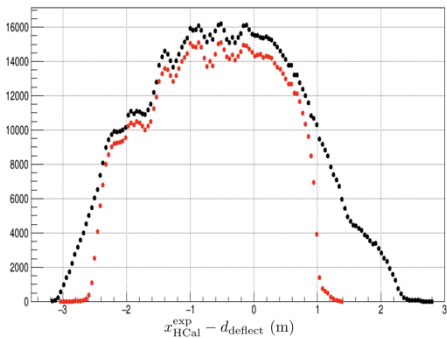


MC



# Proton Relative Rate Information

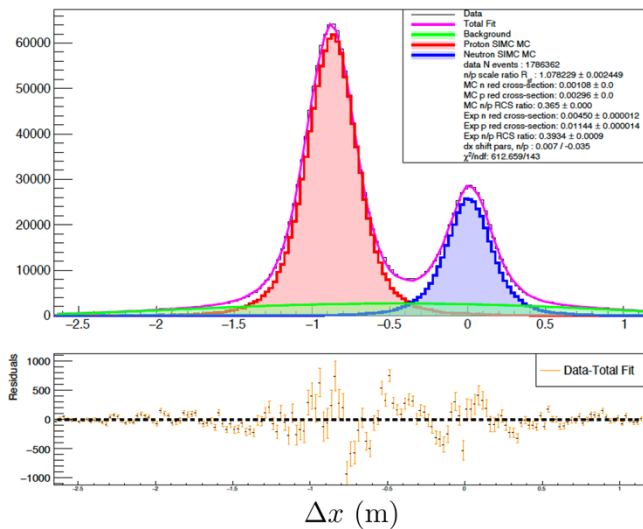
Data Combined



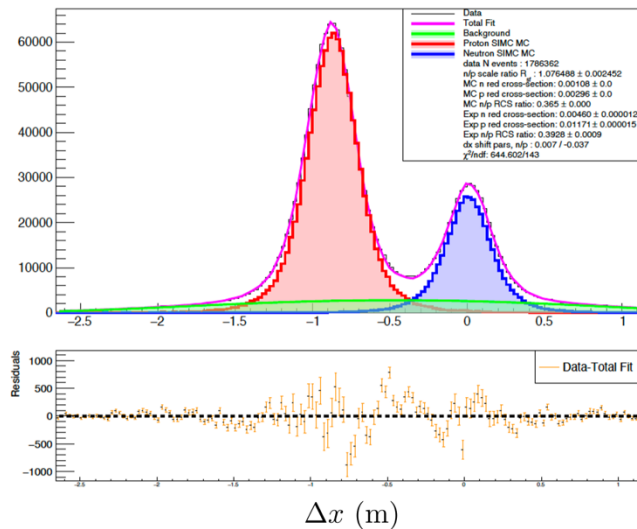
# HCal Non-uniformity Systematic

Setting	$R_{sf}^{n/p}$ from Uncorrected MC	$R_{sf}^{n/p}$ from SBS-8 Map Corrected MC	Absolute Difference
SBS-8 50%	1.0842	1.0845	0.0003
SBS-8 70%	1.0782	1.0764	0.0018
SBS-8 100%	1.0678	1.0666	0.0012
SBS-9 70%	1.0876	1.0823	0.0053

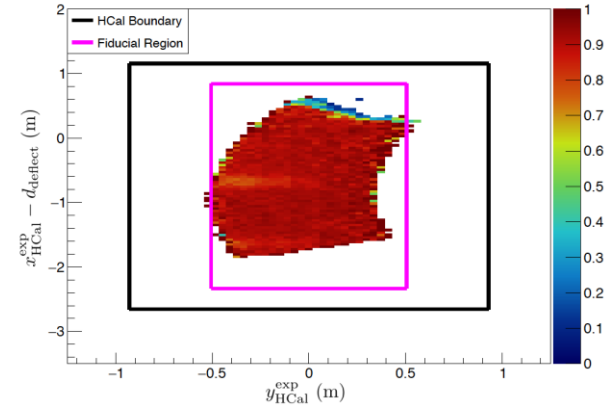
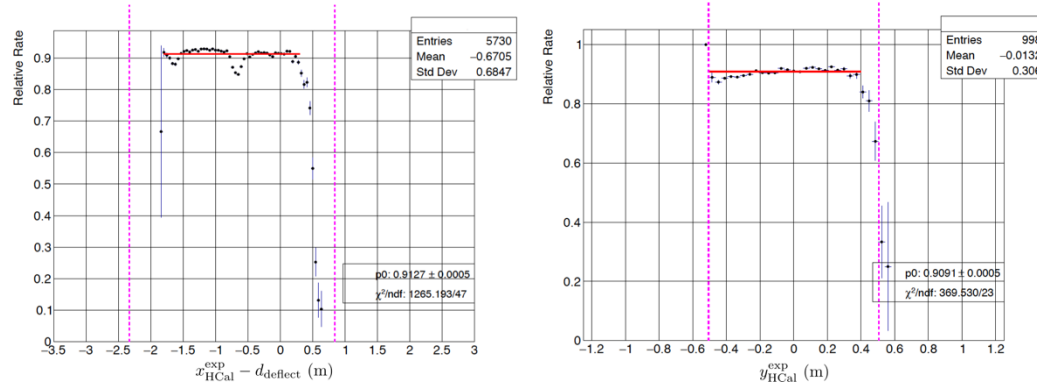
Uncorrected MC



MC Corrected for HCal Non-Uniformity

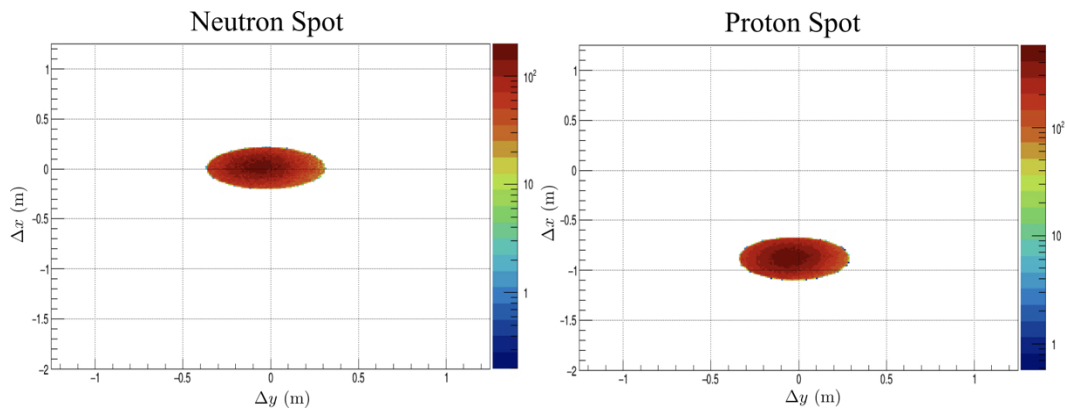


# SBS-9 Proton Relative Rate

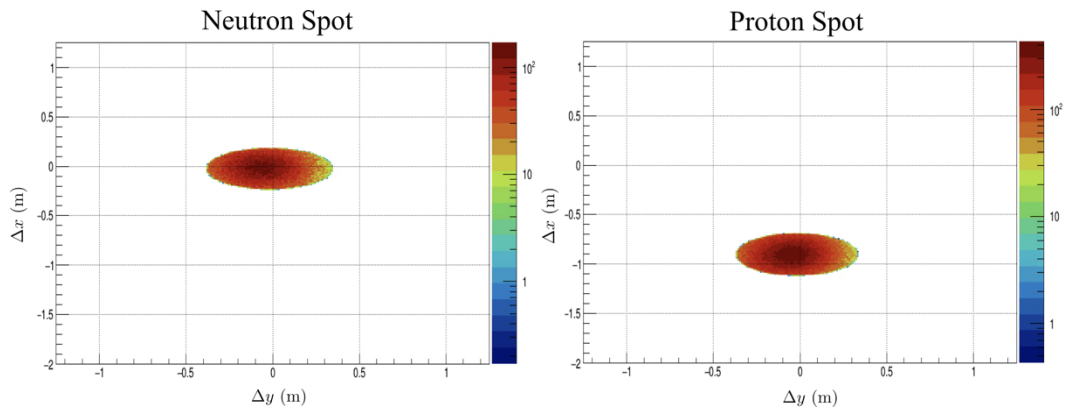


# Spot Cuts for HCal Non-uniformity

SBS-8

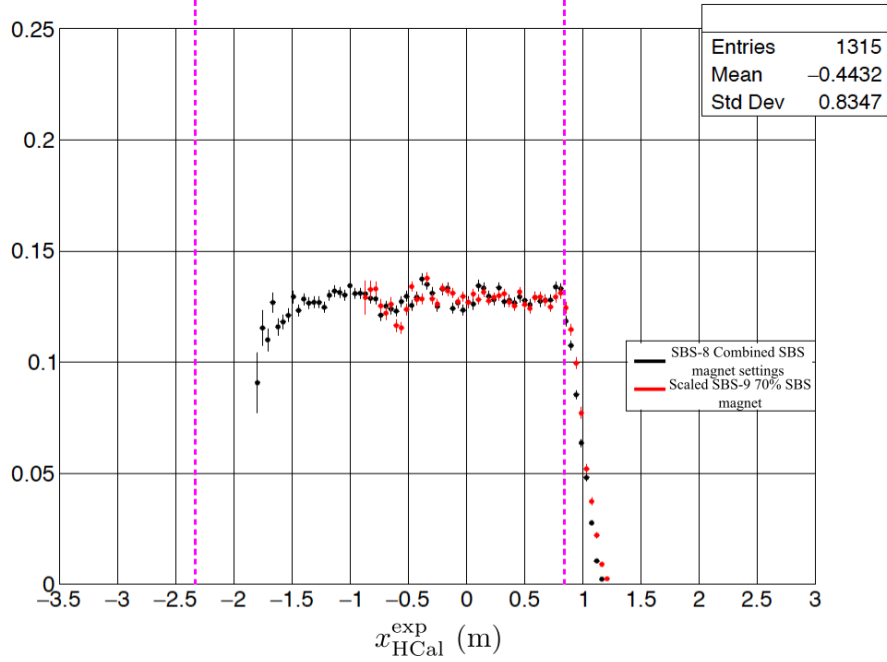


SBS-9

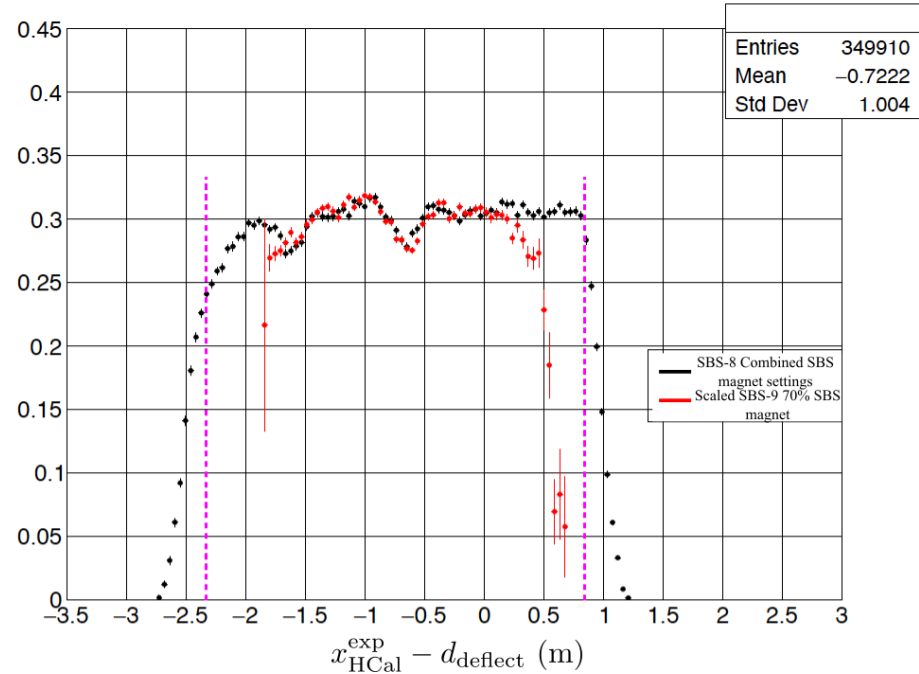


# SBS-8 and SBS-9 Comparison

neutron

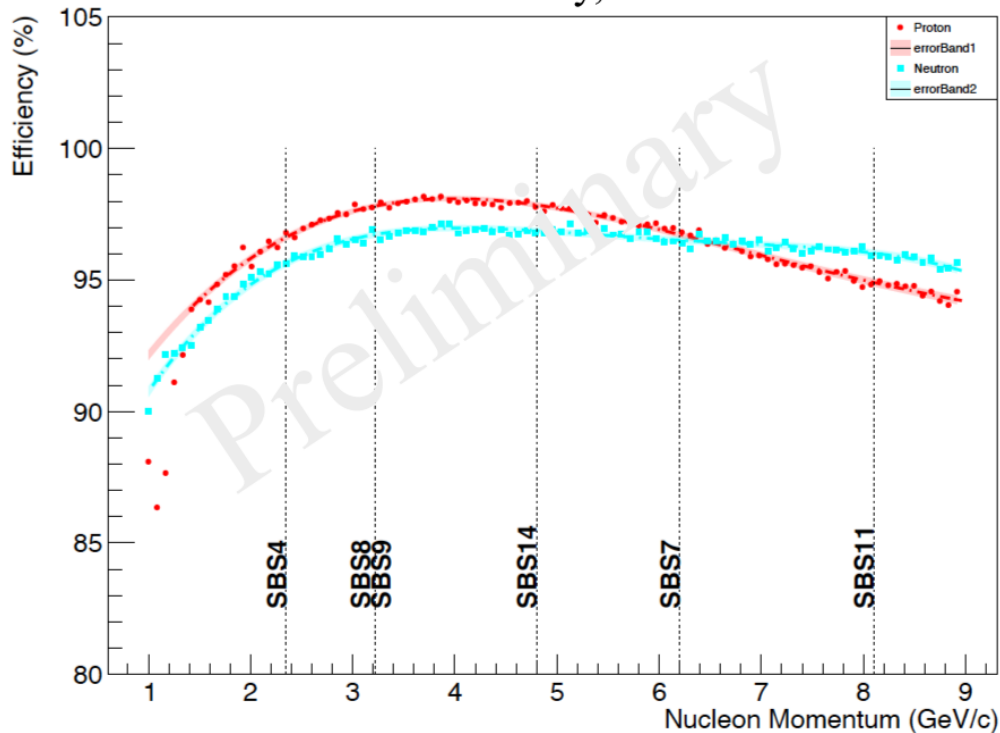


proton



# Detection Efficiency (MC)

HCal Efficiency, SBS8

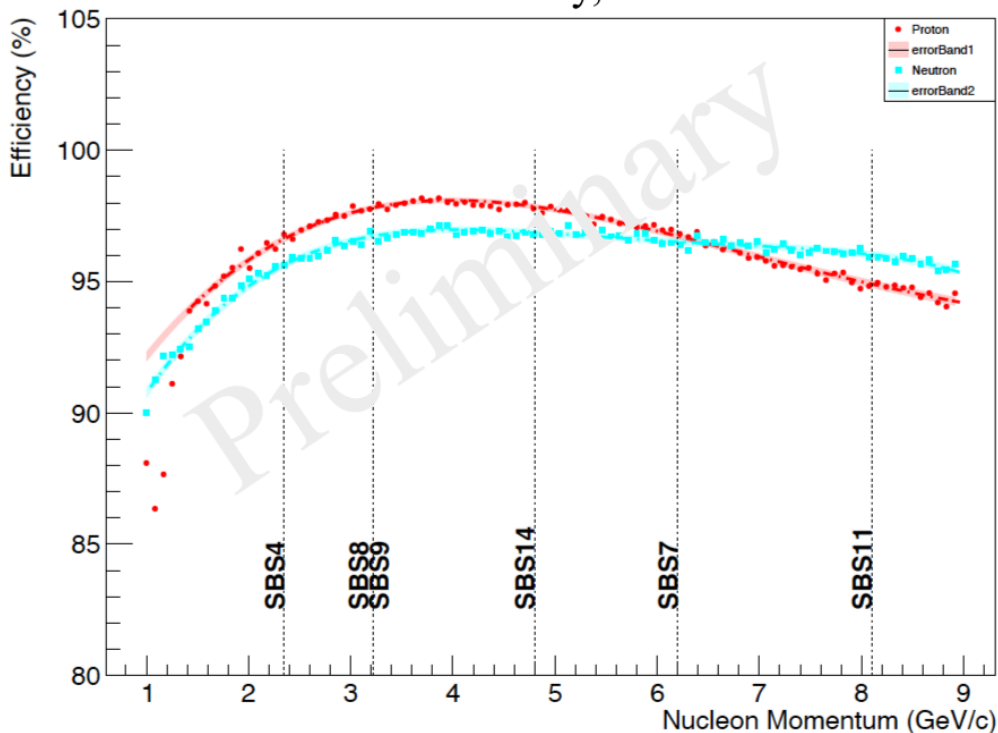


Method:

- Simulate, digitize, replay protons and neutrons separately, with momentum 1-9 GeV. Throw flat and populate 1000 events/channel.
- Get energy spectra vs nucleon momentum. Fit each peak to determine mean E for p bin.
- **Total:** Populate energy per p bin regardless.
- **Pass:** Separately populate energy per p bin  $> E_{\text{mean}}/4$ .
- By looping over p bins, evaluate the integral of energy histograms so Efficiency = **Pass** / **Total**.

# Detection Efficiency (MC)

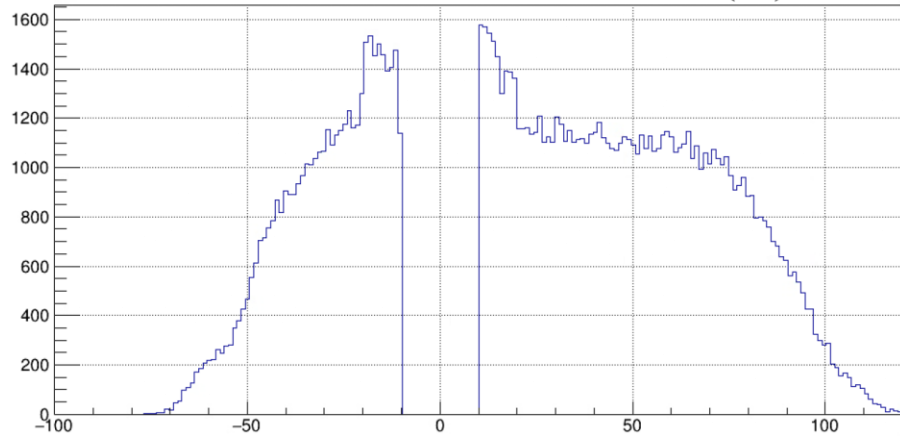
HCal Efficiency, SBS8



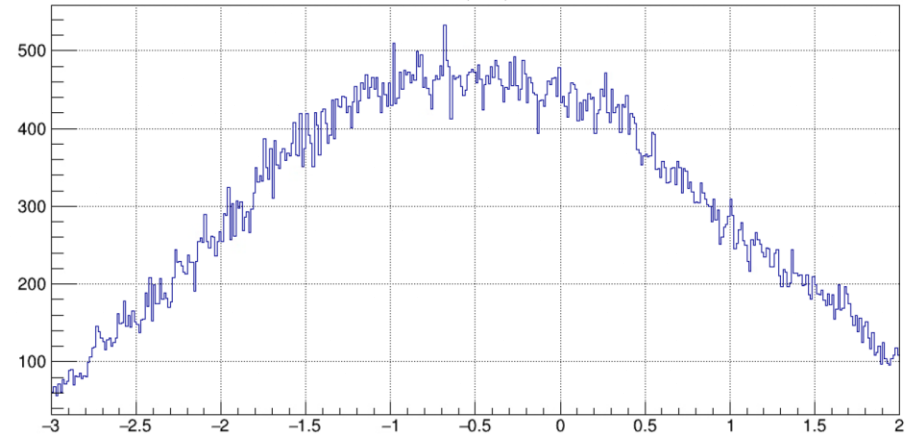
	Proton Efficiency	Neutron Efficiency
SBS4	96.6%	95.6%
SBS8	97.8%	96.7%
SBS9	97.8%	96.7%
SBS14	97.9%	96.9%
SBS7	96.7%	96.5%
SBS11	94.9%	96.0%

# Coincidence Time Anti-cut

HCal - SH ADC coincidence time (ns)

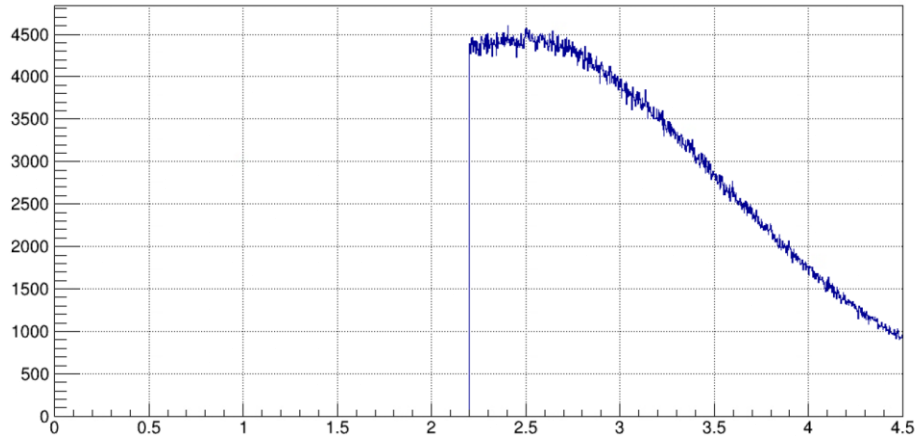


$\Delta x$  (m)

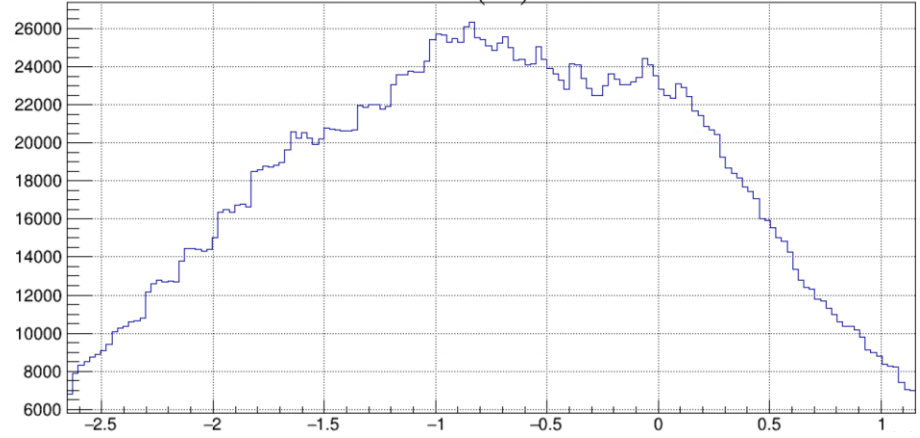


# $W^2$ anti-cut

$W^2$  (GeV<sup>2</sup>)



$\Delta x$  (m)



# Inelastic Background Systematic

Bkgd Model	$R_{sf}^{n/p}$ value			
	SBS-8 50%	SBS-8 70%	SBS-8 100%	SBS-9 70%
Gaussian	1.0655	1.0658	1.0611	1.0680
Polynomial-2	1.0787	1.0732	1.0651	1.0648
Polynomial-3	1.0639	1.0687	1.0554	1.0692
$\Delta t$ Anti-Cut	1.0813	1.0762	1.0681	1.0729
$W^2$ Anti-Cut	1.0869	1.0823	1.0828	1.0681

# Weighted Mean SBS-8

Weighted Mean Formula:  $\bar{R}_{sf,w} = \frac{\sum_{i=1}^3 R_{sf,i} w_i}{\sum_{i=1}^3 w_i}$ , where  $w_i = \frac{1}{\sigma_{uncorr,i}^2}$

Uncertainty on the weighted mean, for uncorrelated uncertainties:  $\sigma_{mean,uncorr}^2 = 1 / \sum_{i=1}^3 w_i$

Uncertainty on the weighted mean, for correlated uncertainties, procedure:

1. Add the correlated error,  $\sigma_{corr,i}$ , for a given data set to the scale factor,  $R_{sf,i}$ :  $R_{sf,i}^{+1} = R_{sf,i} + \sigma_{corr,i}$
2. Apply step 1 for every data set
3. Calculate a new weighed mean from the above formula with all  $R_{sf,i}^{+1}$ s, call it  $\bar{R}_{sf,w}^{+1}$
4. The correlated uncertainty on the weighted mean is the absolute value between  $\bar{R}_{sf,w}^{+1}$  and  $\bar{R}_{sf,w}$ :

$$\sigma_{mean,corr} = |\bar{R}_{sf,w}^{+1} - \bar{R}_{sf,w}|$$

5. Repeat Steps 1 through 5 but considering  $R_{sf,i}^{-1} = R_{sf,i} - \sigma_{corr,i}$ . This should obtain the same value for  $\sigma_{mean,corr}$

Total Uncertainty on the weighted mean is  $\sigma_{mean,total} = \sqrt{\sigma_{mean,uncorr}^2 + \sigma_{mean,corr}^2}$

Values for SBS8

$$\bar{R}_{sf,w} = 1.07113$$

$$\sigma_{mean,total} = 0.01036, \text{ or } 0.97\%$$

$$\sigma_{mean,uncorr} = 0.00538$$

$$\sigma_{mean,corr} = 0.00886$$